AD NUMBER

AD905182

LIMITATION CHANGES

TO:

Approved for public release; distribution is unlimited.

FROM:

Distribution authorized to U.S. Gov't. agencies only; Test and Evaluation; 06 NOV 1972. Other requests shall be referred to Naval Underwater Systems Center, New London, CT 06320.

AUTHORITY

usnusc ltr, 23 aug 1971

NUSC Technical Report 4319

Computer Programs to Calculate Normal Mode Propagation And Applications to Analysis of Explosive Sound Data in the BIFI Range

WILLIAM G. KANABIS
Ocean Science Department

6 November 1972

NAVAL UNDERWATER SYSTEMS CENTER

UNLimited

ADMINISTRATIVE INFORMATION

This work was performed under NUSC Project No. A-650-09, and Navy Subproject No. SF 11 552-008-14054, "Shallow Water Acoustic Theory and Measurements for Sonar Systems Design and Operation," Principal Investigators, W. R. Schumacher and B. Sussman, Code TA11, Program Manager, J. Reeves, NAVSHIPS PMS-302-44.

The Technical Reviewer for this report was Dr. F. R. DiNapoli, Code PA41.

REVIEWED AND APPROVED: 6 November 1972

W. A. Von Winkle
Director of Science and Technology

Inquiries concerning this report may be addressed to the author,
New London Laboratory, Naval Underwater Systems Center,
New London, Connecticut 06320

NAVAL UNDERWATER SYSTEMS CENTER
HEADQUARTERS
NEWPORT, RHODE ISLAND 02840

NEWPORT, R. I. 02840
AREA CODE 401
841 – EXT.
AUTOVON 948 + EXT.

NEW LONDON, CONN. 06320
AREA CODE 203
442 – 0771 – EXT.
AUTOVON 636 + EXT.

IN REPLY REFER TO:
LA152:WFS:jj
5600
Ser: 682

28 NOV 1972

From: Commanding Officer, Naval Underwater Systems Center
To: Distribution List

Subj: Forwarding of documents

Encl: (1) NUSC Technical Report 4319, "Computer Programs to Calculate Normal Mode Propagation and Applications to Analysis of Explosive Sound Data in the BIFI Range"

1. Enclosure (1) is forwarded for information and retention.

W. F. Saars

W. F. SAARS
By direction

Distribution List

CNO, Op-311, cy 2 Op-9420, cy 6 Op-23T, cy 10
OP-32, cy 3 Op-950, cy 7
Op-95, cy 4 Op-954, cy 8
Op-96, cy 5 Op-9814, cy 9
Oceanographer of the Navy, cy 11
ONR, Code 400-A2, cy 12 Code 481, cy 16
466, cy 13 Code 485, cy 17
468, cy 14 Code 102-OS, cy 18
480, cy 15 Code 102-)S (LCdr. McCluskey), cy 19
NOO, Code 7200 and 9320, cys 20, 21
ASWSPO (CNM-PM-4), ASW 211, cy 27 ASW-22, cy 29
ASW-23, cy 28 ASW-24, cy 30
Commander, Fleet Numerical Weather Central, cy 31
NADC, (2) (C. Bartberger), cys 32, 33
NOL, cy 34
NUC, San Diego, cy 35
NRL, cy 36

Distribution List (continued)

Applied Physics Laboratory, University of Washington, cy 37
Marine Physical Laboratory, Scripps Institution of Oceanography, cy 38
Ordnance Research Laboratory, Pennsylvania State University, cy 39
WHOI, cy 40
Naval Postgraduate School, Monterey, Calif., cy 41
Center for Naval Analyses, cy 42
Committee on Undersea Warfare, National Research Council, cy 43
DDC, cys 44, 45
DDR&E, (S. A. Peterson, G. Cann), cys 46, 47
Naval Electronic Systems Command (PME-124), cy 48
OASN (R&D), cy 49

--- 17 OF 22
-- 1 - AD NUMBER: 905182
-- 2 - FIELDS AND GROUPS: 12/5, 19/9, 20/4
-- 5 - CORPORATE AUTHOR: NAVAL UNDERWATER SYSTEMS CENTER NEWPORT R I
-- 6 - UNCLASSIFIED TITLE: COMPUTER PROGRAMS TO CALCULATE NORMAL MODE
-- PROPAGATION AND APPLICATIONS TO ANALYSIS OF EXPLOSIVE SOUND DATA IN
-- THE BIFI RANGE.
-- 9 - DESCRIPTIVE NOTE: RESEARCH REPT.,
--10 - PERSONAL AUTHORS: KANABIS,WILLIAM G. ;
--11 - REPORT DATE: NOV 06, 1972
--12 - PAGINATION: 105P MEDIA COST: $ 5.35
--14 - REPORT NUMBER: NUSC-TR-4319
--20 - REPORT CLASSIFICATION: UNCLASSIFIED
--33 - LIMITATION CODES: 1

ABSTRACT

This report describes two computer programs that use normal mode theory to predict acoustic propagation and discusses the use of these programs in analyzing explosive data taken in a series of shallow water tests. Program S1441 calculates normal mode propagation in a medium in which the stratification is constant with range; program S1548 computes normal mode propagation when the horizontal stratification is assumed to vary slowly with range. The results of the tests indicate that the introduction of horizontal stratification in program S1548 provides an improved comparison with measured data. Physical explanations are provided for the previously observed minimum in propagation loss at about 125 Hz and for the nonlinear relationship, at certain frequencies, between propagation loss and size of the negative sound gradient observed. In addition, bottom loss was determined in the BIFI (Block Island Fishers Island) range for a wide range of frequencies and thermal conditions.

TABLE OF CONTENTS

TABLE OF CONTENTS (Cont'd)

LIST OF ILLUSTRATIONS

*The figures appear at the end of their respective sections.

REVERSE BLANK

LIST OF TABLES

COMPUTER PROGRAMS TO CALCULATE NORMAL MODE PROPAGATION AND APPLICATIONS TO ANALYSIS OF EXPLOSIVE SOUND DATA IN THE BIFI RANGE

INTRODUCTION

Past studies have shown that normal mode theory can be useful in the prediction of acoustic propagation. This report describes two FORTRAN V computer programs, S1441 and S1548, that can be used for this purpose and describes the use of these programs in the analysis of explosive data taken in a series of shallow water acoustic tests.

Program S1441 (discussed in section 1 of this report) is an extension of a program, written for the Navy Underwater Sound Laboratory* by A. D. Little, Inc. (references 1 and 2), that considers normal mode propagation in a medium in which the stratification is constant with range. In the A. D. Little program, the amplitude distribution of an acoustic signal as a function of depth is determined for a given mode by means of the numerical solution of the acoustic wave equation for given boundary conditions. Program S1441 extends the A. D. Little program by calculating and producing calcomp plots of the following values for any mode, frequency, and velocity profile:

a. Amplitude as a function of depth, and the ray equivalent of any mode

b. Group velocity, phase velocity, excitation pressure, and the angle of incidence of sound waves striking the boundaries

c. Propagation loss as a function of range.

Program S1548 (discussed in section 2 of this report) uses normal mode theory to predict acoustic propagation, in a medium whose velocity profile varies slowly with distance from the acoustic source, over an ocean bottom whose depth and acoustic impedance change slowly with range. It calculates and produces calcomp plots of the following values for given modes at any frequency:

*Now the New London Labaratory of the Naval Underwater Systems Center (NUSC).

a. Amplitude as a function of depth, and the ray equivalent of any mode at given distances from a source

b. Propagation loss as a function of range.

The two programs were used in the analysis of data taken in a series of acoustic tests conducted in Block Island Sound between August 1967 and October 1968. In these tests, referred to as "Experiment 2" in reference 3, propagation loss was measured under a wide range of thermal conditions, using explosives as sound sources. In section 3 of this report, these propagation loss measurements are compared with the values predicted by normal mode theory.

This report is based on material contained in

- W. G. Kanabis, "A Computer Program to Calculate Normal Mode Propagation Over a Flat Homogeneous Ocean Bottom," NUSL Technical Memorandum No. 2211-296-69, 13 October 1969.

- W. G. Kanabis, "A Computer Program to Calculate Normal Mode Propagation in a Medium in Which Stratification Is a Function of Position," NUSL Technical Memorandum No. 2211-11-71, 14 January 1971.

- W. G. Kanabis, "Propagation of Explosive Sound in the BIFI Range," NUSL Technical Memorandum No. 2211-311-70, 9 November 1970.

Section 1

A COMPUTER PROGRAM (S1441) TO CALCULATE NORMAL MODE PROPAGATION OVER A FLAT, HOMOGENEOUS BOTTOM

NORMAL MODE THEORY

Normal mode theory is based on the assumption that at large distances from a source the main part of the sound field consists of standing waves formed by energy striking the boundaries in certain preferred directions.

There are three methods by which the preferred directions and the amplitude distribution of the standing waves may be determined. First, one may find the solution of the wave equation in closed form:

$$\nabla^2 \Phi = \frac{1}{c^2} \frac{\partial^2 \Phi}{\partial t^2}, \tag{1}$$

where Φ is a displacement or a velocity potential and c is the velocity of sound in the medium considered. This is done in reference 4 by integrating equation (1) subject to the boundary conditions in the complex plane and approximating the normal mode solution for the standing waves by the evaluation obtained from the residues in the integration.

Second, one may obtain the solution of equation (1) by direct numerical integration, as done by A. D. Little, Inc., by means of the computer program described in references 1 and 2.

Third, as shown in reference 5, one may consider as the descriptions of the modes those ray paths that undergo total reflection at the boundaries and whose successive upgoing and downgoing rays are in phase.

SOLUTION OF THE WAVE EQUATION BY DIRECT NUMERICAL INTEGRATION

The basis of this program is the rapid evaluation afforded by the use of a high-speed computer.

When equation (1) is solved for Φ, the incremental pressure p is found by definition

$$p = -\rho \frac{\partial^2 \Phi}{\partial t^2} \quad , \tag{2}$$

where Φ is the displacement potential and ρ is the material density at the point considered.

We find that equation (1) is separable in terms of range r and depth z, so that the pressure amplitude can be written as

$$p_a = F(r) \cdot u(z) \tag{3}$$

and a differential equation in terms of $u(z)$ may be obtained:

$$\frac{d^2 u}{dz^2} + \left(\frac{\omega^2}{c^2} - k_r^2 \right) u = 0 \quad , \tag{4}$$

where

ω is the radial frequency,

c is the sound velocity (a function of z),*

$u = u(z)$ is the pressure amplitude distribution as a function of depth, and

k_r is the horizontal wave number

$$\frac{\omega}{c} \sin \theta \quad , \tag{5}$$

in which θ is measured relative to the normal to the ocean bottom and c and θ are measured at the same depth.

The physical picture presented by equation (3) is of a standing wave that has a particular pressure amplitude distribution as a function of depth, $u(z)$, and that travels unchanged in shape as it progresses in the r direction.

Equation (4) may be written as

$$\frac{d^2 u}{dz^2} + f(z) u = 0 \quad , \tag{6}$$

*The z dependence will be dropped henceforth in the notation c.

where

$$f(z) = \frac{\omega^2}{c^2} - k_r^2 \quad . \tag{7}$$

In solving equation (4), we must impose two constraints on any solution: the boundary conditions at the interface between the water and the bottom material and at the water surface. First, because there must be continuity of pressure and particle velocity in the vertical direction at the bottom interface, it is necessary that

$$\frac{1}{u_1}\frac{du_1}{dz} = \frac{\rho_1}{\rho_b}\sqrt{k_r^2 - \frac{\omega^2}{c_b^2}} \quad , \tag{8a}$$

where the terms with subscript b refer to quantities in the bottom material while those with subscript 1 refer to the water side of the interface. Second, since we assume a pressure-release surface at the air-water boundary, then

$$u = 0 \tag{8b}$$

at this surface.

Also, we assume that only "unattenuated" modes compose the sound field. These modes, by definition, involve propagation with energy that strikes the bottom at angles larger than the critical angle so that "total reflection" occurs. Since the critical angle θ_c measured relative to the normal to the interface is given by

$$\sin\theta_c = \frac{c_1}{c_b} \quad ,$$

then

$$\sin\theta > \frac{c_1}{c_b}$$

must hold for all energy striking the bottom. (Naturally, c_b must be greater than c_1 to ensure the existence of a critical angle.)

Since

$$k_r = \frac{\omega}{c} \sin \theta \quad ,$$

using equation (7) and the above inequality, we obtain

$$\left|f(z)\right| < \frac{\omega^2}{c_1^2} - \frac{\omega^2}{c_b^2} \tag{8c}$$

at the bottom interface.

Upon examining equation (6), we can see that a solution of the equation is

$$u(z) = B(z)e^{i\sqrt{f(z)}\, z}$$

for given values of c, ω, and k_r. B is a constant. If f(z) is positive, u(z) is in the form of a sinusoid. This form of solution is obtained for the interference pattern between upgoing and downgoing waves in the water. If f(z) is negative, u(z) is in the form of an exponential. This is a consequence of Sturm's comparison theorem (reference 6).

The value f(z) is negative everywhere in the bottom and in the water at depths that correspond to shadow zones caused by the vertexing of rays that form a mode. Both distributions are a result of the condition of continuity of pressure in the medium. Thus, when there is total reflection at a level (either by vertexing or reflection from a boundary) and the pressure is finite at that level, then at adjacent levels there is a decay (whose rate is determined by the boundary conditions) but not a discontinuous step to zero pressure. Examples of a distribution involving both exponentials are shown in figure 1,* which presents the amplitude distribution as a function of depth, and in figure 2, which presents the ray equivalent of the mode. This concept of the ray equivalent is discussed in more detail in the next subsection of this report. In figure 2, it is seen that the ray equivalent of the normal mode vertexes at a depth of 48 ft; therefore, in figure 1, the pressure amplitude distribution is in the form of an exponential between the surface of the ocean and a depth of 48 ft. It can also be seen in figure 1 that the pressure amplitude distribution in the bottom is in the form of an exponential.

*Figures 1 through 16 appear at the end of this section, pages 23 through 33.

To integrate equation (6) numerically, formulas relating u_{n+1} and its derivative u'_{n+1} with the quantities u_n and u'_n must be obtained (the subscripts signify the depth at which the quantities are calculated). This is done by writing a Taylor series for u_{n+1} and u'_{n+1} and retaining all terms of the third order or less. The details of this procedure are given in references 1 and 2; the results are summarized in equations (9) and (10):

$$u_{n+1} = \frac{\left(1 + \frac{h}{3} f_n\right) u_n + h u'_n}{1 + \frac{h^2}{6} f_{n+1}} \tag{9}$$

$$u'_{n+1} = \frac{\left(1 - \frac{h}{3} f_{n+1}\right) u'_n - \frac{h}{2}\left(f_n + f_{n+1} - \frac{h^2}{6} f_n f_{n+1}\right) u_n}{1 + \frac{h^2}{6} f_{n+1}}, \tag{10}$$

where

h is the increment between level n and level $n + 1$ and

f_n and f_{n+1} are the values of $f(z)$ at n and $n + 1$, respectively.

Equations (9) and (10) are recursion relationships that permit calculation of u and u' at all levels in the water if the given values for u_1 and u'_1 are the values of u and u' just above the bottom.

Since we are interested in normalized values of u over the water column, we can select u_1 to be any arbitrary value ($u_1 = 1$ is convenient). For an arbitrary value of the horizontal wave number k_r that is restricted by equation (8c), we can evaluate u'_1 by equation (8a). Then we can determine u for all levels by using equations (9) and (10) repeatedly. If the value of k_r corresponds to a mode, equation (8b) will be satisfied at the surface of the water. Each mode has, at most, one such solution for a given frequency. There is a low cut-off frequency for each mode, so that at frequencies below the cut-off frequency, equation (8b) can not be satisfied.

After finding the amplitude distribution of a mode, we must define the mode number. For a finite frequency, the mode number is equal to the number of nodes in the amplitude distribution. Thus, the first mode has a node only at the surface. A representation of the amplitude distribution of the first mode is shown in figure 1.

THE RAY EQUIVALENT

Corresponding to the definition of a mode discussed above is a more physical approach in which the ray equivalent of the solution to the wave equation is considered. Additional information concerning this approach is contained in references 4, 5, 7, 8, and 9.

For simplicity, let us consider a two-layer medium of constant water depth H, density ρ_1, and sound velocity c_1, lying over an infinite bottom of density ρ_2 and sound velocity c_2, as shown in figure 3. At large ranges from a point source, we may consider sound to be propagated by plane waves. It is clear from figure 3 that for certain waves whose direction is defined by an angle θ, there will be constructive interference between that wave and a plane wave undergoing one more bottom and surface reflection. For constructive interference to exist, the phase difference between points A and B of figure 3 must be $2(n-1)\pi$ degrees; i.e., the phase difference must satisfy the equation

$$\frac{2\pi}{\lambda_n}\left[\frac{H}{\cos\theta} + \frac{H}{\cos\theta}\cos 2\theta\right] - \epsilon - \pi = 2(n-1)\pi$$

or

$$\frac{2\pi}{\lambda_n}\left[2H\cos\theta\right] - \epsilon - \pi = 2(n-1)\pi \quad , \tag{11}$$

where λ_n is the wavelength of the preferred mode, ϵ is the phase change undergone by a plane wave upon bottom reflection, n is the mode number, and the phase change upon reflection from the water surface is assumed to be $-\pi$. If the sound velocity in the water layer varies with depth, the first term of equation (11) would be different from that given above; however, the discussion below applies to either case.

If, for a given wavelength λ_n and angle θ, there is constructive interference between plane waves suffering different numbers of bottom and surface reflections, then propagation consists of a series of upgoing and downgoing waves, as shown in figure 4. The left-hand term of equation (11) is the phase change, 2Δ, undergone in the z direction when a ray makes a surface-bottom-surface cycle. For finite frequencies, $\pi > \epsilon \geq 0$ as $\pi/2 > \theta \geq \theta_c$. Therefore, the phase change, Δ, undergone in the z direction over the water depth is limited by

$$\Delta < n\pi \quad . \tag{12}$$

The pressure is zero at the surface, the phase change upon reflection is $-\pi$, and the direction of propagation is reversed upon reflection from the surface. Therefore, the sound field in the vertical direction is the sum of two sine waves representing the upgoing and downgoing waves in the z direction. These waves are shown for the first two modes in figure 5. Because of equation (12), the number of nodes in this amplitude distribution is equal to the mode number. Thus, there is a correspondence between the definitions of mode number in the solution of the wave equation and the ray equivalent solution.

Now let us consider the procedure actually used in the computer programs to determine the ray equivalent. When the wave equation is solved numerically, values of $f(z)$ are obtained; $f(z)$ is given in equation (7) by

$$f(z) = \frac{\omega^2}{c^2} - k_r^2 \quad , \tag{13}$$

where k_r is given in equation (5) by

$$k_r = \frac{\omega}{c} \sin \theta \quad . \tag{14}$$

Therefore, given positive $f(z)$, one can determine, from equations (13) and (14), the cosine of the angle of inclination of the equivalent ray as a function of z:

$$\cos \theta = \frac{c}{\omega} \sqrt{f(z)} \quad . \tag{15}$$

If the ray between two points z_1 and z_2 is continuous, then $\Delta z = z_1 - z_2$ may be given in terms of the horizontal distance $\Delta R = R_1 - R_2$ and one particular value of the $\tan \theta$ over the path. This relationship is

$$\frac{\Delta R}{\Delta z} = \tan \theta = \frac{c \sin \theta}{c \cos \theta} = \frac{c}{c_v \cos \theta} \quad ,$$

where c_v, the vertex velocity, equals $c/\sin \theta$.

If the value of θ does not vary appreciably between z_1 and z_2, then we can approximate $\tan \theta$ by

$$\tan \theta = \frac{\tan \theta_1 + \tan \theta_2}{2} \quad ,$$

where θ_1 and θ_2 are taken at $z = z_1$ and z_2, respectively. Thus (reference 10),

$$\frac{\Delta R}{\Delta z} \approx \frac{1}{c_v} \frac{c_1 + c_2}{\cos \theta_1 + \cos \theta_2} , \tag{16}$$

where

c_v is the vertex velocity,

c_1, c_2 are the sound velocities at z_1 and z_2, respectively, and

θ_1, θ_2 are the angles relative to the normal of the ray at z_1 and z_2, respectively.

Thus, given values of $f(z)$, one can construct a ray equivalent. If vertexing takes place, the depth z_v at which it occurs is the level whose value of sound velocity equals c_v.

The ray equivalent has a counterpart in the analysis of sound propagation using ray theory. In ray theory, rays corresponding to a continuum of angles of propagation are summed at the receiver. Most groups of rays effectively cancel each other and contribute little to the sound field. This leaves a discrete number of rays that sum constructively to form the sound field. These rays correspond to the ray equivalent of modes that compose the sound field. According to ray theory, the rays that contribute to the sound field are determined by interference effects, and hence, as in normal mode theory, the geometry of the dominant rays changes as a function of frequency. Also as in normal mode theory, the sum of these rays is influenced by the source-receiver geometry. However, there are two factors that limit the correspondence between normal mode and ray theory. First, in ray calculations the sound field is often obtained by simply adding all rays without regard to their phase. Second, the geometrical approximation limits the validity of ray tracing. This limitation can produce differences not only in the theoretical pressure field but also in the ray representations in ray tracing and normal mode methods.

If the velocity profile assumed in the calculations contains only a monotonic variation in sound velocity with depth (as, for example, in figure 6) or describes a simple sound channel, a relatively simple ray equivalent obtains (as in figure 2). However, let us consider the ray equivalent associated with the more complicated velocity profile shown in figure 7. This profile describes two sound channels at depths of about 60 and 120 ft, respectively. The associated ray equivalent of

mode 1 at a frequency of 200 Hz is shown in figure 8. It can be seen that the ray equivalent consists of two traveling waves, one for each of the two sound channels in the water column. This phenomenon of wave "leakage" through a layer is described in reference 11.

PHASE VELOCITY AND GROUP VELOCITY

The phase velocity V_p is given by the relationship

$$V_p = \frac{c}{\sin \theta} \quad , \tag{17}$$

where θ is the direction of propagation of a plane wave where the sound velocity has a value c. Equation (17) can also be written

$$V_p = c_v \quad , \tag{18}$$

where c_v is the vertex velocity.

The group velocity V_g can be considered from two points of view. First, V_g may be considered as a measure of the speed of propagation in the horizontal direction of a number of frequencies in a band $\Delta\omega$ centered about ω. V_g may be given by (reference 12)

$$V_g = \frac{\Delta\omega}{\Delta\kappa} \tag{19}$$

or by (reference 11)

$$\frac{V_g}{c} = \frac{V_p}{c} + (\kappa H) \frac{d\left(\frac{V_p}{c}\right)}{d(\kappa H)} \quad , \tag{20}$$

where H is the water depth.

It can be seen that this approach to the calculation of group velocities involves the calculation of derivatives, which is not desirable in a computer program since it produces inaccuracies and makes it necessary to obtain an unnecessarily large number of values of phase velocity as a function of frequency.

Second, Tolstoy (reference 13) has used a general theorem by Biot (reference 14) to show the equivalence of V_g in equations (19) and (20) to the rate of energy transport in the horizontal direction. The group velocity is given by

$$V_g = \frac{1}{V_p} \frac{\nu}{\sigma} \quad , \tag{21}$$

where

$$\nu = \int_{-\infty}^{+\infty} \rho \phi^2 \, dz \tag{22}$$

$$\sigma = \int_{-\infty}^{+\infty} \frac{\rho}{c^2} \phi^2 \, dz \quad , \tag{23}$$

in which ρ and c are, respectively, the density and sound velocity at z, and ϕ is given in the equation

$$\Phi = \phi(z) e^{i(\pm \alpha x - \omega t)} \tag{24}$$

in which Φ is the displacement potential in equation (1).

Since, by equation (2),

$$p = -\rho \frac{\partial^2 \Phi}{\partial t^2} ;$$

and u is the value of pressure (normalized to maximum amplitude) as a function of z; then, by equations (2) and (24),

$$u \propto \rho \varphi \quad , \tag{25}$$

where φ is the normalized value of ϕ. Thus, by equation (25) we can obtain φ once u is known since we are interested only in the normalized values of u and φ for given ω.

Given ρ_1 in the water, ρ_b in the bottom, and u normalized to maximum pressure amplitude; to obtain φ, the normalization of ϕ, we first obtain

$$\varphi_{1,\, u_u(z)} = \frac{u(z)}{\rho_1}$$

$$\varphi_{b,\, u_u(z)} = \frac{u(z)}{\rho_b} \quad , \tag{25a}$$

where 1 and b signify water and bottom, respectively, and u_u signifies unnormalized. Since the maximum value of u lies in the water and ρ_b is greater than ρ_1 and because $u(z)$ is normalized with respect to maximum amplitude, we multiply both expressions in equation (25a) by ρ_1 to obtain φ normalized with respect to maximum amplitude, so that

$$\varphi_1 = u(z)$$

$$\varphi_b = u(z)\ \rho_1/\rho_b \quad . \tag{25b}$$

The normalized value for ϕ is represented by φ and may be used in place of ϕ in equations (21) through (23).

EXCITATION PRESSURE AND PROPAGATION LOSS

The sound field produced by a simple harmonic source in a two-layered halfspace (figure 9) with a free surface at $z = 0$ and the boundary between two fluids at $z = H$ is given by the solution of equation (1). The solution is given in reference 12 by

$$\Phi = -i\ \frac{1}{\sqrt{r}}\,\frac{1}{\omega^2} \sum_m P_m e^{-i(\kappa_m r - \omega t - \pi/4)} \quad , \tag{26}$$

where

r is the horizontal range,

ω is the radial frequency,

m is the mode number,

κ_m is the horizontal wave number k_r for mode m, and

$$P_m = p_m\,\frac{1}{\rho_s}\,\varphi_m(z)\ \varphi_m(z_o) \quad , \tag{27}$$

in which

ρ_s is the water density at the source,

$\varphi_m(z)$ is the normalized displacement potential, a function of depth,

z_o is the source depth,

z is the receiver depth, and

m is the mode number.

The notation p_m is the excitation function given by

$$p_m = 2\pi\,(\rho_o c_o S)^{1/2}\,\frac{\rho_o}{\nu_m\sqrt{\kappa_m}}\quad , \tag{28}$$

where

ρ_o is the water density at the source,

c_o is sound velocity at the source,

S is the power output of an omnidirectional source,*

κ_m is the horizontal wave number, and

$$\nu_m = \int_{-\infty}^{+\infty} \rho\varphi_m^2\,dz\quad , \tag{29}$$

where φ_m is the normalized displacement potential.

If the source produces a unit sound pressure level, then the following relationship (reference 11) must be satisfied:

$$4\pi\left(\frac{Sc_o\,\rho_o}{2\pi}\right)^{1/2} = 1\quad . \tag{30}$$

Substituting equation (30) into equation (28), we obtain for the excitation pressure

*This quantity is represented by Π in reference 12.

$$P_m = \frac{\rho_o (2\pi)^{1/2}}{2 \nu_m \sqrt{\kappa_m}} \quad . \tag{31}$$

The excitation pressure is the sound pressure amplitude produced by a source that generates a unit pressure level at unit range when both source and receiver are at antinodes. It is essentially a measure of the source level of mode m for a unit source.

From equation (26) we determine the pressure amplitude characteristics of the sound field, and this amplitude, p_a, is given by

$$p_a = \frac{\rho_o}{\sqrt{r}} \left\{ \left[\sum_m P_m \cos \left(\kappa_m r - \frac{\pi}{4} \right) \right]^2 + \left[\sum_m P_m \sin \left(\kappa_m r - \frac{\pi}{4} \right) \right]^2 \right\}^{1/2} \quad . \tag{32}$$

Since p_a is the sound pressure amplitude at range r from a generator with unit source level, the value of propagation loss L_r at range r for given depths of source and receiver is

$$L_r = -20 \log p_a \quad . \tag{33}$$

It can be seen from equations (27) and (32) that, once φ_m is known, one can easily determine the effect of the source and receiver depths on the sound field at a given range. If the source depth, z_o, is such that $\varphi_m(z_o)$ is a node, the mode m will be suppresed in the sound field; conversely, if z_o is such that $\varphi_m(z_o)$ is an antinode, the sound field of mode m will be greater than it would be at depths for which $\varphi_m(z)$ is less than $\varphi_m(z_o)$. The same relationships apply to the effect of the receiver depth upon the sound field.

It can also be seen from equations (27), (28), and (29) that the pressure amplitude does not depend upon the normalization of $\phi(z)$.

For small attenuations of individual modes, equation (32) may be rewritten to include, for mode m, losses at the boundaries as a function of range and losses caused by absorption of sound energy in the water, so that

$$p_a = \frac{\rho_o}{\sqrt{r}} \left\{ \left[\sum_m P_m 10^{(-D_m r/20 - ar/20)} \cos \left(\kappa_m r - \frac{\pi}{4} \right) \right]^2 + \left[\sum_m P_m 10^{(-D_m r/20 - ar/20)} \sin \left(\kappa_m r - \frac{\pi}{4} \right) \right]^2 \right\}^{1/2} , \tag{34}$$

where D_m* is a measure of bottom loss in decibels of loss per unit increment of range and a is the attenuation coefficient given in reference 15 by

$$a \frac{dB}{kyd} = \frac{0.1 f^2}{1 + f^2} + \frac{40 f^2}{4100 + f^2} ,$$

where f is the frequency in kilohertz.

DESCRIPTION OF PROGRAM S1441

Program S1441 uses normal mode theory to predict acoustic propagation over a flat, homogeneous ocean bottom. The program may be used with any of three options, each of which provides different information about the sound field in a medium for a given frequency, velocity profile, and mode number. The three options provide, as output, the following calcomp plots.

- Option A produces two types of plots for each mode analyzed. One type gives pressure normalized to the maximum amplitude as a function of depth, and the second gives the ray equivalent of the mode.

- Option B produces two types of plots for each mode. One type gives three quantities: phase velocity, group velocity, and excitation pressure as a function of frequency, and the second gives the angles of incidence of energy at the two boundaries as a function of frequency.

- Option C produces a plot of propagation loss versus range for any combination of modes. Plots can be produced for any source depth, receiver depth, and frequency.

Each option provides two plots of the velocity profile: the first plot (figure 6) shows the sound velocity in both the water and the bottom; the second (figure 10) shows the sound velocity in the water in greater detail through the use of an expanded velocity scale.

The format of the input data is presented in table 1. Card group 2 in the table shows the routine for selecting option A, B, or C. The mechanics of the individual options are described below.

*D_m must be specified by the user of the program.

Table 1. Input Data for Program S1441

Card Group	Amount of Cards	Format	Input Parameter	Columns	Data
1	1	20A4		1-80	Heading on each page of output.
2	1	I10	NUMV	1-10	Number of velocities in profile.
		F10.0	VEL 1	11-20	Velocity at origin of calcomp plot of velocity profile (ft/sec)
		4I10	IVOP	21-30	If IRP = 0, when IVOP = 0, option A when IVOP = 1, option B
			IRP	31-40	When IVOP = 1, if IRP = 1, option C
			IVRP	41-50	When IVRP = 1, velocity profile not plotted When IVRP = 0, profile plotted.
			IEX	51-60	Changes increment of k_r (horizontal wave number) by a factor of 10^{-IEX}. Values from 0 to 10.
3	1	5F10.3	ZM	1-10	Water depth (ft)
			CB	11-20	Velocity of sound in the bottom (ft/sec)
			RO	21-30	Density of water (grams/cm^3)
			RB	31-40	Density of bottom (grams/cm^3)
			FSC	41-50	Maximum depth plotted (200 x FSC in all velocity profiles and in plots in option A)
4	NUMV cards	2F10.3	Z(I)	1-10	Height above bottom at which sound velocity is C(I).
			C(I)	11-20	Velocity of sound (ft/sec) at Z(I).
			I = 1, 2, ..., NUMV in order of increasing Z		
5	1	I10	N	1-10	Number of intervals into which depth is to be subdivided in integration of differential equations.

Table 1 (Cont'd). Input Data for Program S1441

Card Group	Amount of Cards	Format	Input Parameter	Columns	Data
5		2F10.3	UM FQ	11-20 21-30	Maximum value of u(z) Frequency (Hz)
6	1	4I10 ↓	ISFQ IEFQ NMOD INCF	1-10 11-20 21-30 31-40	Highest frequency to be analyzed Lowest frequency to be analyzed Number of modes analyzed. Mode number analyzed = 1, 2, ..., NMOD. Decrement in frequency from ISFQ to IEFQ. (In options A and C, ISFQ = IEFQ = FQ. Option B range of frequencies is selected by ISFQ, IEFQ, INCF.)
7 (for option C)	1	4I10 ↓	IRST IREN IRIC NPS 3F10.3 ↓	1-10 11-20 21-30 31-40 41-50 51-60 61-70	Shortest range (ft) at which propagation loss versus range will be plotted. Longest range (ft) at which propagation loss will be plotted. Increment in range to be plotted (ft). Number of propagation loss versus range plots. Source depth (ft) Receiver depth (ft) Increment of range on the calcomp plot per division in nautical miles
8 (for option C)	the smallest integer $\geq \frac{NMOD}{4}$	4F10.5	DD(J)	1-40	Loss at boundaries (dB/ft) as a function of range for the mode J. J = 1, 2,..., NMOD where NMOD is the number of modes analyzed.

Table 1 (Cont'd). Input Data for Program S1441

Card Group	Amount of Cards	Format	Input Parameter	Columns	Data
9 (for option C)	Card a = 1	110	NMS	1-10	Number of modes to be summed in the plot of propagation loss versus range (NM $\leq$ NMOD)
	Card(s) b = the smallest integer $\geq \frac{NMS}{6}$	6110	MDS(J)	1-60	J = 1, 2, ..., NMS The values of MDS(J) are the mode numbers of the modes to be summed in the propagation loss versus range plots. MDS(J) $\leq$ NMOD
(Cards a and b form a set. There is a set of cards for each plot in option C.)					

OPTION A

In option A, first the numerical solution to equation (6) is found, subject to the boundary conditions given by equations (8a), (8b), and (8c); then the ray equivalent of the solution is obtained.

For a given inputted velocity profile (card group 4, table 1), the sound velocity is calculated at N levels (card group 5) equispaced between the surface and bottom by interpolation.

The value of the horizontal wave number k_r is varied subject to the restrictions given in equation (8c). For each value of k_r, the value of u(z) is calculated over the water column of N equispaced levels by means of equations (9) and (10). The values of u(z) are restricted so that u(z) never exceeds UM (card group 5). In addition, mode m must have m zero crossings. After u(z) is calculated for a given k_r value, k_r is incremented by Δk_r so as to obtain the smallest possible value of u at the surface. If the conditions necessary for the existence of a given mode can not be met, the statement "No Mode Found" is printed out.

Once u(z) has been found for a given mode, the ray equivalent can be found by using equation (16). Sample calcomp plots of the amplitude distribution normalized to maximum amplitude and of the ray equivalent are shown in figures 1 and 2.

Where there is a large negative velocity gradient, high-frequency sound is trapped near the ocean bottom. Under these circumstances, it is difficult to obtain a good approximation of the boundary condition at the surface, and one has to decrease the value by which k_r is incremented. This is done by using a large value (up to about 10) of IEX (card group 2, table 1). A large value of IEX will increase the program time since it decreases the increment of k_r by a factor of 10^{-IEX}. Under most circumstances, however, an IEX value of zero is adequate.

OPTION B

In option B, group velocity, phase velocity, excitation pressure, and angle of incidence at the boundaries relative to the normal to the boundary are found over any frequency range (card group 6, table 1). The group velocity for a given frequency is determined by equations (21), (22), and (23); phase velocity by equation (18); excitation pressure by equation (31); and angle of incidence at the boundaries by equation (15). If the ray vertexes before striking a boundary, the angle of incidence is given as 90°. Sample plots obtained from option B are shown in figures 11 and 12.

OPTION C

In option C, propagation loss for a source level at a 1-yd reference is obtained as a function of range for any given frequency and combination of modes. Propagation loss may be calculated by equations (32) and (33). The ranges over which loss is plotted and the source and receiver depths are inputted by card group 7. Values of D_m are inputted by card group 8, and the modes that make up the sound field are inputted by card group 9. A sample calcomp plot is shown in figure 13.

The program was evaluated in two ways. First, a test case was run and the results compared to corresponding calculations obtained from two equivalent procedures described in references 16 and 17. Second, the convergence of the numerical procedure used in solving the wave equation was examined for many cases, and the resulting limitations on the program were noted. The test case used for comparison is illustrated in figure 14, which gives the velocity profile and the assumed sound velocity in the homogeneous semi-infinite bottom.

Since each mode is defined by a unique horizontal wave number κ_m, the values of κ_m obtained by each procedure were compared. Such a comparison is shown in table 2. In the table, the values of κ_m obtained by Bartberger and Ackler (reference 17) are compared with the values obtained by using the method described in this report. It can be seen that the results agree to the fourth decimal place and, hence, tend to support the validity of the two procedures. Furthermore, similar good agreement was obtained for this test case using the Fast Field Program (reference 16).

Table 2. Comparison of Calculated κ_m

Mode	κ_m (Kanabis)	κ_m (Bartberger and Ackler)
1	3.78104	3.78105
2	3.77896	3.77896
3	3.77725	3.77725
4	3.77574	3.77575
5	3.77436	3.77437
6	3.77309	3.77309
7	3.77186	3.77187
8	3.77063	3.77065
9	3.76932	3.76933
10	3.76782	3.76784
11	3.76617	3.76618

Another theoretical result tested was the calculation of propagation loss as a function of range for the test case. The comparison of results with those of DiNapoli (reference 15) is shown in figures 15 and 16. It can be seen from the figures that the interference patterns are virtually identical at all ranges except those very near the source. The differences near the source result from the inclusion by DiNapoli of "attenuated" modes in the sound field. These attenuated modes contribute to the field significantly at short ranges but are attenuated rapidly so that they are usually insignificant at longer ranges. The procedure described in this report considers only "unattenuated" modes, i.e., modes whose angles of incidence exceed the critical angle so that there is "total" reflection at the boundaries. The only major discrepancy in the results lies in the absolute levels of loss calculated. For this example, the results of our program consistently show 3 dB less loss than the values obtained from the two other programs used in the comparison. The source of the difference probably lies in the establishment of a unit source level at unit distance in our procedure.

It was found that the numerical procedure converges in practically all cases considered. However, at high frequencies, and for extremely irregular velocity profiles, the procedure may encounter difficulty in converging. This problem can probably be overcome in most cases at the expense of increased computer time, e.g., by narrowing the interval between grid points over the water column (by increasing N given in card group 5, table 1).

It is difficult to estimate meaningful computer execution times because these times are sensitive to a large number of input parameters. However, the order of magnitude of time for a typical case involving any one of the three options and a moderate number of incremental parameters is one minute on the Univac 1108.

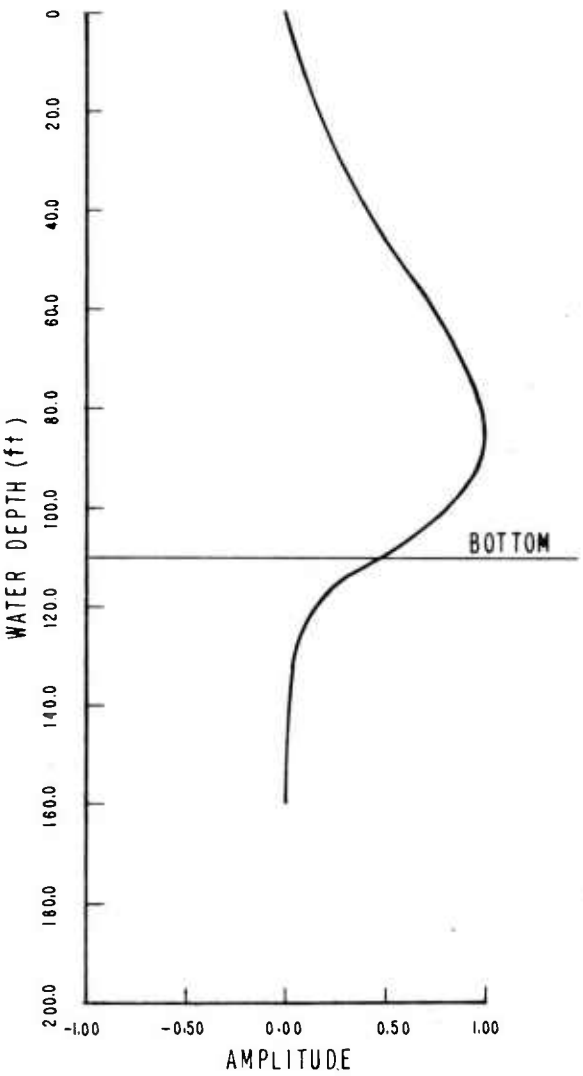

Figure 1. Amplitude versus Depth, Frequency 282 Hz, Mode 1

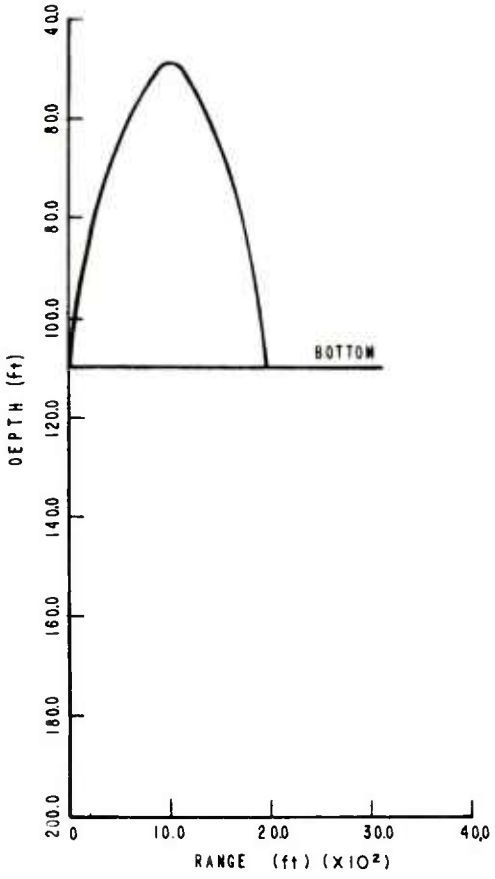

Figure 2. Ray Equivalent, Frequency 282 Hz, Mode 1

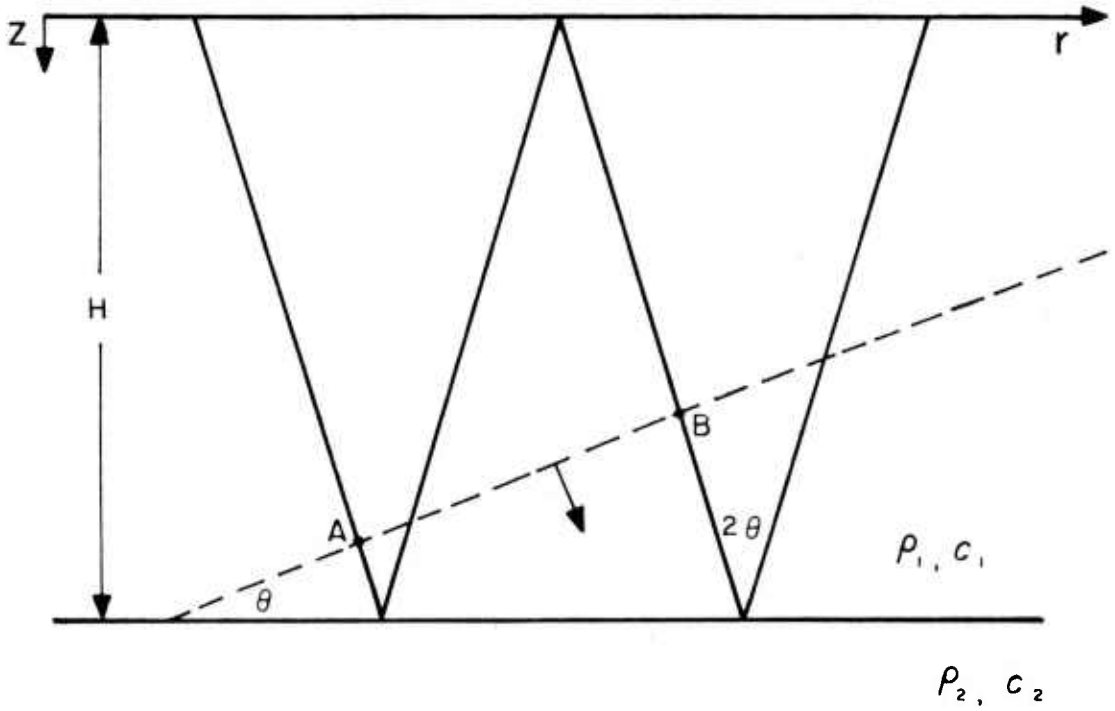

Figure 3. Path of Reflected Waves That Interfere

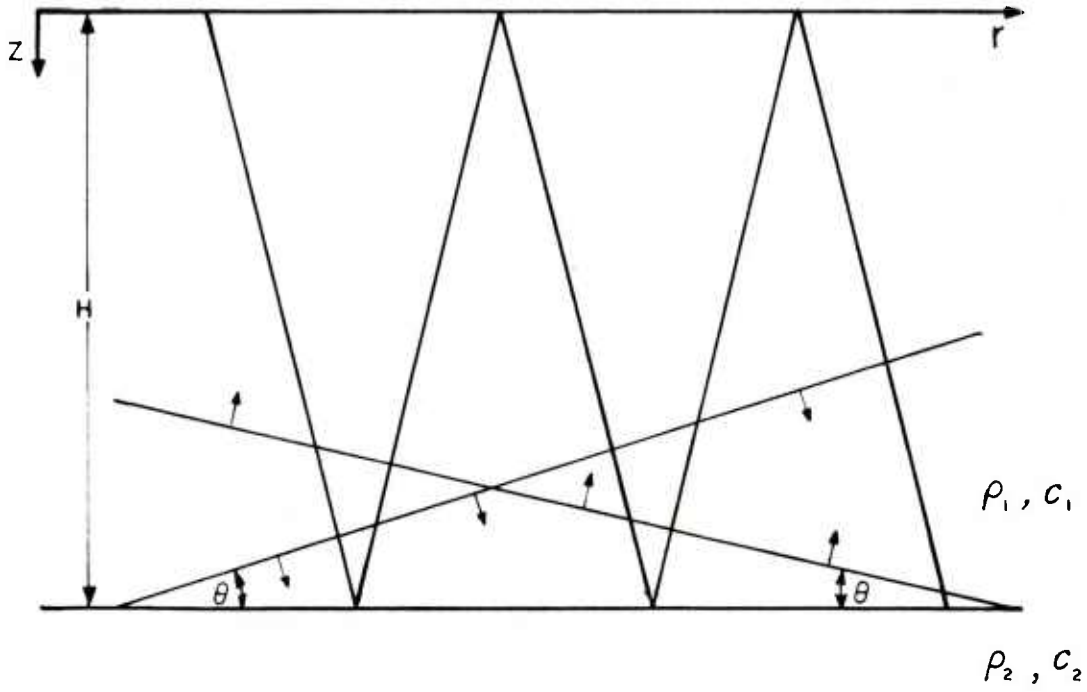

Figure 4. Downgoing and Upgoing Waves

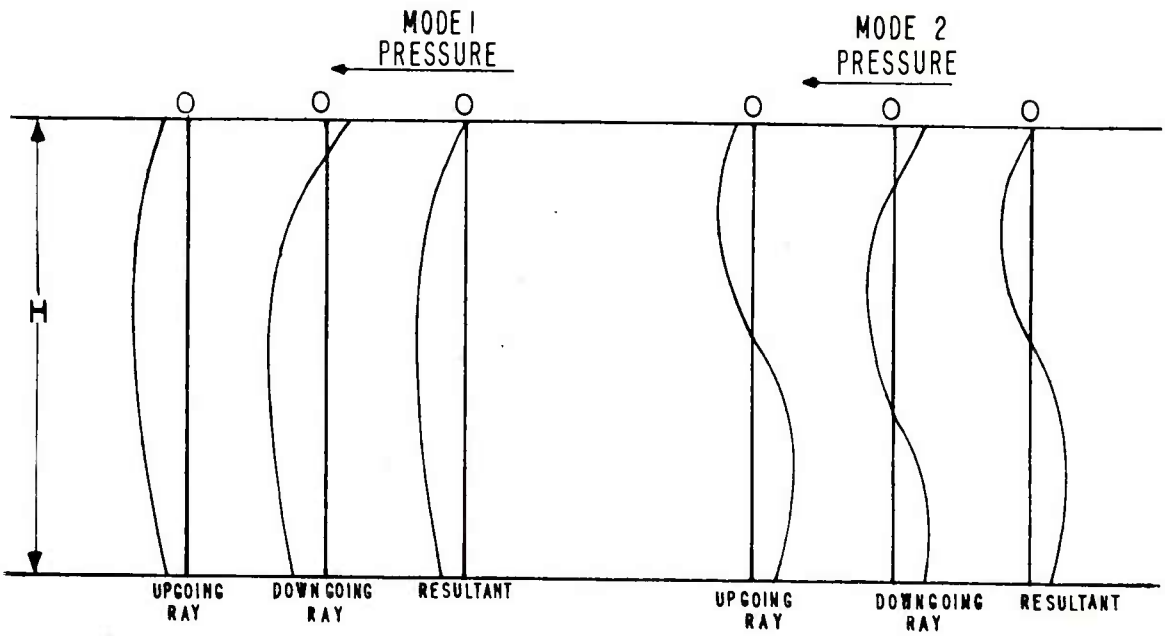

Figure 5. Pressure of Upgoing and Downgoing Rays and the Resultant

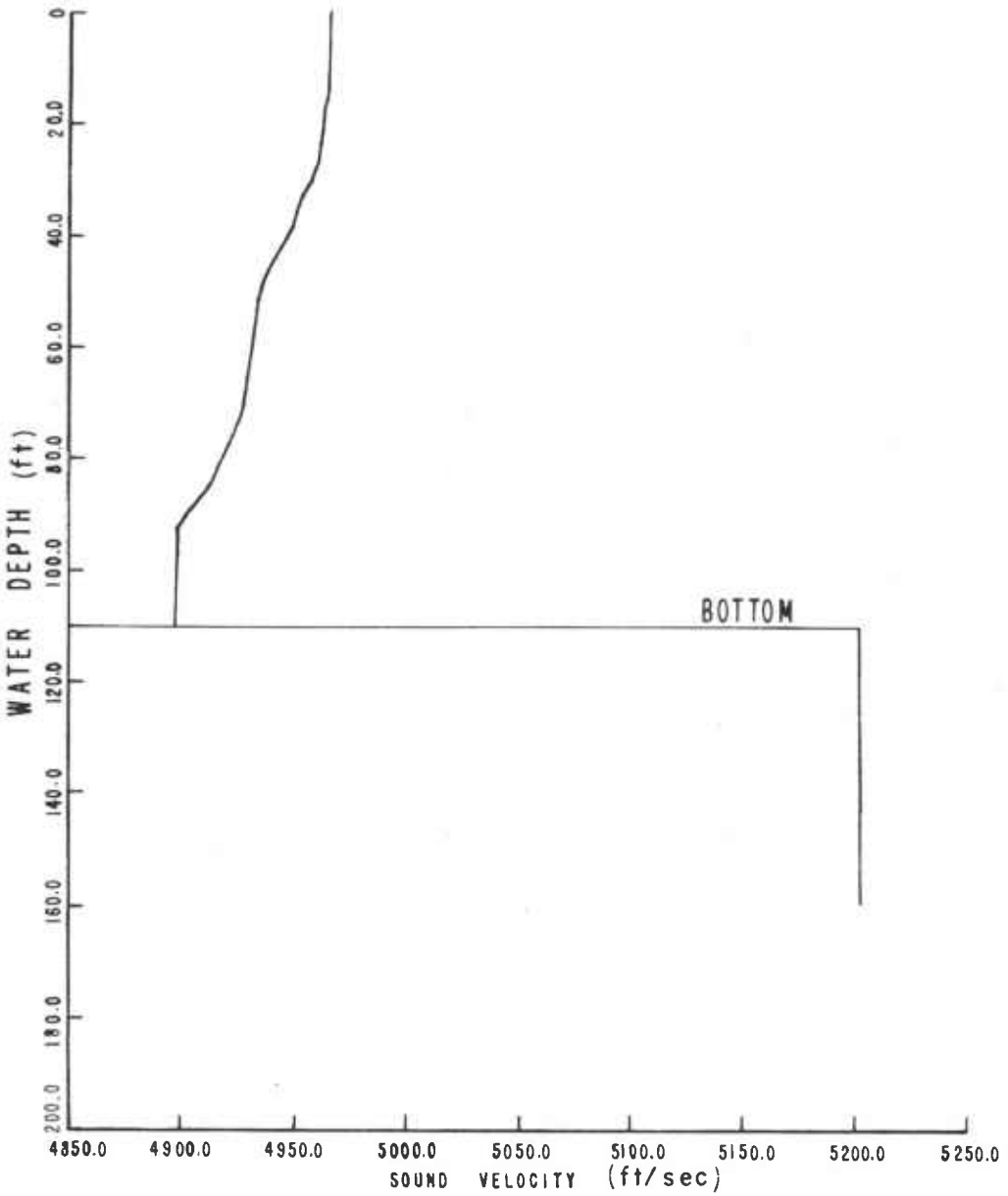

Figure 6. Velocity Profile, Simple Variation

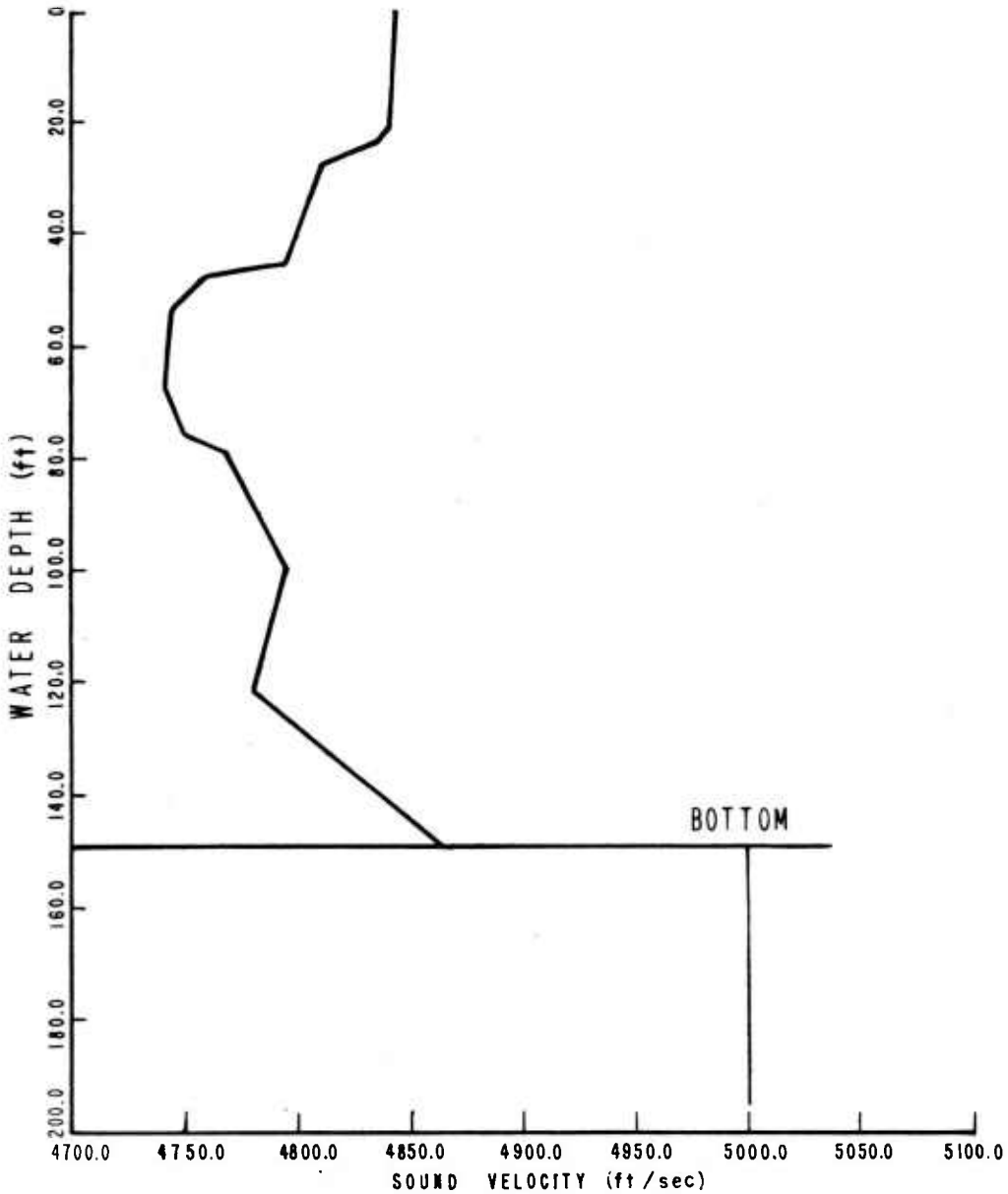

Figure 7. Velocity Profile, Complex Variation

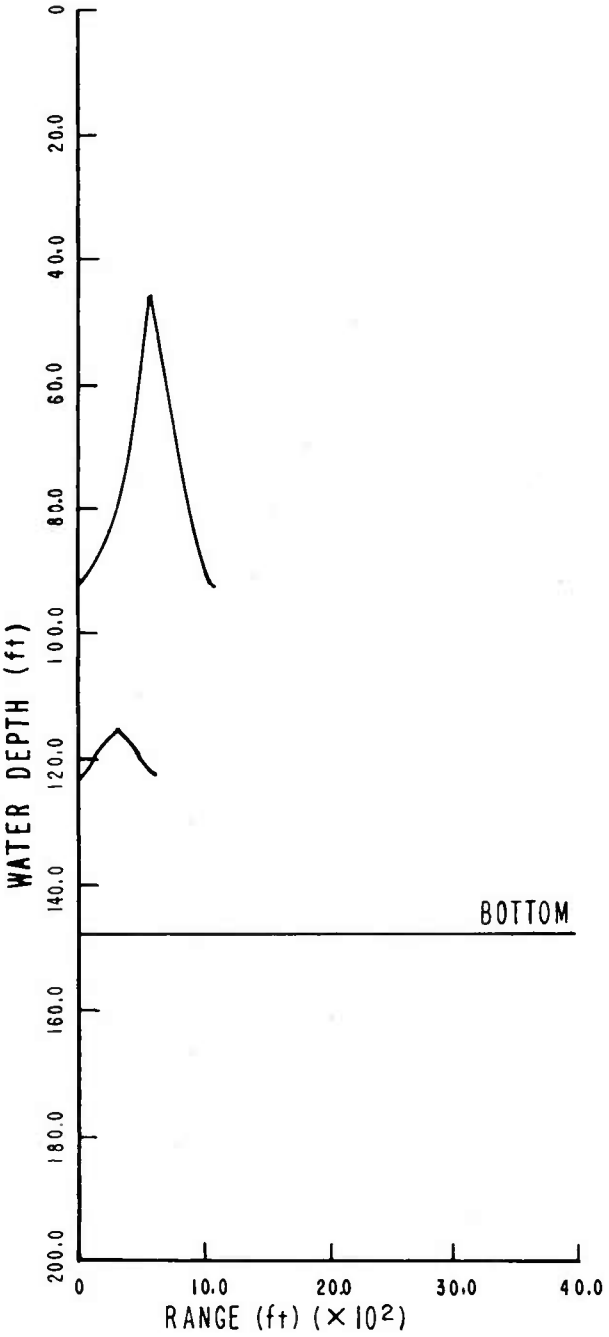

Figure 8. Ray Equivalent, Frequency 200 Hz, Mode 1

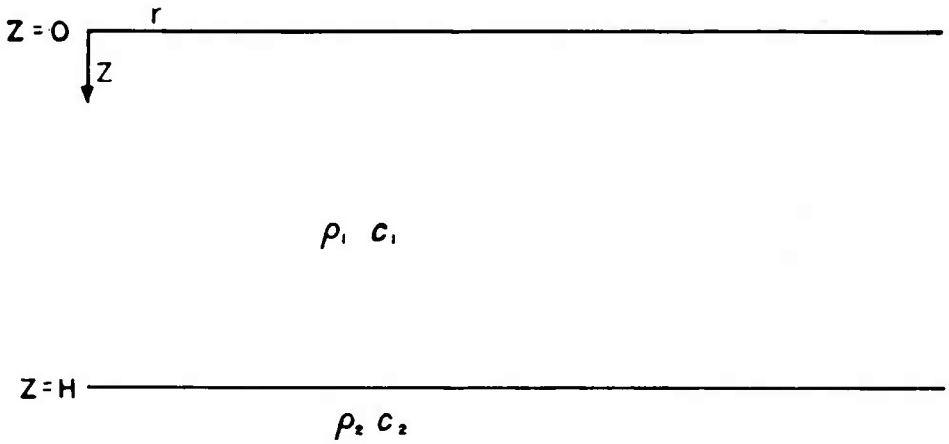

Figure 9. Two-Layered Half-Space

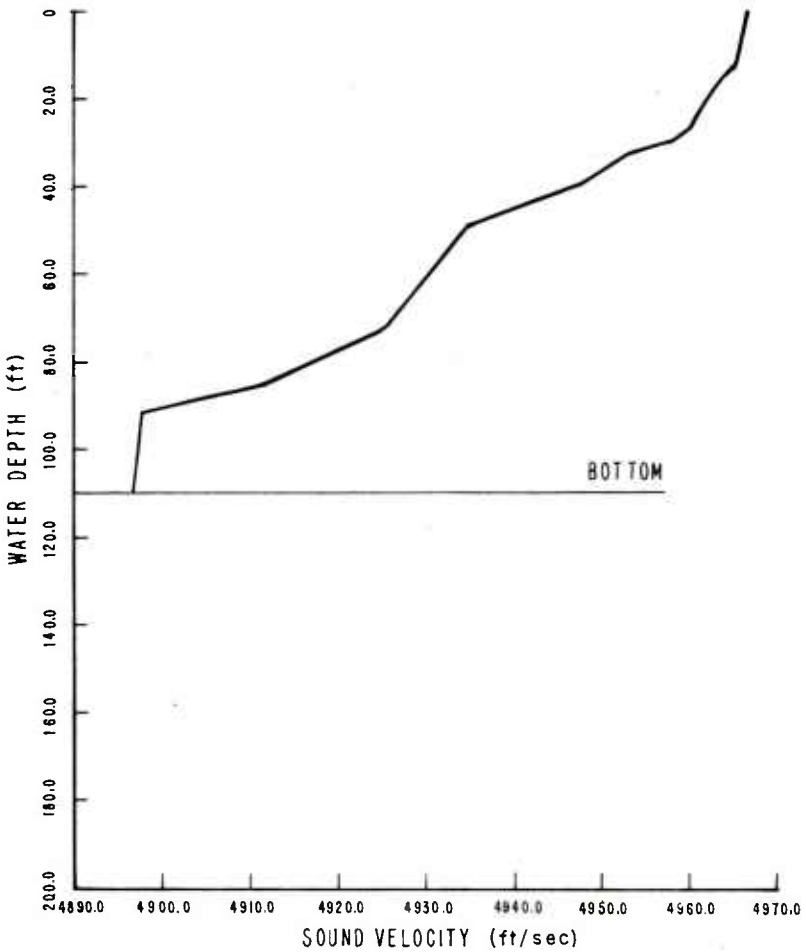

Figure 10. Expanded Velocity Profile

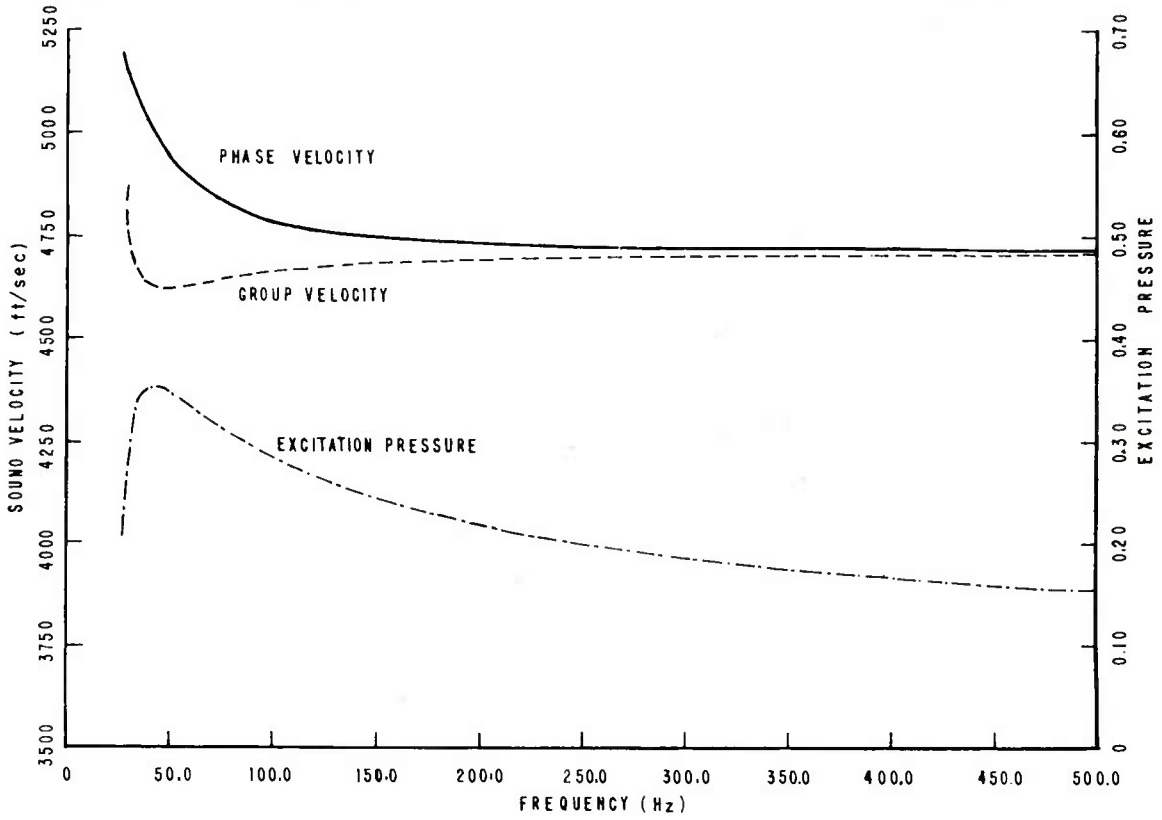

Figure 11. Sound Velocity and Excitation Pressure versus Frequency, Mode 1

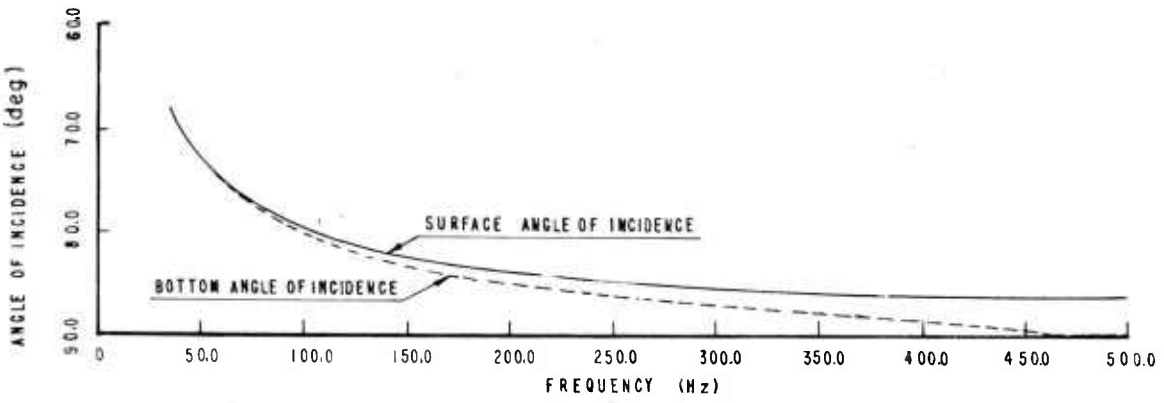

Figure 12. Angle of Incidence versus Frequency, Mode 1

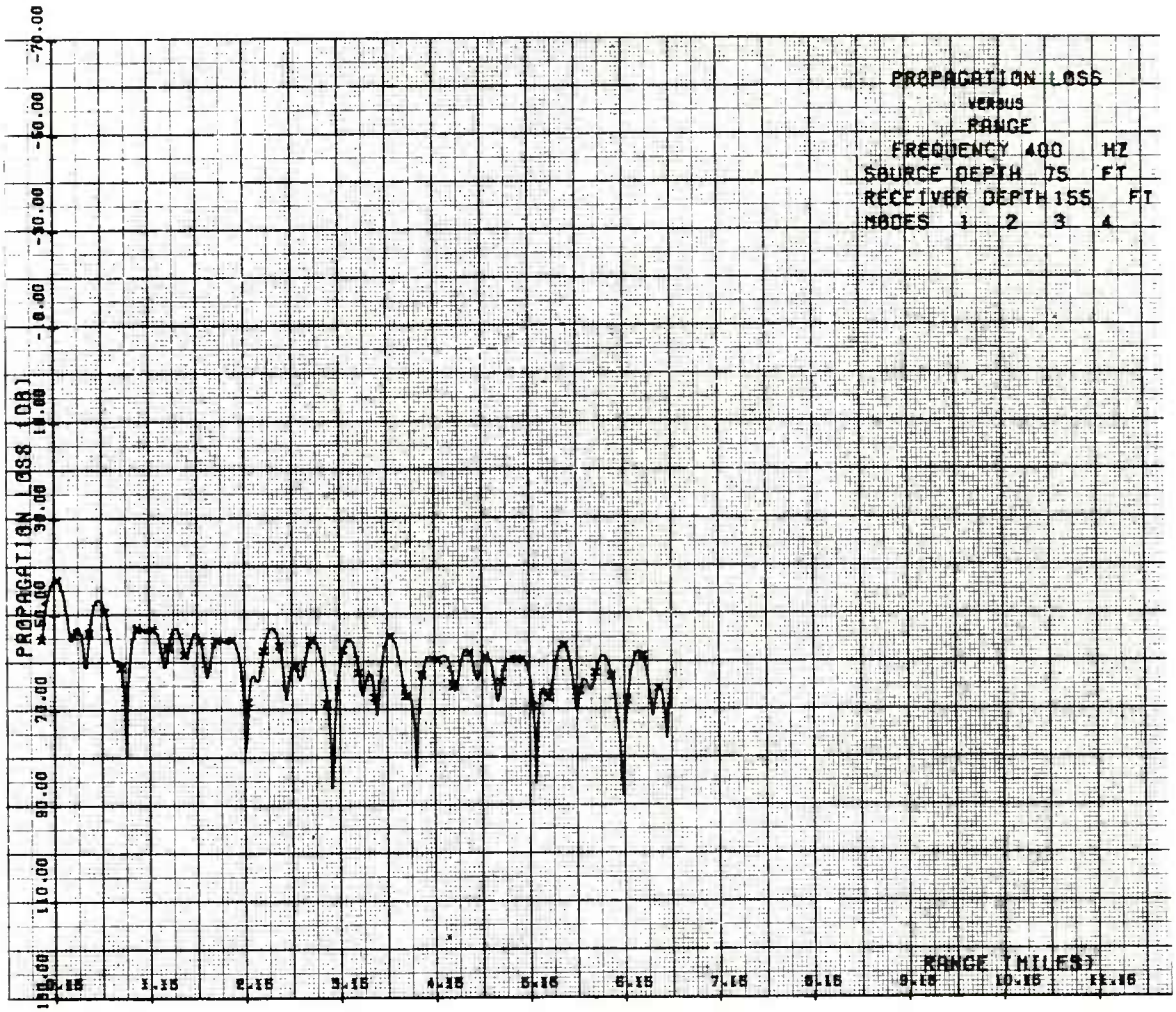

Figure 13. Sample Calcomp Plot

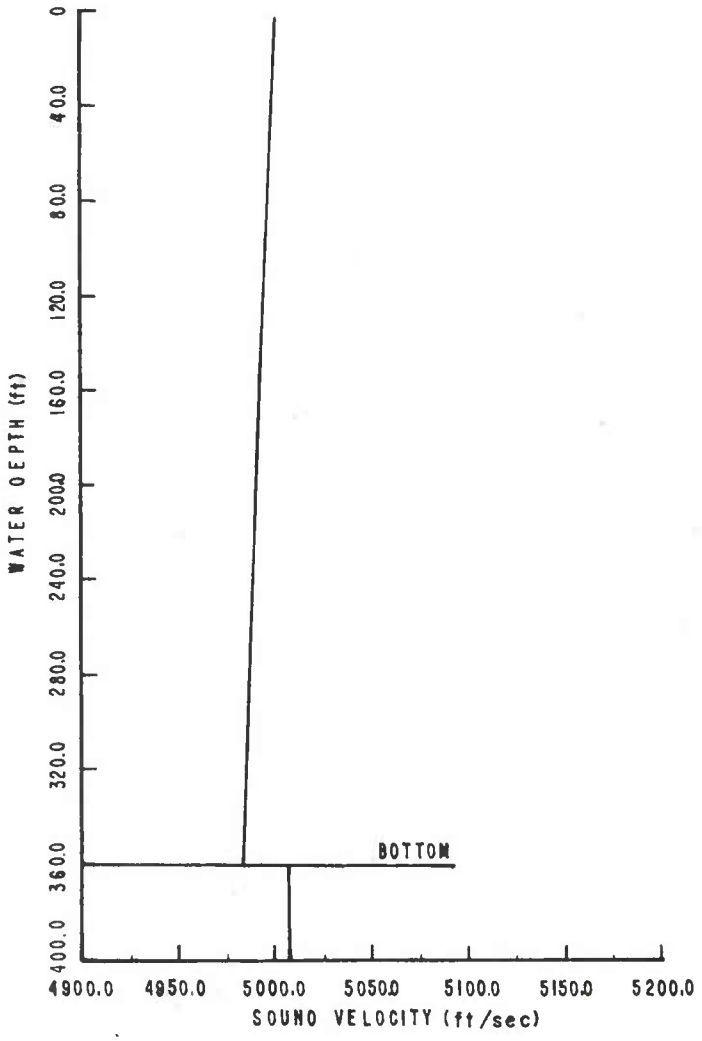

Figure 14. Velocity Profile, Test Case

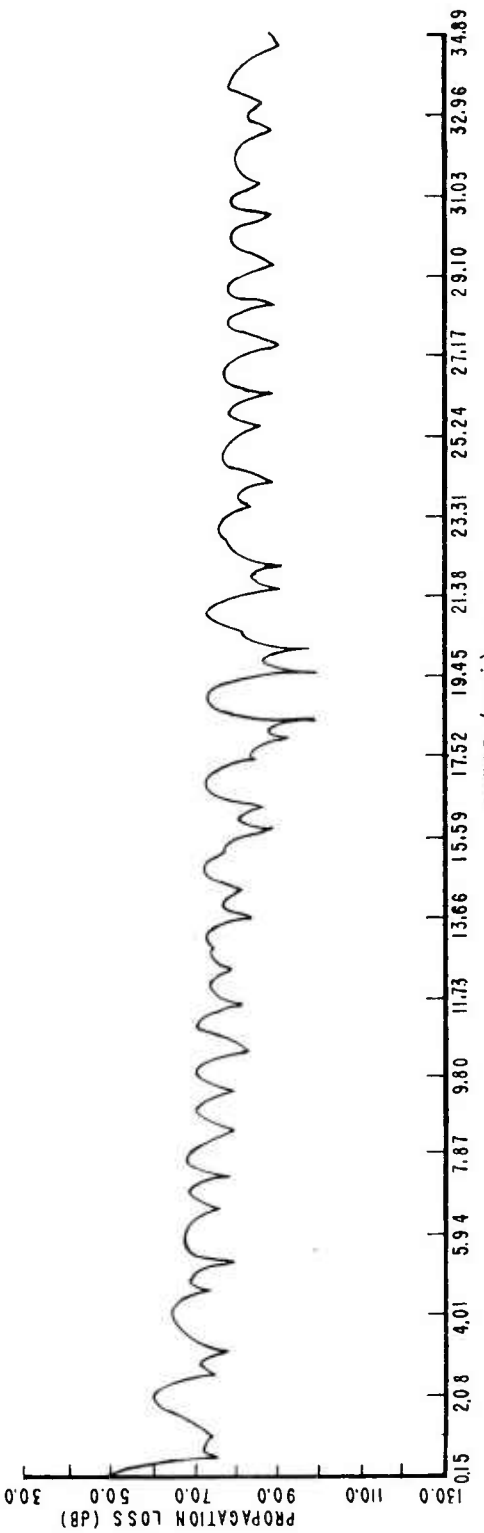

Figure 15. Propagation Loss versus Range, Test Case, Program S1441

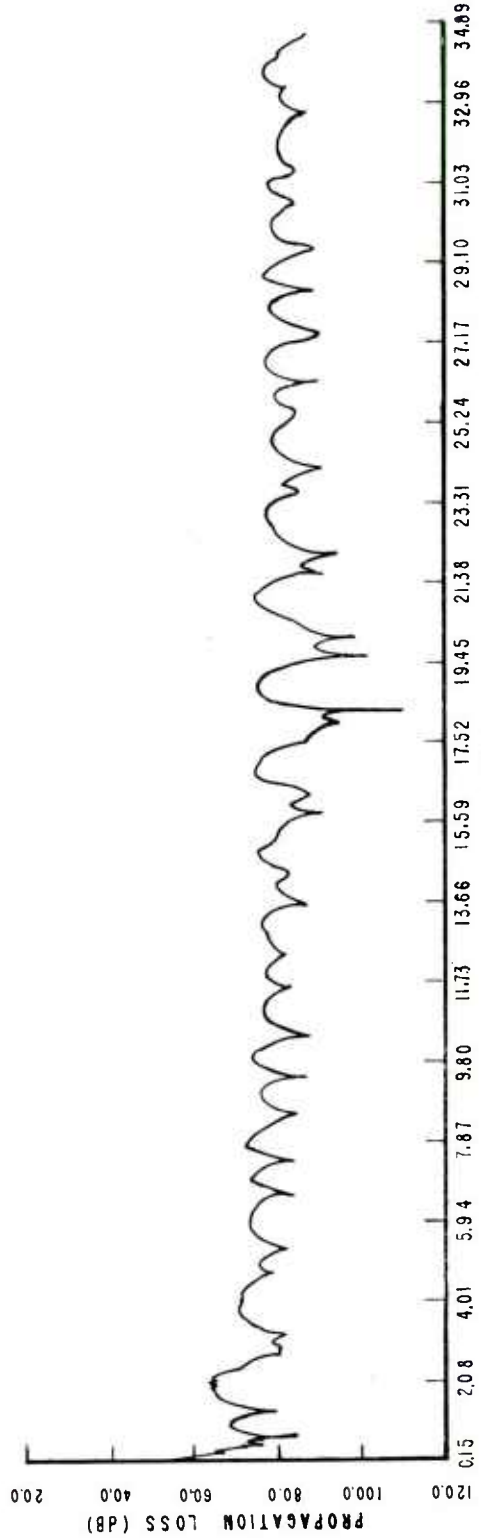

Figure 16. Propagation Loss versus Range, Test Case, FFP Program

Section 2

A COMPUTER PROGRAM (S1548) TO CALCULATE NORMAL MODE PROPAGATION IN A MEDIUM IN WHICH STRATIFICATION IS A FUNCTION OF POSITION

THEORY

The normal mode theory used in calculating the sound field in the case of a flat, homogeneous ocean bottom has been discussed in section 1. The extension of this theory to a homogeneous, semi-infinite bottom whose properties vary with range (reference 12) is discussed here.

In equation (34) of section 1, the pressure amplitude of the sound field produced by a projector with unit source level in an ocean with a flat, homogeneous bottom was described by a function dependent on range. The equation is repeated below.

$$p_a = \frac{\rho_o}{\sqrt{r}} \left\{ \left[\sum_m P_m 10^{-D_m r/20 - ar/20} \cos(\kappa_m r - \pi/4) \right]^2 + \left[\sum_m P_m 10^{-D_m r/20 - ar/20} \sin(\kappa_m r - \pi/4) \right]^2 \right\}^{1/2}, \quad (34)$$

where

a is the attenuation coefficient due to absorption in the water,

ρ_o is the water density,

r is the horizontal range,

m is the mode number,

κ_m is the horizontal wave number for mode m, and

D_m is the attenuation for unit range due to losses at the boundaries.

$$P_m = p_m \frac{1}{\rho_s} \varphi_m(z) \varphi_m(z_o) \quad , \quad (35)$$

where

$$P_m = \frac{\rho_o (2\pi)^{1/2}}{2 \nu_m \sqrt{\kappa_m}},$$

$$\nu_m = \int_{-\infty}^{+\infty} \rho \varphi_m^2 (z)\, dz \quad ,$$

ρ_s is the water density at the source, and

$\varphi_m(z)$ is the normalized displacement potential as a function of depth.

In computing the sound field for a horizontally stratified medium, the following two assumptions (reference 12) are made:

a. The values of $\varphi_m(z)$ correspond to local stratification.

b. The stratification varies slowly from one region to another so that there is no appreciable scattering of energy from one mode to another when sound propagates through the medium.

If the latter assumption holds, then the bottom topography can be approximated by a number of segments of different depth parallel to the surface as shown in figure 17 (reference 18).

The power in a given mode is determined by $\varphi(z_o)$, where z_o is the source depth. The pressure level at the receiver is determined by $\varphi(z)$, where z is the receiver depth. When there is little scattering between modes, we can approximate (reference 19) the pressure level for a given mode by substituting $\overline{P}_m$ for P_m in equation (34), with

$$\overline{P}_m = \left[P_{source}\, P_{receiver}\right]^{1/2} \quad , \qquad (36)$$

where "source" and "receiver" refer to the values of P obtained by taking into account the local stratification at the source or receiver.

Thus, P_{source} is found by calculating P_m in equation (35), using the depth, velocity profile, and bottom composition present in the segment of the range containing the source. In addition, $\varphi_m(z_o)$ should be substituted for $\varphi_m(z)$. Similarly, to calculate $P_{receiver}$, the local stratification at the receiver should be used in equation (35) and $\varphi_m(z)$ should be substituted for $\varphi_m(z_o)$.

In equation (34) the phase of the signal depends upon $\kappa_m r$. In a horizontally stratified medium, κ_m is a function of range since the variation in water depth and bottom composition causes κ_m to vary. The term κ_m can be expressed by (reference 12)

$$\kappa_m(r) = \bar{\kappa}_m + \epsilon_m(r) \quad ,$$

where $\bar{\kappa}_m$ is the average of κ_m over r and $\kappa_m(r)$ is the value of κ_m at a range r. Equation (36) can be used to form a perturbation solution of the plane wave equation

$$\nabla^2\Phi + \frac{\omega^2}{c^2}\Phi = 0 \quad ;$$

in this case, one obtains (reference 12) an approximate solution so that in equation (34), $\kappa_m(r)$ can be replaced by

$$\bar{\kappa}_m r + \Delta S_m \quad ,$$

where

$$\Delta S_m = \int_o^r \epsilon_m(r)\, dr \quad . \tag{37}$$

If the bottom properties vary with range from the source, then the attenuation per unit range due to losses at the boundaries D_m varies as a function of range, and $D_m(r)$ in equation (34) can be replaced by

$$\int_o^r D_m(r)\, dr \quad .$$

Thus equation (34) becomes

$$p_a = \frac{\rho_o}{\sqrt{r}} \left\{ \left[\sum_m \vec{P}_m 10^{-\int_o^r D_m(r)\, dr/20 - ar/20} \cos(\bar{\kappa}_m r + \Delta S - \pi/4) \right]^2 + \left[\sum_m \bar{P}_m 10^{-\int_o^r D_m(r)\, dr/20 - ar/20} \sin(\bar{\kappa}_m r + \Delta S - \pi/4) \right]^2 \right\}^{1/2} \tag{38}$$

and

$$L_r = 20 \log p_a \quad , \tag{39}$$

where L_r is the propagation loss at range r.

The amplitude distribution as a function of depth and the ray equivalent can be calculated for a particular segment of the range by a method identical to that in section 1, using the parameters determined by the local stratification.

The above formulation corresponds to a simple physical picture of the propagation of sound in a medium whose stratification changes with range. Let us consider two plane waves propagating in a medium segmented as described above. Let the first wave correspond to a given order mode in one segment and the second wave correspond to the same order mode in an adjacent segment. If the change in stratification between segments is small, the difference in direction of the two waves is small, and hence the waves are excited at approximately the same level at the source. This level is determined by the excitation pressure of the mode. However, the field at the receiver will correspond to the stratification of the segment in which the receiver is located, and the plane wave that corresponds to the mode considered will dominate the contribution by that mode to the field in the segment. Thus, the field in the segments is determined by the plane wave corresponding to the modes that compose the field. Extending the concept to several segments and several plane waves, we can similarly picture a given mode changing shape in conformance to the local stratification as it moves from segment to segment.

Let us consider, for a specific case, the effect upon sound propagation of differences in c_B, the velocity of sound in the bottom, found in segments of a range. This effect can be seen in table 3, in which θ_1, the angle of incidence at the bottom for the wave corresponding to mode 1 at 127 Hz, is given as a function of c_B for the velocity profile shown in figure 18. Consider the case where c_B varies between 5200 and 6000 ft/sec over a range. The decrease in θ_1 is rather small, 0.9°. Thus it appears that the formulation presented above in equations (38) and (39) can be used for such a variation in c_B, with $D_1(r)$, the bottom loss for mode 1 as a function of range, chosen to correspond to c_B in each segment.

Table 3. Angle of Incidence at Bottom for Mode 1, θ_1, and Critical Angle θ_c as a Function of Velocity of Sound in Bottom c_B, at 127 Hz

c_B (ft/sec)	θ_1	θ_c
5000	83° 30'	82° 22'
5200	82° 0'	72° 22'
5400	81° 30'	66° 36'
5500	81° 24'	64° 18'
5600	81° 18'	62°15'
5800	81° 12'	58° 42'
6000	81° 06'	55° 41'

Let us consider the result when the value of c_B varies from 5000 to 5200 ft/sec. The change in θ_1 is larger (1.5°) than for the case considered previously. Furthermore, the θ_c corresponding to a c_B of 5000 ft/sec is greater than the θ_1 corresponding to 5200 ft/sec. In the situation where c_B increases with increasing range from 5000 to 5200 ft/sec, the ray corresponding to mode 1 for the harder bottom (c_B = 5200 ft/sec) can be highly attenuated because the angle of incidence is less than the critical angle as the ray passes through the segment that contains the softer bottom. If the softer segment is long, there is a high probability that the ray considered can not contribute significantly to the sound field over the hard bottom. Thus, if the ray is highly attenuated, one would expect a dramatic drop in signal level and an unstable field. If, on the other hand, the transition is from a harder to a softer bottom, the value of θ_1 increases, and hence the sound field should be stronger over the softer bottom because of the transition alone. (This subject and pertinent experimental results are discussed in reference 20.)

A change in stratification due to an increase in water depth results in an increase in the θ_1 associated with a given mode. Hence, the result of such a change in stratification is similar to the result of a decrease in c_B. (The effect of a change in depth is discussed in detail in reference 21 in the context of the consequences of a change in water depth due to tide.)

Finally, a change in stratification that can be described by a change in velocity profile with range has two effects. First, like the changes in stratification discussed above, the angle θ_1 associated with a given mode is changed. Second, the angle of propagation of a given wave corresponding to a given mode in one segment is diverted toward the direction corresponding to the same mode in the following segment entered by the wave.

DESCRIPTION OF PROGRAM S1548

Program S1548 uses normal mode theory to predict acoustic propagation in a medium over a bottom whose depth and acoustic properties vary with range. Such a bottom is shown in figure 17,* where the BIFI range is approximated by 73 segments, each of which has a constant depth. The range is divided into four regions, each possessing a different bottom composition. In S1548, provision is made also for the variation in sound velocity profile over the range.

This section describes the following aspects of the program:

a. Input parameters specifying the medium through which sound is transmitted

b. Amplitude versus depth and the ray equivalent

c. Propagation loss versus range.

INPUT PARAMETERS SPECIFYING THE MEDIUM

The number of segments into which a given acoustic range is divided is given by NPCS (card group 2, table 4). The depth, location, size, and bottom properties of each segment are inputs of card group 8. The number of velocity profiles necessary for a full description of the range is given by NVCP (card group 2). The number of the first segment described by a particular velocity profile is given by ICVP (card group 3). This profile describes the velocity conditions from segment ICVP(J) to segment ICVP(J+1). IVPL (card group 6) is the parameter governing the option of a calcomp plot of the profile.

AMPLITUDE DISTRIBUTION AND RAY EQUIVALENT

Each segment of a range has its own amplitude distribution as a function of depth for each mode. With the range divided into 73 segments, it is doubtful that one would want the amplitude distribution and ray equivalent for every segment.

*Figures 17 through 21 appear at the end of this section, pages 45 through 48.

Table 4. Input Data for Program S1548

Card Group	Amount of Cards	Format	Input Parameter	Columns	Data
1	1	20A4		1-80	Heading on each page of output.
2	1	5I10	NPCS	1-10	Number of segments of constant depth into which range is divided.
			NVPC	11-20	Number of velocity profiles in the range.
			NADS	21-30	Number of segments for which amplitude distributions and ray equivalents are plotted.
			NCOR	31-40	Segment number considered to be the effective water depth at the source.
			NMOD	41-50	Number of modes calculated.
3	The smallest integer $\geq \frac{NVPC}{8}$	8I10	ICVP(J)	1-80	ICVP(J) is the number of the bottom segment at which velocity profile J is first used. This profile is used in calculations between segments ICVP(J) and ICVP(J + 1).
4	The smallest integer $\geq \frac{NADS}{8}$	2I10	IADS(J)	1-80	IADS(J) is the number of the bottom segment for which the pressure amplitude distribution and ray equivalent are plotted.
5	1	2I10	IRIC	1-10	Range increments (ft) in propagation loss versus range plot.
			NPS	11-20	Number of propagation loss versus range plots.
		4F10.3	ZS	21-30	Source depth (ft).
			ZRC	31-40	Receiver depth (ft).
			FMI	41-50	Increment in range in nmi/in. on propagation loss curves.
			FSC	51-60	200 x FSC is maximum depth (ft) plotted on curves that have depth as a parameter.

Table 4 (Cont'd). Input Data for Program S1548

Card Group	Amount of Cards	Format	Input Parameter	Columns	Data
5		2F10.3 ↓	FMJ	61-70	Value of propagation loss (dB) at origin of propagation loss curves.
			FMK	71-80	Increment in propagation loss in dB/in. on propagation loss curves.
6	Card a = 1	I10	NUMV	1-10	Number of values in velocity profile.
		F10.0	VEL 1	11-20	Velocity at origin of plot of velocity profile.
		2I10 ↓	IVPL	21-30	If IVPL = 1, velocity profile not plotted.
			IEX	31-40	Changes increment of k_r by a factor of 10^{-IEX}. Values from 0 to 10. (Explained in section 1.)
	Card b = 1	2F10.3 ↓	ZMM	1-10	Water depth (ft) at location of velocity profile.
			CB	11-20	Velocity (ft/sec) of sound in bottom at location of velocity profile.
	Card(s) c = NUMV	2F10.3 ↓	ZZ(I)	1-10	Height (ft) above bottom at which sound velocity is CC(I).
			CC(I)	11-20	Velocity (ft/sec) of sound at ZZ(I).
			I = 1, 2, ..., NUMV in order of increasing Z.		
(Other groups of cards representing a velocity profile should be inserted in front of Group 8 cards that represent the bottom segments ICVP(J), J = 1, NVPC.)					
7	1	I10	N	1-10	Number of intervals into which depth is to be subdivided in integration of differential equations (see section 1).
		2F10.3 ↓	UM	11-20	Maximum value of u(z) (see section 1).
			FQ	21-30	Frequency (Hz).

Table 4 (Cont'd). Input Data for Program S1548

Card Group	Amount of Cards	Format	Input Parameter	Columns	Data
8	Card a = 1	F10.0	ZM	1-10	Depth (ft) of water in a given bottom segment.
		2I10	IRST	11-20	Distance (ft) of a given bottom segment from the source.
		↓	IREN	21-30	Length (ft) of a given bottom segment.
	Card b = 1	3F10.3	CB	1-10	Velocity (ft/sec) of sound in a given bottom segment.
			RO	11-20	Density (grams/cm^3) of water above a given bottom segment.
		↓	RB	21-30	Density (grams/cm^3) of bottom in a given bottom segment.
	Card(s) c = the smallest integer $\geq \frac{NMOD}{4}$	4F10.5	DD(J)	1-40	DD(J) is the loss at the boundaries per unit range for a given bottom segment (dB/ft for mode J). J = 1, 2, ..., NMOD, where NMOD is the number of modes analyzed.
(There are NPCS sets of cards a, b, and c, where NPCS is the number of segments of constant depth into which the range is divided. Set i describes segment i, where i = 1, 21, ..., NPCS.)					
9	Card a = 1	I10	NMS	1-10	Number of modes to be summed in plot of propagation versus range. NMS $\leq$ NMOD.
	Card(s) b = the smallest integer $\geq \frac{NMS}{6}$	6I10	MDS(J)	1-60	J = 1, 2, ..., NMS. The values of MDS(J) are the mode numbers of the modes to be summed in the propagation loss versus range plots. MDS(J) $\leq$ NMOD.
(There are NPS sets of Group 9.)					

Therefore, NADS (card group 2) is the number of segments for which calcomp plots of these functions are desired, and IADS(J) (card group 4) gives the segment numbers for which these plots are generated. NMOD (card group 2) is the number of mades calculated. Sample plots are shown in figures 19 and 20.

PROPAGATION LOSS CURVES

Propagation loss for a source level (dB//1 yd) is obtained as a function of range for any given frequency and cambination of modes. Propagation lass may be calculated from equations (38) and (39). Source and receiver depths and ranges over which loss is ta be plotted are card graup 5 inputs. Input of the modes that make up the sound field is made with card group 9. A sample plot is shown in figure 21.

It can be seen from figure 17 that the choice of the effective water depth at the saurce may nat be a straightforward matter. The water depth at the source is abaut 17 yd, ar 51 ft. However, most modes generated may be influenced mare by segment 12, about 37 yd (110 ft) deep, than by segments 1 through 11, since the modes cansidered travel in a direction characterized by large values of the angle θ measured relative to the normal to the bottam. If one wishes to alter the effective saurce depth, one would choose NCOR equal to the number of the segment having the desired water depth. If one were ta want the effective source depth ta be that af segment 1, NCOR would be set ta 1. In the case described, ane might chaose a value of NCOR equal ta 12. Propagation loss curves will be platted starting at ranges carrespanding ta segment NCOR.

No "unattenuated" mode can possibly be formed at frequencies below the cutaff frequency for a given mode. If this situatian occurs in any segment of the range, the propagatian lass curve will be discontinuous at thase ranges carresponding ta the locatian af the particular segment. The effect af the baundaries represented by $\int_a^r D_m(r)dr$ aver this segment is calculated and added to the integral in equatian (38) anly when it is possible for "unattenuated" modes to prapagate over a range beyand the range of discantinuity.

SUMMARY

Program S1548 is designed to calculate and plat many quantities af interest in the study af a saund field in an acean whase baundaries vary in depth and acaustic praperties. Changes in the velacity prafile aver the range may also be included in the calculatians.

The limitations an the velacity prafile pertinent ta program S1441 (sectian 1) must be applied also to program S1548.

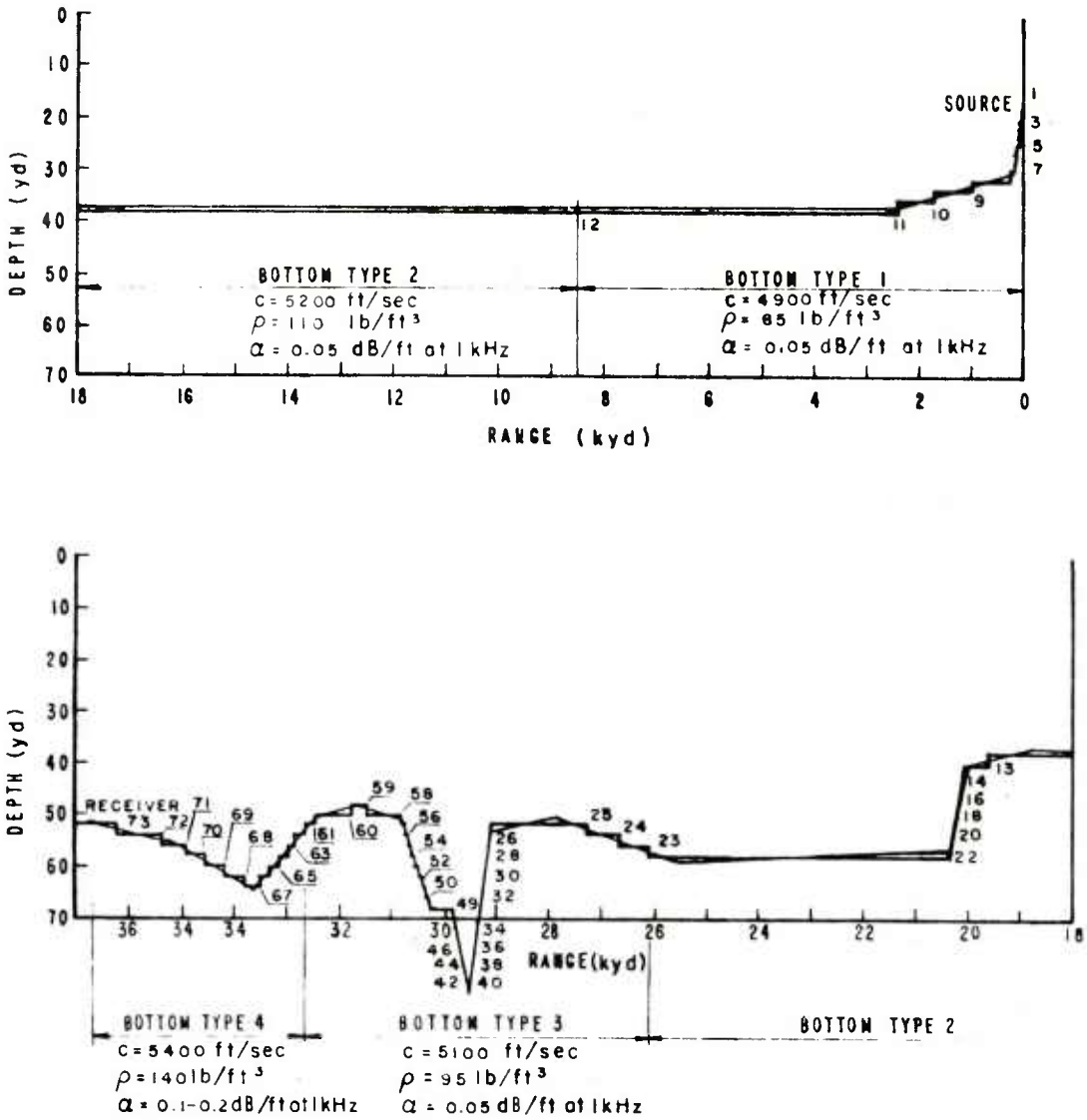

Figure 17. Model of BIFI Range

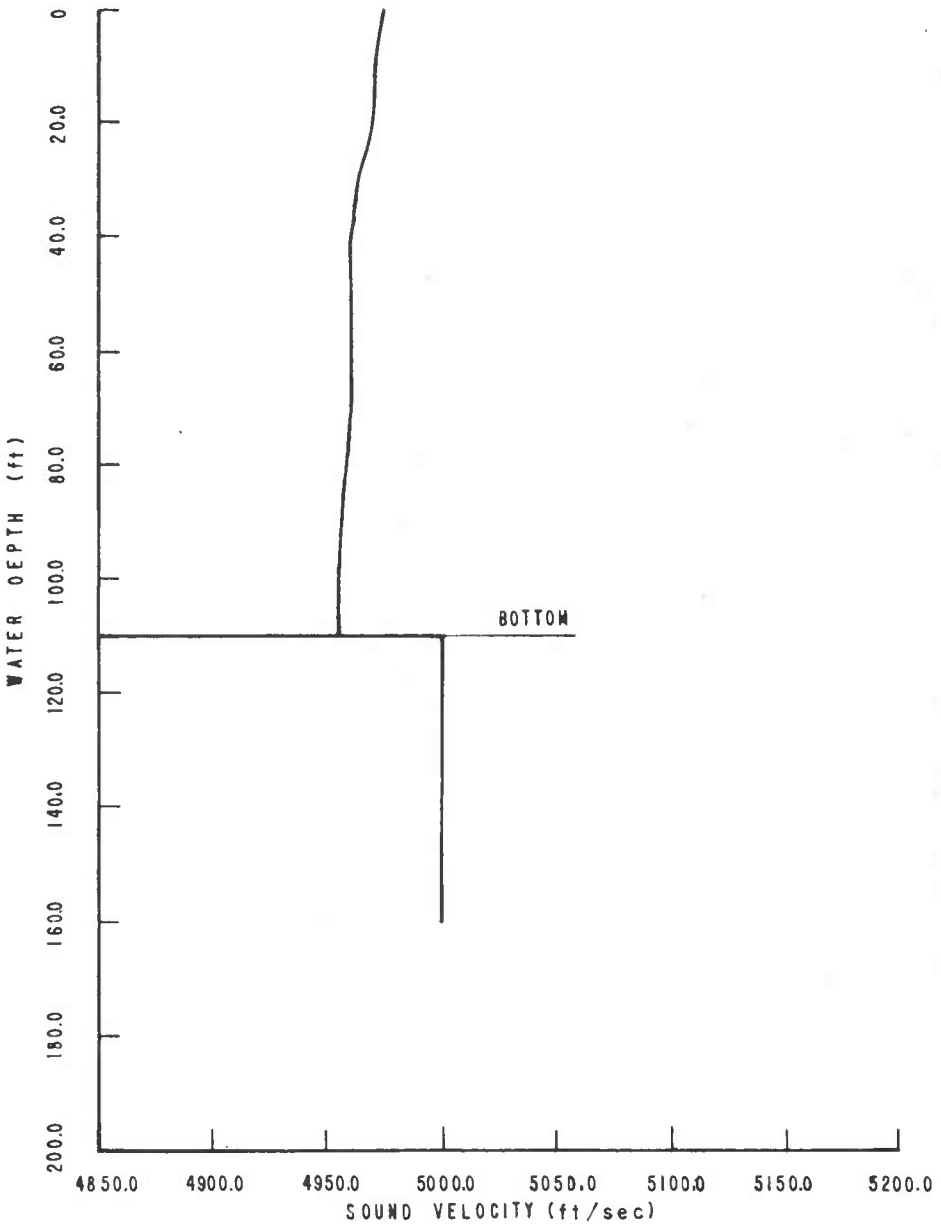

Figure 18. Velocity Profile Input to Program S1548

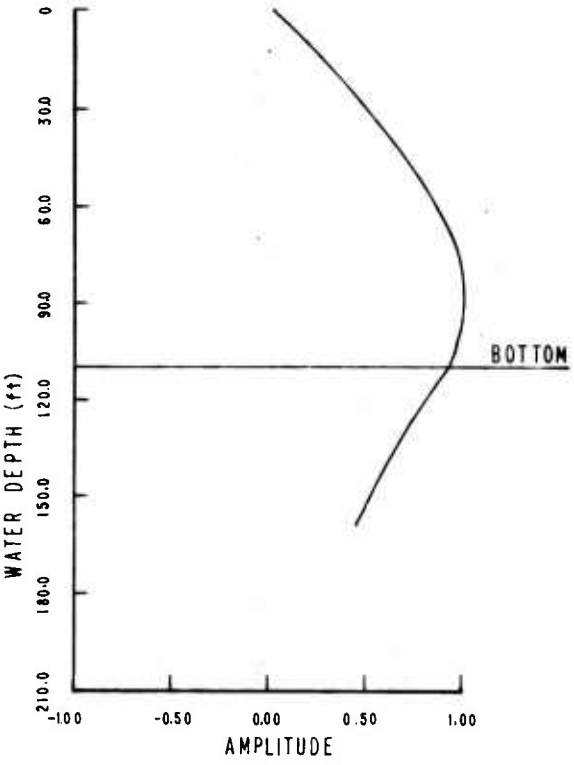

Figure 19. Amplitude versus Depth, Frequency 46 Hz, Mode 1

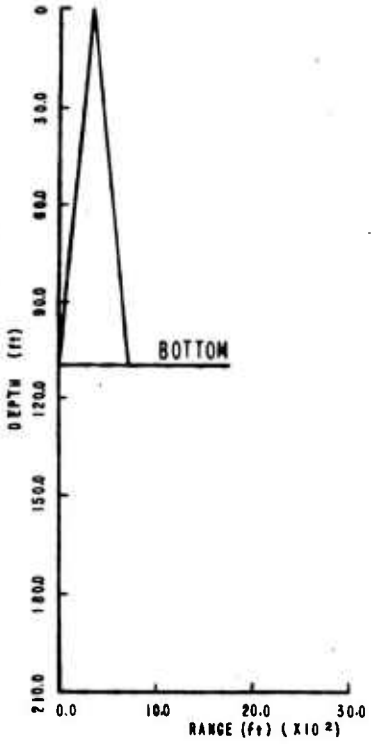

Figure 20. Ray Equivalent, Frequency 46 Hz, Mode 1

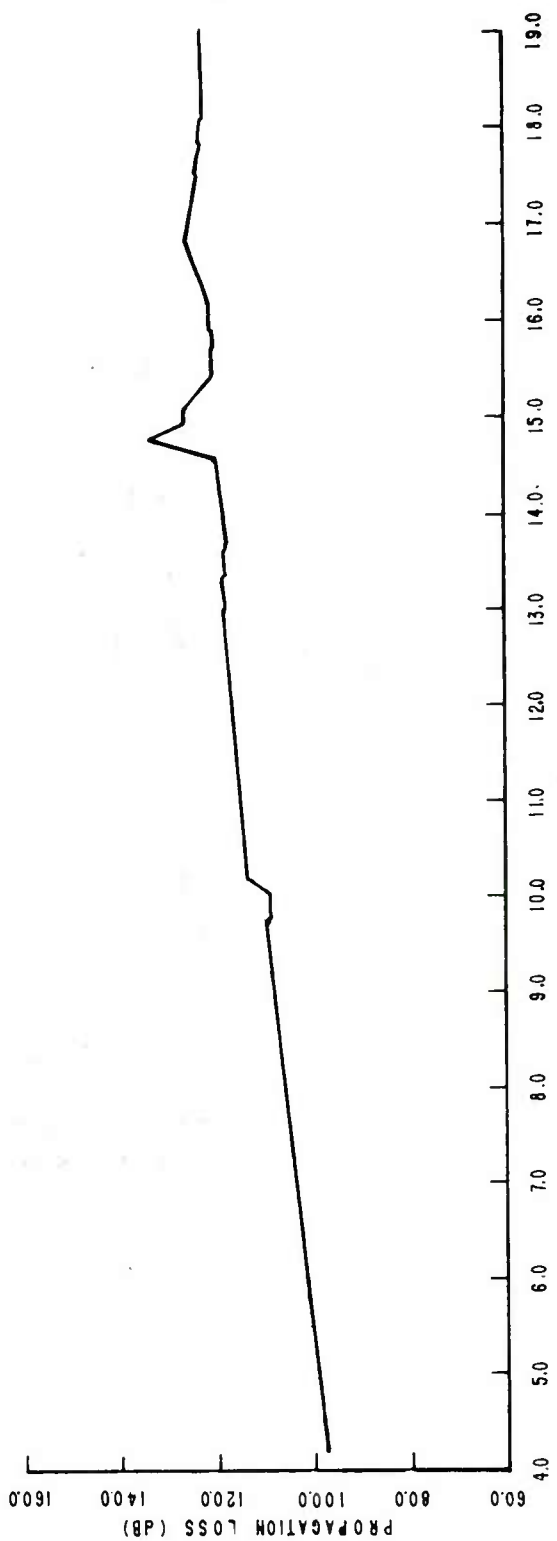

Figure 21. Propagation Loss versus Range, Frequency 500 Hz, Source Depth 50 ft, Receiver Depth 104 ft, Mode 1

Section 3
PROPAGATION OF EXPLOSIVE SOUND IN THE BIFI RANGE

PROCEDURE

For all the tests discussed, explosives were detonated at depths of 50 and 75 ft at point A in figure 22,* near Block Island. Signals were received by a bottom-mounted hydrophone located at a depth of 155 ft at point B, off Fishers Island. The explosive charges used were 1/2- and 1-lb blocks of TNT.

THEORY

Most of the theory of sound propagation by normal modes has been discussed in sections 1 and 2. Section 1 contains a description of NUSC program S1441, which deals with normal mode propagation over a flat, homogeneous bottom in a medium whose velocity profile is constant with distance from an acoustic source. Section 2 describes NUSC program S1548, which uses normal mode theory to predict acoustic propagation over an ocean bottom whose depth and acoustic impedance vary slowly with range and in a medium whose velocity profile varies slowly with distance from an acoustic source. These two procedures will be referred to as normal mode predictions for a flat bottom and an irregular bottom, respectively.

The prediction of propagation loss for a flat bottom is a function of the depth, velocity profile, and bottom characteristics, each of which is assumed constant with distance from an acoustic source. The prediction of propagation loss for an irregular bottom is dependent on the values of these three parameters at both the source and receiver. Thus, if the parameters have large variations with distance from an acoustic source, the two methods may predict significantly different values of propagation loss.

One special case where the predicted values do, indeed, vary significantly should be mentioned. It occurs when velocity profile and bottom characteristics remain relatively constant over an entire range but a large variation exists between the depth assumed for a flat bottom and the depth at the source or receiver. Vertexing of the rays can account for a marked disparity between the sound fields at the receiver. As shown in figure 23, H_1 is the assumed depth for a flat bottom case and H_2 is the depth at the source or receiver in the irregular bottom case; the source or receiver is at the bottom. In the irregular, but not the flat, bottom case the hydrophone is in a "shadow zone" and the calculated propagation loss is consequently

*Figures 22 through 37 appear at the end of this section, pages 60 through 73.

much larger since the omplitude of the pressure fields shows on exponentiol decoy in o shodow zone (reference 8). The example considered occurs in the winter ond where H_1 = 110 ft is the overage depth used for o flat bottom ond H_2 = 150 ft is the depth at the receiver.

It has been previously determined (references 7 ond 8) thot ot the frequencies considered in these tests (about 56 to 560 Hz), the first mode dominates in the signols received ot point B in figure 22. Therefore, it hos been ossumed in the theoretical colculotions of propagation loss thot the pressure field at the receiving hydrophone contains only the first mode. Since the first mode is dominant, there is little difference in the pressure field produced by explosives ond detected ot 50 ond 75 ft. As in references 7 ond 8, the meosurements ot the two depths ore combined. Theoreticol colculations ore for o source 75 ft deep.

Let us consider the generol chorocteristics of propagotion loss os o function of frequency in cases where the first mode dominates. All calculotions are made assuming the velocity profile shown in figure 24. Figure 11 is o typicol plot of excitation pressure (defined in section 1 of this report) versus frequency for the first mode. At the frequencies considered here, excitation pressure decreases with frequency. Thus, less energy goes into the higher frequency modes and, because of this factor olone, propagation loss will increose with increasing frequency. It is possible (reference 8) to construct a ray equivalent of a particular mode, os shown in figure 25; it is therefore possible to determine the skip distance between bounces off the bottom of the medium. The angle at which energy strikes the surfoce θ_s or bottom θ_b, relotive to the normal to the bottom, increases with frequency (reference 8). Thus, as shown in figures 25 ond 26, the skip distonce tends to increase with frequency, thereby reducing the number of bounces over o given ronge. However, if a velocity grodient exists in the medium, the skip distance increoses with the frequency until there is a vertexing ot the interface, as presented in figure 27. In generol, this represents the lorgest skip distance attainable. As the frequency is increased further, the depth of the vertexing recedes from the interface ond the skip distonce decreoses, os shown in figure 28. Thus, propagation loss will decrease with increasing frequency as o result solely of the effect of skip distonce; however, the effect of vertexing con modify this relationship.

In the irregulor bottom cose, mony depths and velocity profiles moy exist. Obviously, then, there are many possible ways to determine the skip distance. One woy is to toke on averoge skip distonce for the vorious sections of an acoustic ronge. However, the sections of the range with the largest gradients should produce the greotest effect on the propagation loss. Therefore, in the onalysis of these tests, whenever the velocity profile varied considerably over the ronge, the skip distonce was determined by using the largest grodient measured ot o depth thot was close to the averoge depth of the range.

RESULTS OF TESTS

Propagation loss as a function of frequency was determined for all five tests conducted. The results were obtained by finding the energy content of each received shot for a 1-Hz band at logit frequencies from 56 to 562 Hz. The levels thus derived were subtracted from the source level for the explosives as given by Weston (reference 22).

For each test, the theoretical propagation loss values were calculated in both the irregular and flat bottom cases with the assumption that no bottom loss was suffered by the first mode. Velocity profiles measured at the time of the tests were used. The profiles obtained during the five tests ranged from those with large negative gradients to those with small positive gradients. In the flat bottom case, the velocity profile with the largest gradient was chosen to apply to the whole range if more than one profile was taken. The water depth assumed for the flat bottom was 110 ft. The difference between experimental and theoretical values of propagation loss was interpreted as a measure of bottom loss, and the internal consistency of the theoretical and experimental results was observed. The outcomes of the individual tests are given below.

AUGUST 1967

The August 1967 tests were conducted when the velocity profile possessed a large negative gradient, as shown in figure 24. Since this was the only velocity profile taken during these tests, it was used to represent velocity conditions over the entire range. As shown in figure 29, propagation loss as a function of frequency is nonlinear, with the minimum at 141 Hz. The results and the theoretical analysis are given in table 5. The differences between theoretical predictions of propagation loss for the flat and irregular bottom cases are small, since in both cases only one velocity profile was used to represent the entire range. The increase in theoretical loss with frequency is a result mainly of the variation of the excitation pressure with frequency. At low frequencies, the skip distance increases with frequency, as shown in figures 25 and 26. This increase continues until a frequency is reached at which the ray vertexes near the surface (figure 27). This event corresponds to 141 Hz in table 5, at which point the skip distance is maximum and the angle at which the energy first strikes the surface becomes 90°. Thereafter, as shown in figure 28, the ray vertexes at increasing depth for higher frequencies and the skip distance decreases. The loss per nautical mile is minimum at 141 Hz, and the loss per bounce is on the order of 0.5 dB over the frequency range considered. The maximum loss per bounce was determined to occur at 141 Hz, which is probably a result of the assumption that the particular velocity profile measured is a good approximation at all points along the range.

Table 5. Results of August 1967 Tests

Frequency (Hz)	Skip Distance (ft)	θ_b (deg)	θ_s (deg)	Theoretical Loss		Measured Loss (dB)	Flat Bottom		Irregular Bottom		Number of Bounces
				Flat (dB)	Irregular (dB)		Bottom Loss (dB/nmi)	Loss Per Bounce (dB)	Bottom Loss (dB/nmi)	Loss Per Bounce (dB)	
45	710	71.4	74.0	55.8	57.0	117.8	3.33	.39	3.32	.39	155
56	840	73.6	76.6	56.8	58.2	104.5	2.61	.36	2.53	.35	131
70	1020	75.8	79.5	58.2	59.8	98.3	2.19	.37	2.10	.36	107
89	1280	77.7	82.3	59.9	61.6	93.9	1.86	.40	1.76	.38	86
112	1700	79.2	85.1	61.6	63.3	89.5	1.52	.43	1.43	.41	65
141	3420	80.4	90.0	63.2	64.9	87.2	1.31	.74	1.22	.69	32
178	1890	81.4	90.0	64.6	66.3	92.1	1.50	.47	1.41	.44	58
224	1730	82.2	90.0	65.8	67.6	96.6	1.68	.49	1.58	.46	63
282	2100	82.9	90.0	66.7	68.8	101.4	1.90	.66	1.78	.62	52
355	1800	83.4	90.0	67.6	70.1	107.7	2.19	.66	2.05	.62	61
446	1150	84.0	90.0	68.7	71.6	109.2	2.21	.42	2.05	.39	95
562	1050	84.6	90.0	70.6	73.5	115.3	2.44	.43	2.28	.40	105

JANUARY 1968

The tests in January 1968 were conducted when the typical velocity profile had a small positive gradient. All five profiles taken over the range were similar to that shown in figure 30 (taken from reference 23). For comparison, figure 31 exhibits plots of propagation loss as a function of frequency for both the January 1968 and the August 1967 tests. It can be seen that propagation loss was much greater in August than in January, and that the difference in propagation loss between the two sets of tests is particularly large for frequencies above 200 Hz. The results and theoretical analysis pertaining to the January tests are shown in table 6. It can be seen that the predicted propagation loss values for an irregular bottom are much larger than those for a flat bottom, especially at the higher frequencies. This is attributed to the previously described effect caused by irregularity in depth near the receiver and a positive velocity gradient. In both cases, the predicted propagation loss increases with frequency, as expected. The skip distance increases with frequency since vertexing would not occur until θ_b equals 90° at about 700 Hz.

It should be noted that the physical pictures suggested by the analysis of a flat and an irregular bottom differ. For the flat bottom, the loss per bounce is on the order of 0.2 dB at all frequencies considered. However, the skip distance increases (number of bounces decreases) with frequency, and thus bottom loss decreases with frequency, as demonstrated by values of bottom loss in dB per nautical mile.

In the irregular bottom analysis, the loss per bounce decreases sharply with increasing frequency as the angle of incidence of energy striking the bottom, θ_b, increases from 74.4 to 89.3°. This, when combined with the increase in skip distance with frequency, explains the decreased bottom loss with frequency. At frequencies of 355 to 562 Hz, the predicted values of propagation loss are lower than the measured values by about 2 dB, and bottom loss and loss per bounce are negative. At low frequencies, the skip distances for August and January are about the same. However, the angle of incidence is larger during January, a fact that explains the decrease in propagation loss in January at these frequencies. At higher frequencies, both the angle of incidence and the skip distance are larger in January than in August. Thus, the larger seasonal increase in propagation loss at the higher frequencies is explained.

Table 6. Results of January 1968 Tests

Frequency (Hz)	Skip Distance (ft)	θ_b (deg)	θ_s (deg)	Theoretical Loss		Measured Loss (dB)	Flat Bottom		Irregular Bottom		Number of Bounces
				Flat (dB)	Irregular (dB)		Bottom Loss (dB/nmi)	Loss Per Bounce (dB)	Bottom Loss (dB/nmi)	Loss Per Bounce (dB)	
56	780	74.4	74.1	56.6	59.2	93.3	2.01	.26	1.86	.24	141
70	930	76.7	76.5	58.3	61.2	85.3	1.48	.23	1.32	.20	118
89	1140	79.2	78.8	60.3	63.6	80.2	1.09	.21	0.91	.17	96
112	1380	81.2	80.5	62.4	66.2	75.0	0.69	.16	0.48	.11	80
141	1680	82.8	82.0	64.7	68.9	75.9	0.61	.17	0.38	.11	65
178	2050	84.3	83.3	67.3	71.9	78.3	0.60	.21	0.35	.12	54
224	2520	85.5	84.3	70.0	75.1	78.3	0.45	.19	0.17	.07	44
282	3120	86.5	85.1	73.0	78.6	79.9	0.38	.20	0.07	.04	35
355	3980	87.5	85.8	76.1	82.5	80.9	0.26	.17	-0.09	-.06	28
446	5640	88.5	86.2	79.6	87.0	84.8	0.28	.27	-0.12	-.11	19
562	6160	89.3	86.3	83.6	92.7	90.6	0.38	.39	-0.11	-.12	18

APRIL 1968

The tests in April 1968 were conducted when the velocity profile varied considerably over the range, as shown in figure 32 (taken from reference 23). As can be seen, the profile possessed a small negative gradient approximately 18 nmi from the source and a fairly large negative gradient in the middle of the range. For comparison, plots of propagation loss as a function of frequency for the April and January tests are shown in figure 33. It is apparent that the propagation loss at most frequencies was slightly greater in April than in January. The April results and the theoretical analysis are presented in table 7. The differences between the theoretical propagation loss predictions for a flat and an irregular bottom are small since there is little variation in the velocity profile near the source and receiver. As expected, the theoretical propagation loss increases with frequency. The skip distances and angles of incidence at the surface and bottom were calculated for about 12 nmi from the source, using the velocity profile shown in figure 32. By comparing the values of skip distance and θ_b in tables 6 and 7, one sees that these quantities are nearly the same in January and April for low frequencies, so that similar bottom losses would be expected. However, at higher frequencies, the skip distance and θ_b are greater in January, so that one would expect slightly lower values of propagation loss in January. This seems to be the case, although the differences at 112 and 141 Hz are larger than anticipated. The loss per bounce in the higher frequency ronge was on the order of 0.3 dB.

AUGUST 1968

The tests in August 1968 were conducted when the velocity profiles* taken over the range exhibited large negative gradients, as shown in figure 34 (taken from reference 23). The profile near the source, however, possessed only a slightly negative gradient, smaller thon the gradient in the profile observed during the August 1967 tests.

Figure 35 gives plots of propagation loss as a function of frequency for the August 1968 and the August 1967 tests. It can be seen that the propagation loss at most frequencies was slightly greater in 1968 than in 1967. These results and the theoretical analysis for the August 1968 tests are provided in table 8. There are only moderate differences between the theoretical predictions of propagation loss for a flat and an irregular bottom, since there is only a moderate difference between the velocity profiles at the source and at the receiver. Again, the theoretical propagation loss increases with frequency.

The skip distance is maximum at 178 Hz, compared with the maximum skip distance at 141 Hz in August 1967. In August 1968, the minimum propagation loss at 141 Hz is slightly less pronounced than the minimum loss for August 1967.

*These profiles were token a doy after the tests were performed.

Table 7. Results of April 1968 Tests

Frequency (Hz)	Skip Distance (ft)	θ_b (deg)	θ_s (deg)	Theoretical Loss		Measured Loss (dB)	Flat Bottom		Irregular Bottom		Number of Bounces
				Flat (dB)	Irregular (dB)		Bottom Loss (dB/nmi)	Loss Per Bounce (dB)	Bottom Loss (dB/nmi)	Loss Per Bounce (dB)	
56	860	74.7	75.8	56.5	59.0	94.2	2.06	.30	1.92	.28	128
70	1040	77.1	78.4	58.1	60.9	80.6	1.23	.21	1.08	.19	106
89	1280	79.3	80.9	60.1	63.2	83.0	1.25	.27	1.08	.23	86
112	1570	81.0	83.1	62.2	65.6	82.4	1.10	.29	0.92	.24	70
141	1960	82.4	85.1	64.4	68.2	81.5	0.93	.31	0.73	.24	56
178	2560	83.6	87.3	66.9	70.9	81.0	0.77	.33	0.55	.24	43
224	3580	84.6	90.0	69.4	73.7	83.0	0.74	.44	0.51	.30	31
282	2840	85.4	90.0	72.0	76.5	87.3	0.84	.40	0.59	.28	39
355	3160	86.0	90.0	74.7	79.3	89.0	0.78	.41	0.53	.28	35
446	4110	86.5	90.0	77.4	81.5	89.7	0.67	.46	0.45	.31	27
562	2640	87.0	90.0	80.3	81.6	94.2	0.76	.33	0.69	.30	42

Table 8. Results of August 1968 Tests

Frequency (Hz)	Skip Distance (ft)	θ_b (deg)	θ_s (deg)	Theoretical Loss		Measured Loss (dB)	Flat Bottom		Irregular Bottom		Number of Bounces
				Flat (dB)	Irregular (dB)		Bottom Loss (dB/nmi)	Loss Per Bounce (dB)	Bottom Loss (dB/nmi)	Loss Per Bounce (dB)	
89	1330	79.1	81.8	59.1	62.3	94.8	1.95	.43	1.78	.39	83
112	1670	80.7	84.1	60.8	64.4	90.0	1.60	.44	1.60	.39	66
141	2230	82.1	86.7	62.6	66.6	89.6	1.48	.55	1.26	.47	49
178	2920	83.2	90.0	64.3	68.8	93.7	1.61	.78	1.36	.66	38
224	2490	84.1	90.0	65.9	70.9	99.0	1.81	.75	1.54	.64	44
282	2500	84.9	90.0	67.4	72.8	104.8	2.04	.85	1.75	.73	44
355	2190	85.5	90.0	68.6	74.5	108.2	2.16	.79	1.84	.67	50
446	2140	86.0	90.0	69.8	76.0	110.5	2.22	.79	1.89	.67	51
562	2190	86.5	90.0	71.0	77.2	112.4	2.26	.82	1.92	.70	50

SEPTEMBER 1968

The September 1968 tests were performed when the velocity profiles* taken over the range exhibited moderately negative gradients, as shown in figure 36 (taken from reference 23). The profiles near the source and receiver were less negative than those toward the center of the range. Figure 37 gives plots of propagation loss as a function of frequency for the September 1968 and August 1967 tests. The loss is lower in August at low frequencies and lower in September at the higher frequencies. Table 9 shows that in September the maximum skip distance occurs at 355 Hz; in August the skip distance is maximum at 141 Hz. Since the skip distances are longer in August at lower frequencies and longer in September at higher frequencies, it is not surprising that relatively less loss occurs at the higher frequencies in September and at the lower frequencies in August.

*These profiles were obtained two days after the tests were performed.

Table 9. Results of September 1968 Tests

Frequency (Hz)	Skip Distance (ft)	θ_b (deg)	θ_s (deg)	Theoretical Loss		Measured Loss (dB)	Flat Bottom		Irregular Bottom		Number of Bounces
				Flat (dB)	Irregular (dB)		Bottom Loss (dB/nmi)	Loss Per Bounce (dB)	Bottom Loss (dB/nmi)	Loss Per Bounce (dB)	
70	980	76.1	77.9	57.4	60.3	105.5	2.63	.43	2.47	.40	112
89	1190	78.0	80.2	59.1	62.4	101.2	2.30	.46	2.12	.42	92
112	1440	79.6	82.2	60.8	64.6	97.2	1.99	.48	1.78	.43	76
141	1770	80.8	83.9	62.6	67.0	94.4	1.74	.51	1.50	.44	62
178	2230	81.8	85.6	64.4	69.4	98.8	1.88	.70	1.61	.60	49
224	2950	82.6	87.3	66.0	71.8	105.9	2.18	1.07	1.86	.92	37
282	3630	83.1	90.0	67.4	74.1	106.6	2.14	1.30	1.78	1.07	30
355	4860	83.6	90.0	68.3	76.1	108.9	2.22	1.80	1.79	1.45	23
446	3270	83.9	90.0	68.8	77.8	103.5	1.90	1.03	1.40	.77	34
562	1770	84.3	90.0	69.3	79.0	108.6	2.15	.63	1.62	.48	62
707	1620	84.6	90.0	70.7	79.8	112.7	2.30	.62	1.80	.49	68

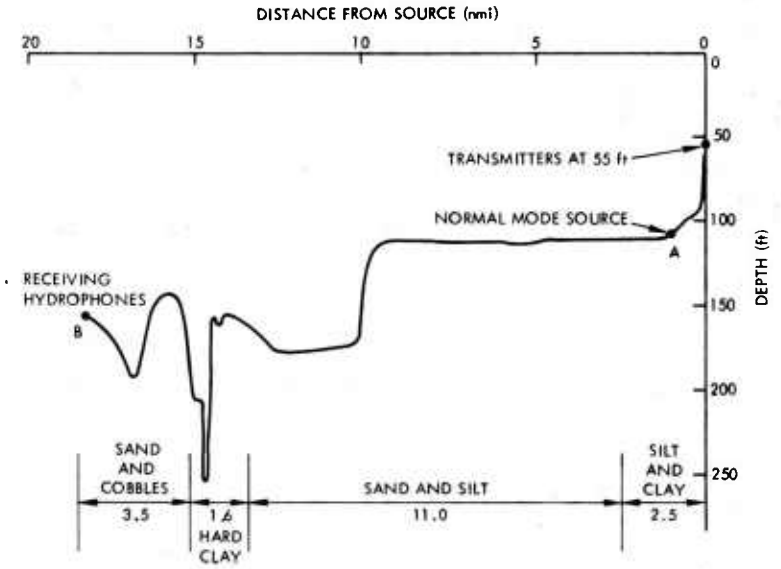

Figure 22. Depth Profile, BIFI Range

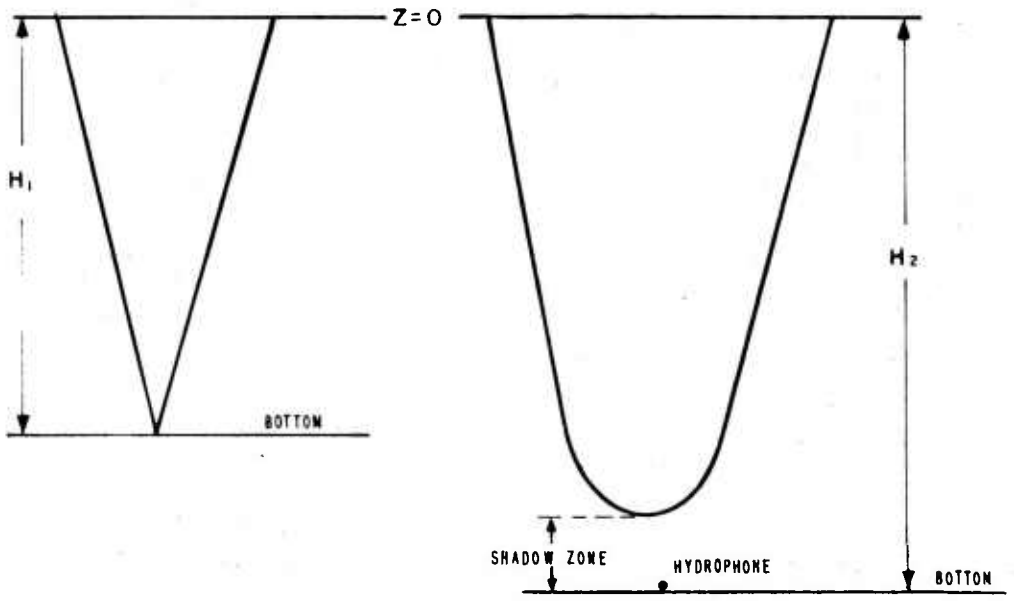

Figure 23. Effect of Variable Depth on Rays

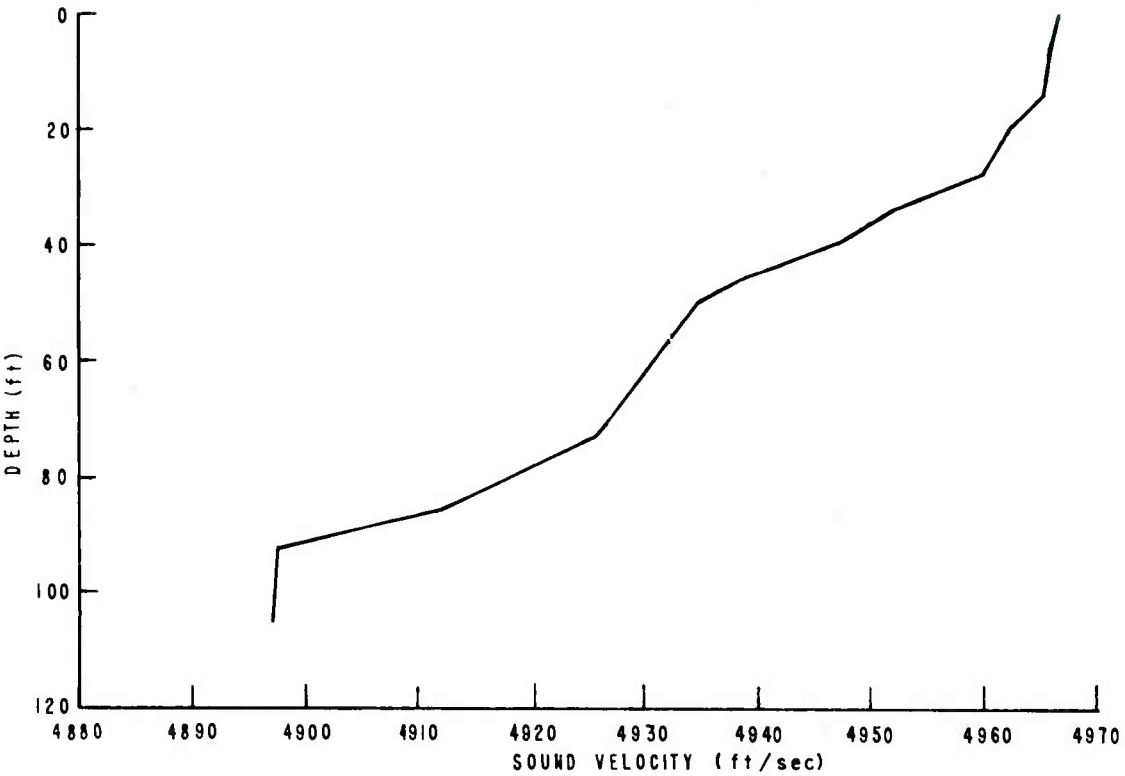

Figure 24. Velocity Profile, 8 August 1967

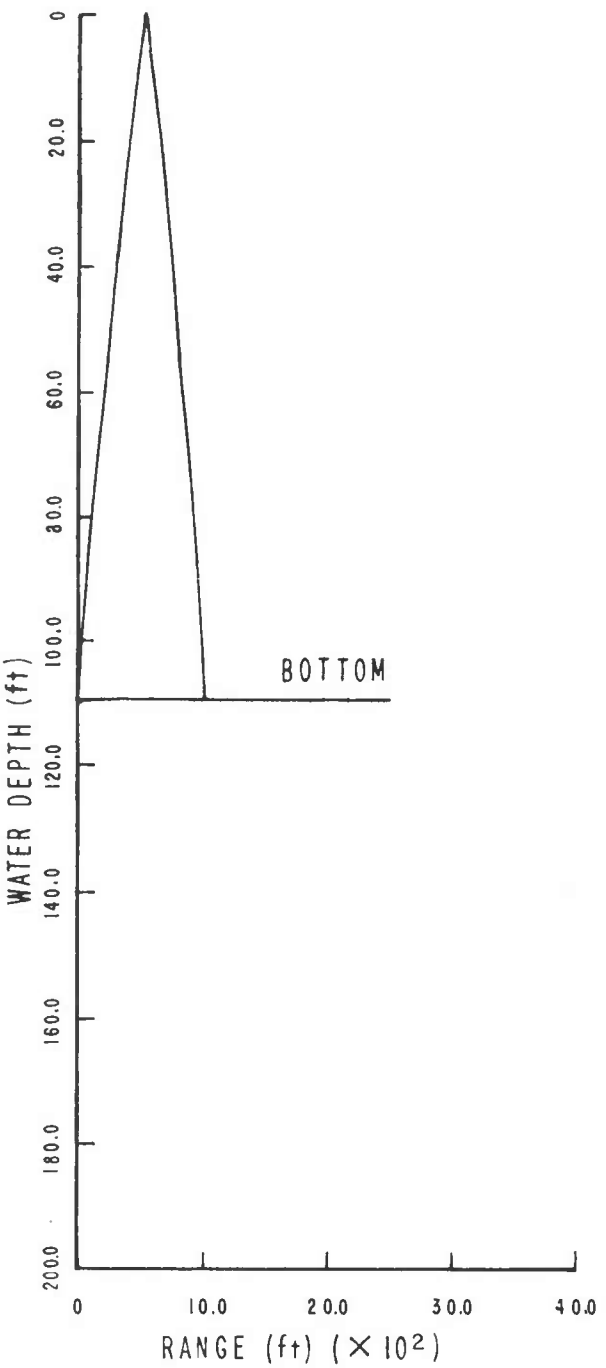

Figure 25. Ray Equivalent, Frequency 70 Hz, Mode 1

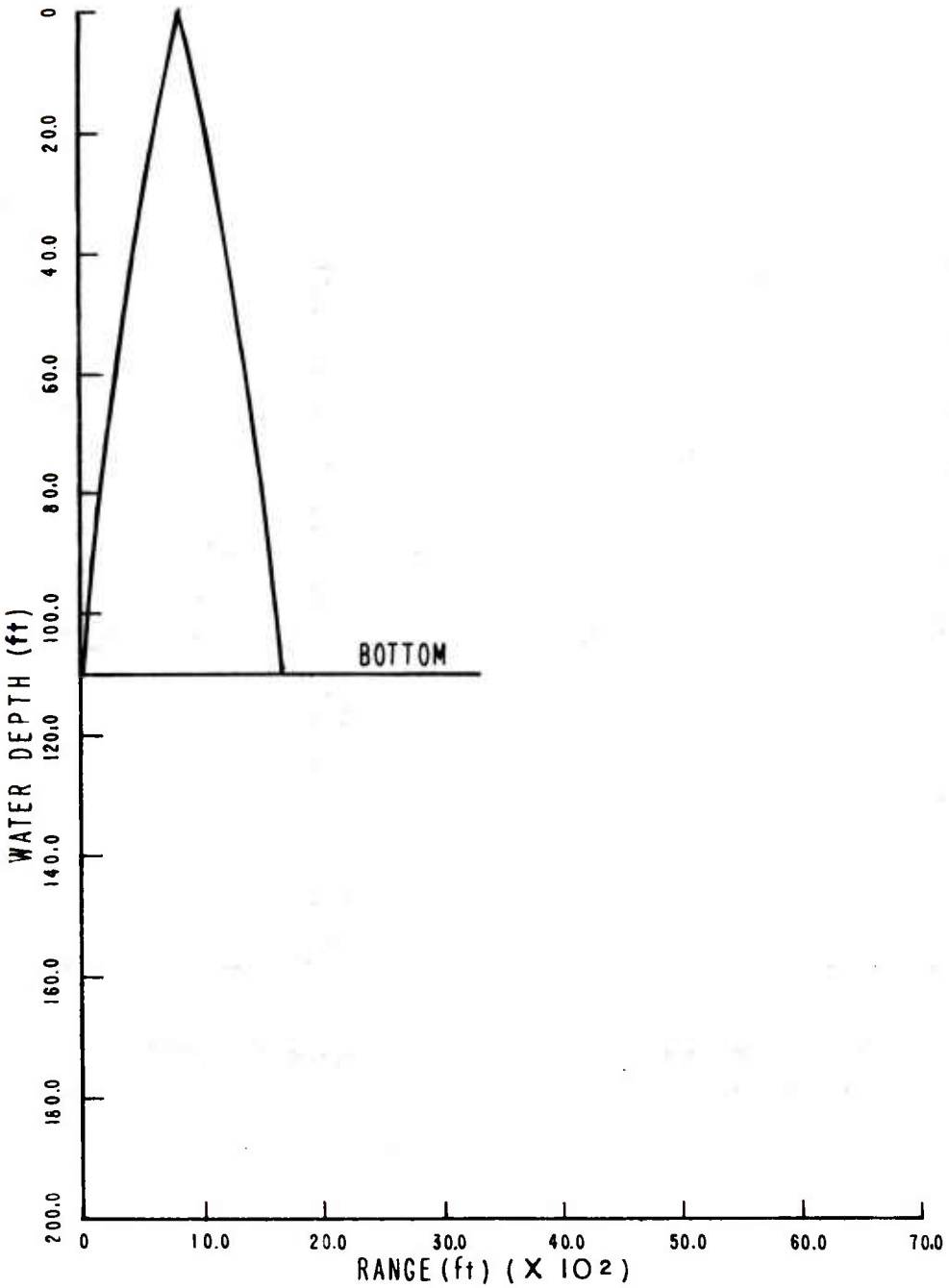

Figure 26. Ray Equivalent, Frequency 112 Hz, Mode 1

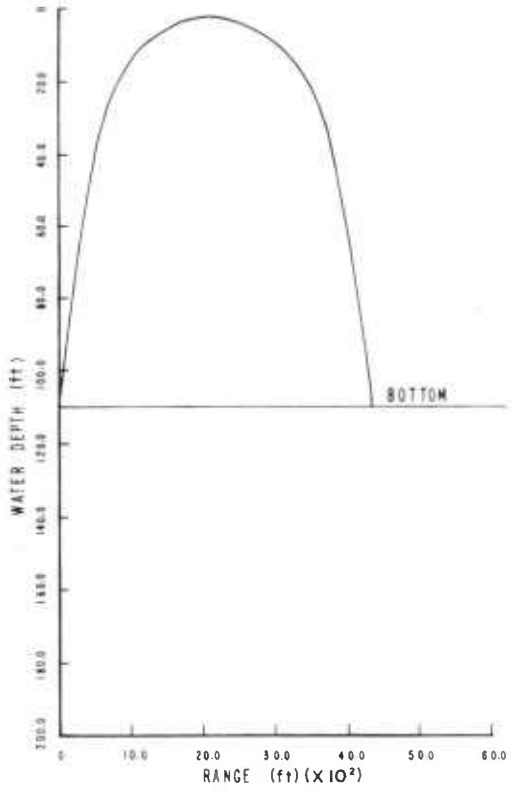

Figure 27. Ray Equivalent, Frequency 141 Hz, Mode 1

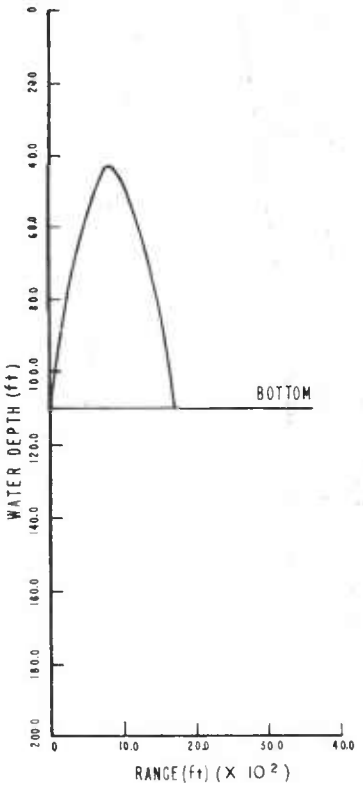

Figure 28. Ray Equivalent, Frequency 224 Hz, Mode 1

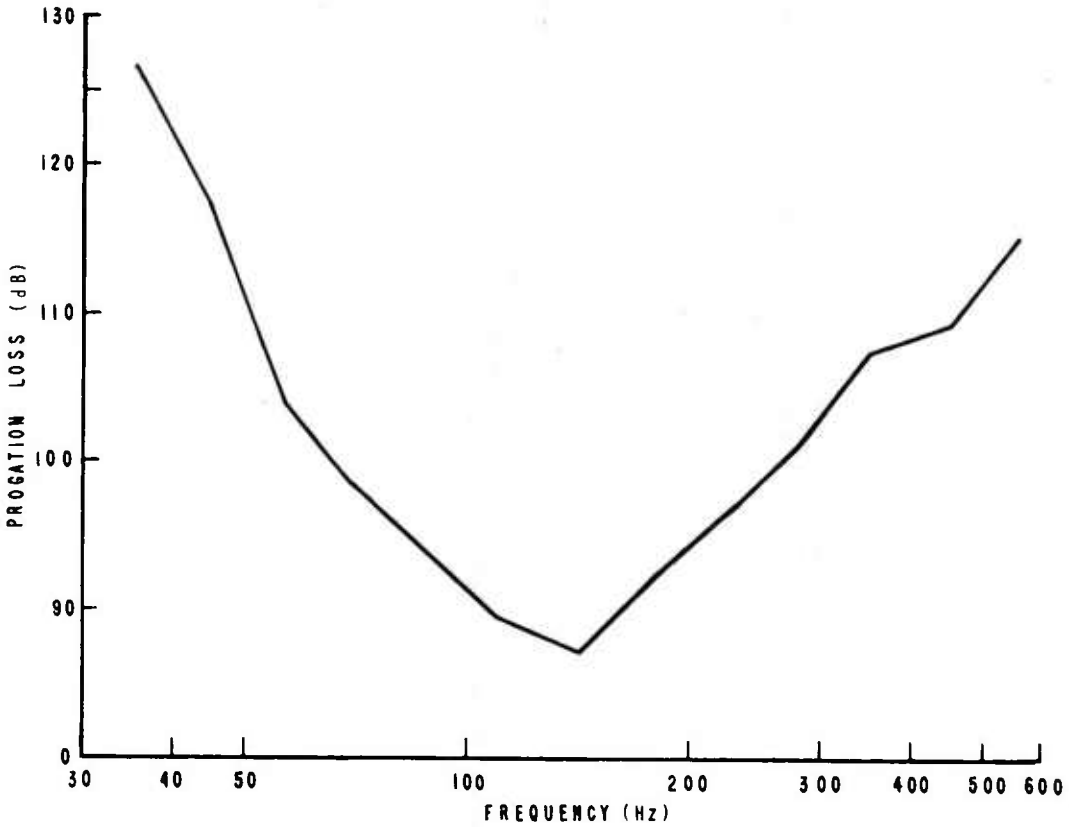

Figure 29. Propagation Loss versus Frequency, August 1967

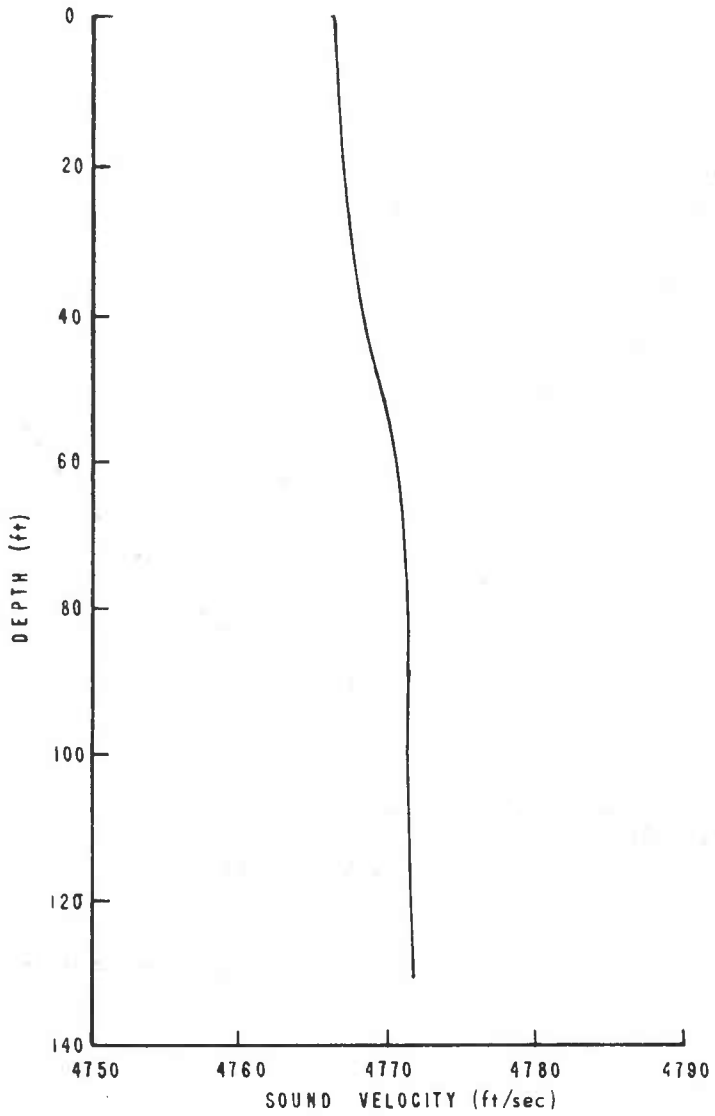

Figure 30. Velocity Profile, 30 January 1968

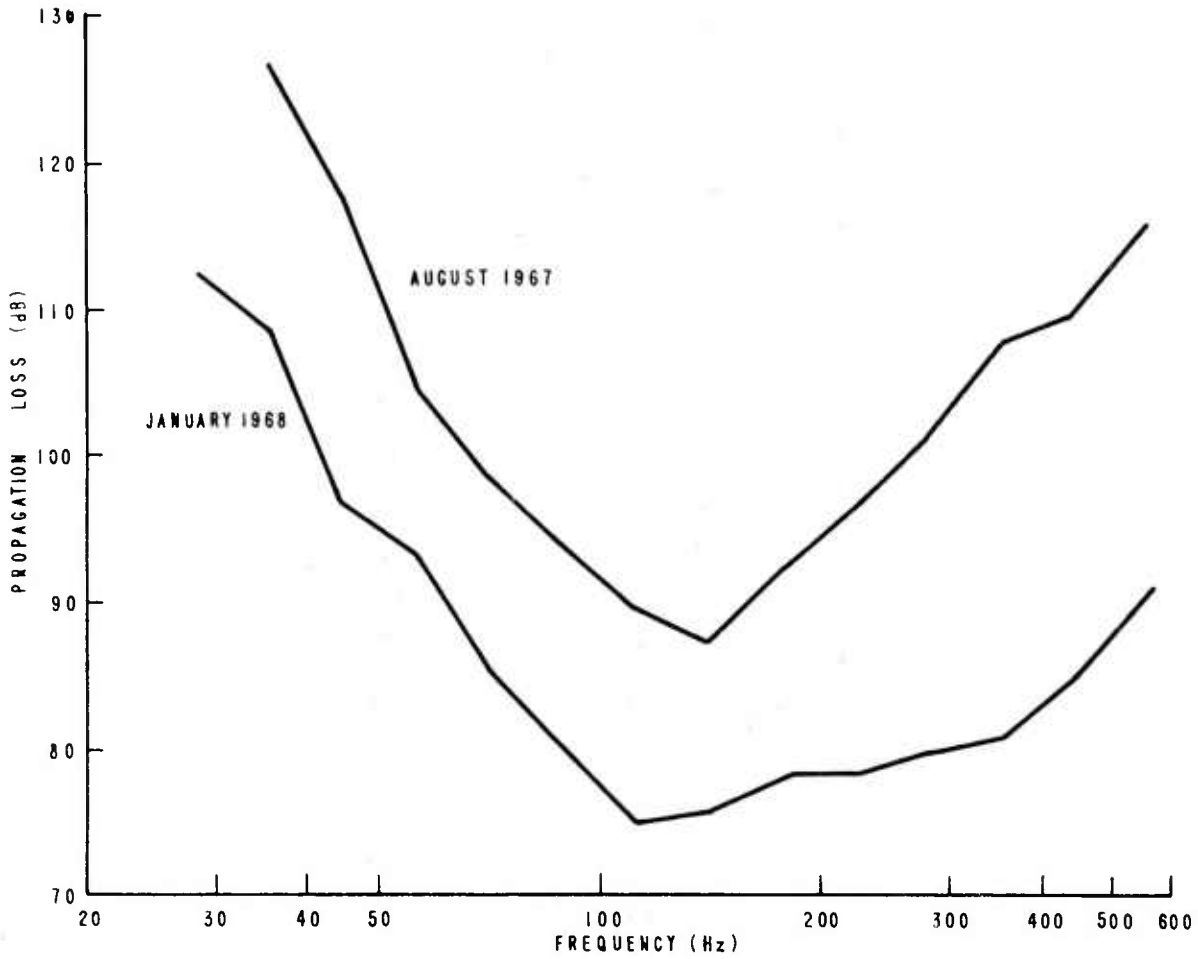

Figure 31. Propagation Loss versus Frequency, January 1968 and August 1967

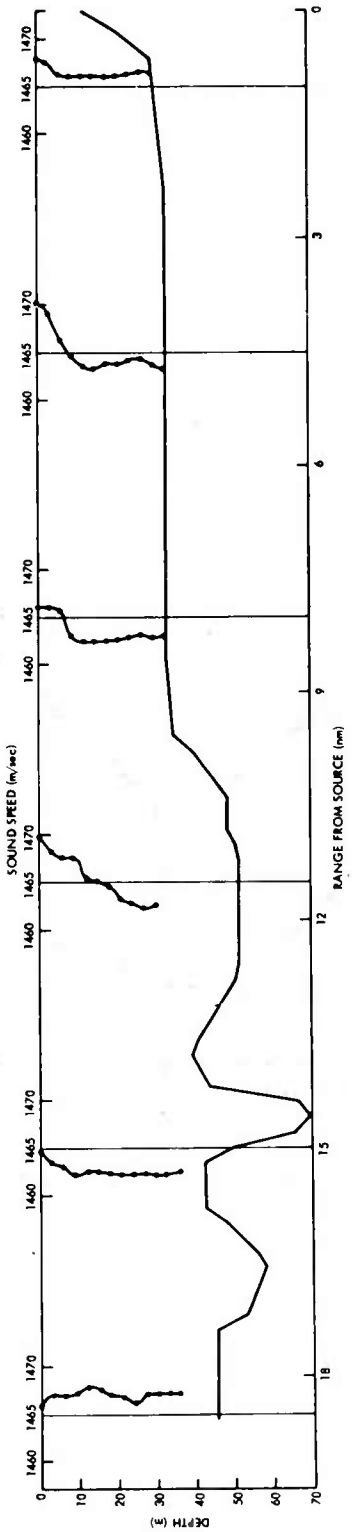

Figure 32. Velocity Profiles, 19 April 1968

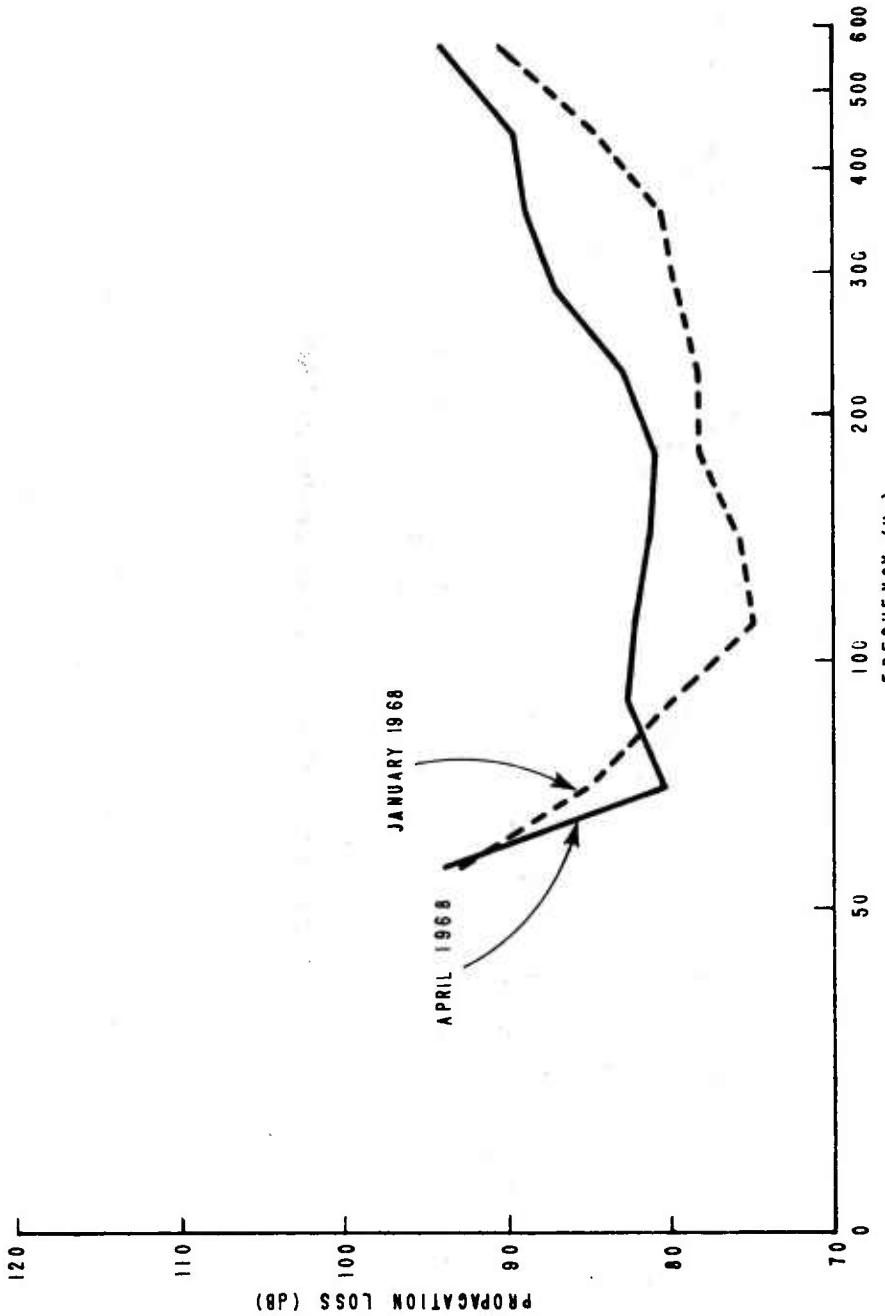

Figure 33. Propagation Loss versus Frequency, January and April 1968

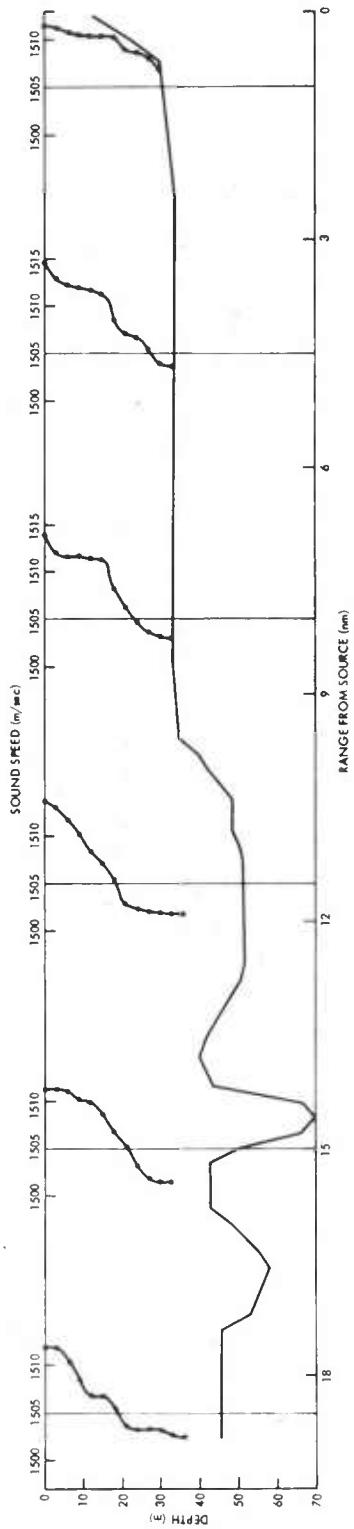

Figure 34. Velocity Profiles, 28 August 1968

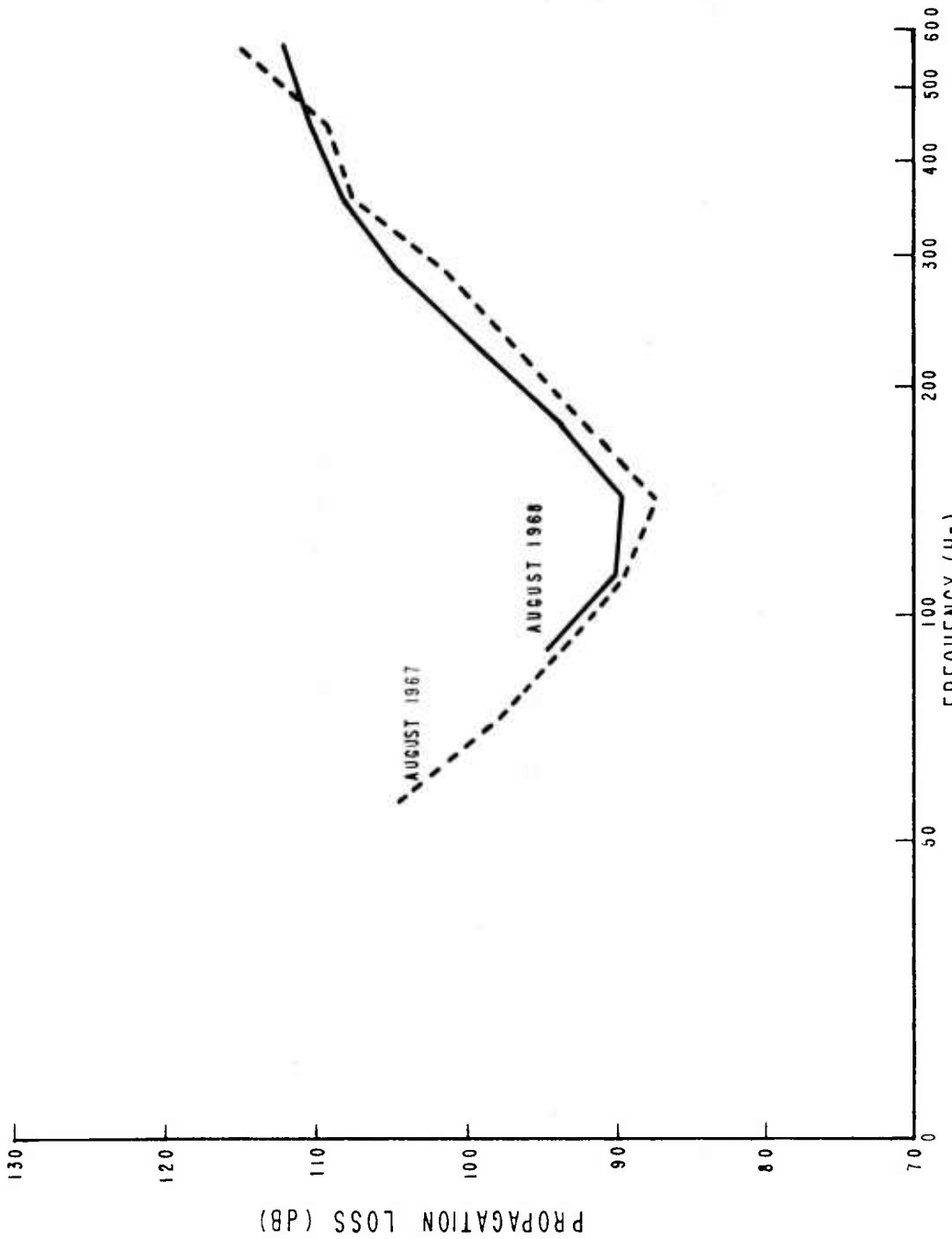

Figure 35. Propagation Loss versus Frequency, August 1967 and August 1968

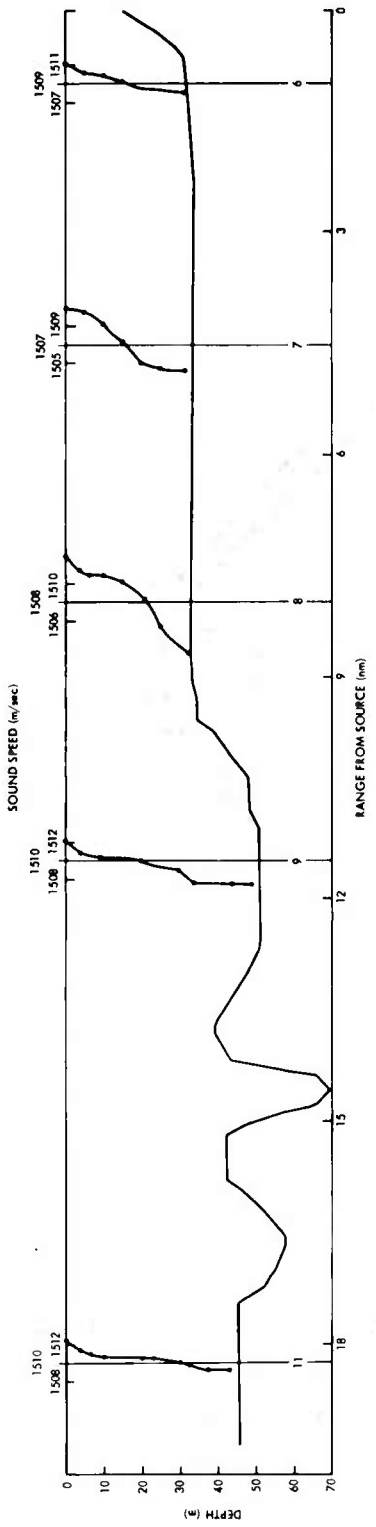

Figure 36. Velocity Profiles, 2 October 1968

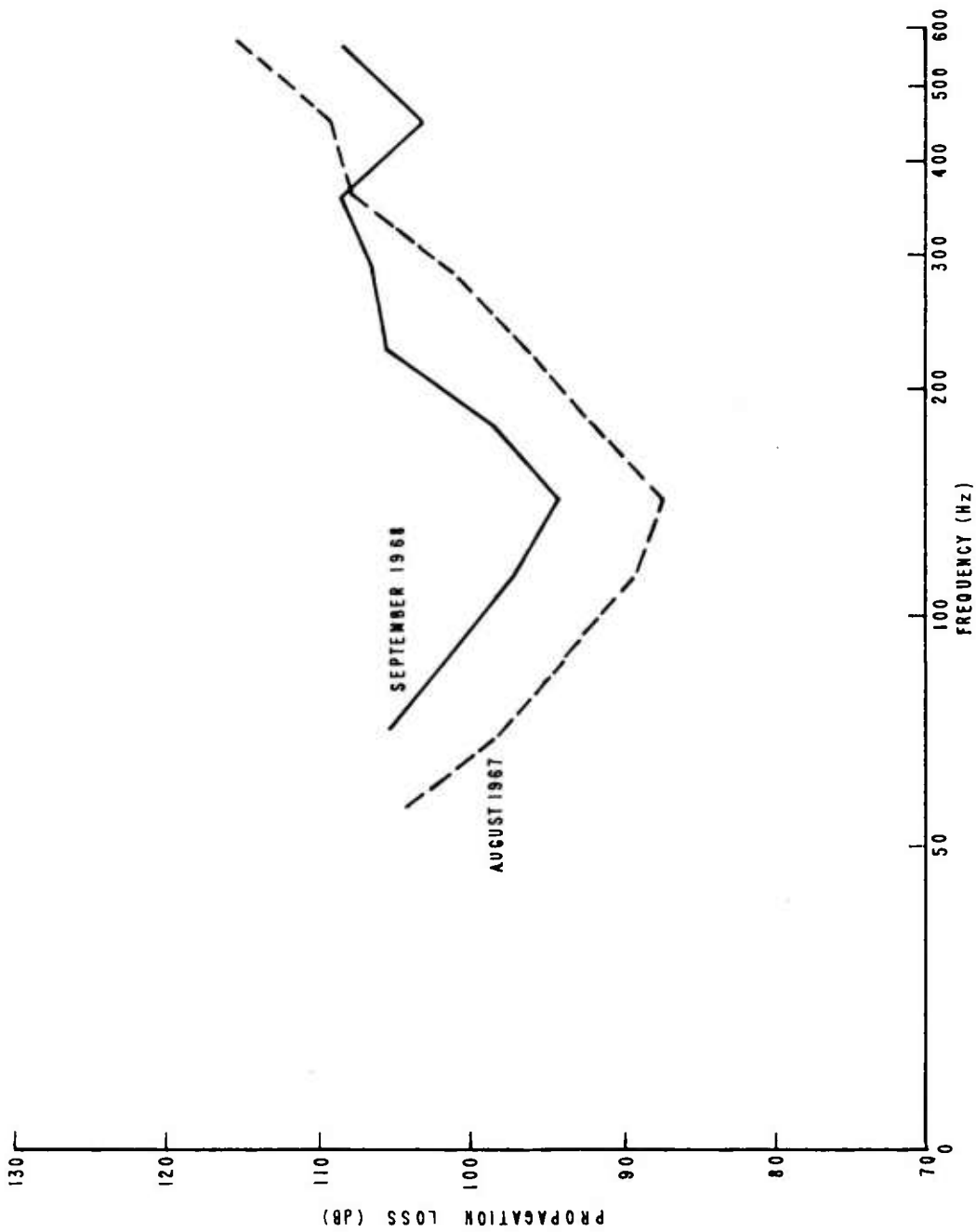

Figure 37. Propagation Loss versus Frequency, August 1967 and September 1968

Section 4
SUMMARY AND CONCLUSIONS

Program S1441 is designed to calculate and plot many quantities of interest in the study of a sound field in an ocean bounded by flat parallel boundaries. The problem of acoustic propagation is approached from the standpoint of physical and ray acoustics.

Program S1548 is designed to calculate and plot many quantities of interest in the study of a sound field in an ocean whose boundaries vary in depth and acoustic properties. Changes in the velocity profile over the range may also be included in the calculations.

The theoretical predictions using programs S1441 and S1548 differ by small or moderate amounts in four of the explosive tests considered. In the January 1968 tests, the difference is considerable, and predictions using program S1548 are physically more plausible. This is true also to a lesser degree in the other explosive tests. Therefore, assumption of a medium in which stratification is a function of position seems to be an improvement over that of a medium with constant stratification with range.

The results derived from the explosive tests are consistent with normal mode predictions. Three major factors account for the relationship between propagation loss and frequency. First, excitation pressure decreases with increasing frequency, which has the effect of increasing propagation loss with increasing frequency. Second, skip distance, in general, increases with frequency, thereby decreasing propagation loss with increasing frequency. In the BIFI range, these two effects seem to cause the minimum propagation loss at a frequency around 100 to 200 Hz. This minimum is either enhanced or depressed by the third factor, the frequency at which vertexing commences. If vertexing occurs near the minimum, as in August 1967 and August 1968, the minimum is enhanced; if it occurs away from the minimum, the minimum is rendered less pronounced.

An interesting effect explained by the normal mode analysis is the dependence of propagation loss on the size of the negative gradient of the velocity profile. In general, propagation loss will increase with the size of the negative gradient because an increase in the negative gradient will tend to decrease the angle, θ_b, at which energy strikes the bottom, thereby decreasing the skip distance. However, this increase in negative gradient also lowers the frequency at which vertexing first occurs, which normally corresponds to the largest skip distance at any frequency. So, in August 1967 and August 1968, propagation loss at the lower frequencies is less than

the corresponding loss in September 1968, even though much larger negative gradients were observed in the velocity profiles taken during the August tests. This circumstance may be attributed to the fact that vertexing took place at about 150 Hz in August and at about 350 Hz in September. The August skip distances at low frequencies were larger than the corresponding skip distances in September. This is compatible with normal mode theory, which states that at low frequencies, propagation loss should increase to maximum as the gradient becomes negative and then decrease with a further increase in the size of the negative gradient. At the higher frequencies in the case of the profiles considered, propagation loss increases with increasingly negative gradients.

The determination of the exact skip distance is a major problem in normal mode analysis. As explained previously, the skip distance assumed over the entire range was calculated by using the velocity profile with the largest gradient. As a consequence, whenever there is a large variation in the velocity profile over the range, there is a bias in the calculations of skip distance as a function of frequency. This can be seen in table 9, where the calculated loss per bounce is extremely high at 355 Hz, the frequency at which the skip distance is maximum. The bias is especially severe when the bottom loss is high and the velocity profile varies significantly over the range.

An alternative method of determining skip distance would be to take an average of the skip distance over each segment as weighted by the length of each segment. One drawback to this method is that segments with large gradients would be weighted evenly with those possessing small gradients; the effect of the small-gradient segments on propagation loss might be smaller than the effect of the large-gradient segments. If an analysis similar to the one described here is performed in the future, program S1548 should be modified to do the calculations suggested, and the results should be compared with skip distances calculated for the segment with the largest velocity gradient. Ideally, an investigator would want to know the bottom loss per bounce in each segment so that he could determine the total loss by summing the product of loss per bounce by the number of bounces in each segment. However, experimental determination of bottom loss as a function of frequency for angles of about 75 to 90°, relative to the normal, would be extremely difficult to perform.

As expected, it was found that, for a given frequency, loss per bounce decreased as the angle of incidence relative to the normal increased. Loss per bounce as a function of frequency did not show any marked trends except for the January

data in the case of an irregular bottom. Here, the angle of incidence increased extremely rapidly with frequency, and the bottom loss went to zero as the rays nearly vertexed close to the bottom. Since the angle of incidence at the bottom increases with frequency, it might be concluded in the other cases that the bottom loss for a constant incident angle would also increase with frequency.

The theoretical predictions for flat and irregular bottoms differ by small or moderate amounts in four out of the five tests considered. In the January 1968 tests, the difference is considerable, with the predictions for the irregular bottom physically more plausible. This is true also to a lesser degree in the other tests. Therefore, the assumption of an irregular bottom seems to be an improvement over the assumption of a flat bottom.

Further investigation of the effects described in this report will be conducted during daily propagation tests at frequencies of 127, 400, and 1702 Hz.

REVERSE BLANK

LIST OF REFERENCES

1. Arthur D. Little, Inc., Design of an Arroy to Excite Individual Normol Modes in the BIFI Range, Report No. C-70673, 31 Januory 1969.

2. Arthur D. Little, Inc., "A Memorandum Describing the Computer Program Used to Calculate Normol Modes in the BIFI Range," February 1969.

3. W. R. Schumacher, "Shollow Water Acoustical Studies: Informotion Concerning," NUSL Technicol Memorondum No. 2211-18-68, 17 Januory 1968.

4. C. L. Pekeris, "Theory of Propagotion of Explosive Sound in Shallow Water," Geological Society of Americo Memoir No. 27, 15 October 1948.

5. C. B. Officer, "Normal Mode Propagation in Three Loyered Liquid Half-Space by Ray Theory," Journal of Applied Physics, vol. 23, 1952, p. 997.

6. G. Birkhoff and G. Rota, Ordinory Differential Equations, Ginn and Company, New York, 1962.

7. W. G. Kanobis ond H. F. Bernier, "Propagation in BIFI Range Using Explosive Sources," NUSL Technical Memorandum No. 2211-93-68, 25 March 1968.

8. W. G. Kanabis, "BIFI Propagation Tests of 30 Jonuary 1968," NUSL Technical Memorandum No. 2211-185-68, 8 July 1968.

9. C. B. Officer, Introduction to the Theory of Sound Transmission, McGrow-Hill Book Company, Inc., New York, 1958.

10. H. Weinberg and L. T. Einstein, "Eigenray Analysis for an Ocean Model with a Sloping Bottom," NUSL Technicol Memorondum No. 2070-25-67, 26 January 1967.

11. L. M. Brekhovskikh, Waves in Layered Media, Acodemic Press, Inc., New York, 1960.

12. I. Tolstoy and C. B. Clay, Ocean Acoustics, McGraw-Hill Book Company, Inc., New York, 1966.

13. I. Tolstoy, "Shallow Water Test of the Theory of Layered Wave Guides," Journal of the Acoustical Society of America, vol. 30, 1958, p. 340.

14. M. A. Biot, "General Theorems on Equivalence of Group Velocity and Energy Transport," The Physical Review, vol. 105, 1957, p. 1129.

15. W. H. Thorp, "Deep Ocean Sound Attenuation in the Sub- and Low-Kilocycle-per-Second Region," Journal of the Acoustical Society of America, vol. 38, 1965, p. 648.

16. F. R. DiNapoli, Fast Field Program for Multilayered Media, NUSC Report No. 4103, 26 August 1971.

17. C. L. Bartberger and L. L. Ackler, Normal Mode Solutions and Computer Programs for Underwater Sound Propagation, NADC report (in preparation).

18. R. O. Davidson and G. A. Leibiger, Computer Program for Normal Mode Propagation in a Shallow Water Acoustic Test Range, Vitro Laboratories Report No. VL-1028-9-0, 3 March 1969.

19. A. O. Williams and M. N. Lewis, Approximate Normal Mode Method of Calculation for Sound Propagation in Shallow Water, Brown University Technical Report No. 56-1, 1956.

20. W. G. Kanabis and H. J. Arens, Determination of Acoustic Parameters, Using Normal Mode Theory, NUSC Technical Report 4335 (in preparation).

21. W. G. Kanabis, BIFI Forty-Eight Hour Tests, NUSC Technical Report 4441 (in preparation).

22. D. E. Weston, "Underwater Explosives As Acoustic Sources," Proceedings of the Physical Society (London), August 1960.

23. R. G. Williams, T. Azarovitz, and J. Lamoureux, Seasonal Variations of Temperature and Sound Speed in Block Island Sound, NUSC Report No. 4131, 30 December 1971.

Appendix A

LIST OF PROGRAM S1441

```
      DOUBLE PRECISION     F,U,UP
      DOUBLE PRECISION               K2,    W2,P2,H,ZP,   CZ,G,H2,DEN
      DOUBLE PRECISION S,K20,DK2,GAM,BA
      DOUBLE PRECISION E,V
      DOUBLE PRECISION  UMAX
      DOUBLE PRECISION  COS2 , CCC  , CV
      DIMENSION HED(20),Z(100),C(100),F(500),UP(500) ,U(500) ,
     1  ZMP(1000), XMP(1000), COS2(500), CCC(500)
     1  , ZZP(500) , ZPP(500),  VV(500),  DATA(1024) , UU(500)
     1  ,PM(3000)           ,DDT(100)
     1  , ZR(500) , CR(500) ,RP(3000),ZBT(5) , ZBF(5)
     1,DD(100),PPT(3000),PCT(3000),PST(3000),MDS(100),USR(100),URR(100),
     1  PMM(100),FMR(100)  ,FDS(100)
     1 ,GVEL(2000), PVEL(2000), FQP(2000), T1(2000), T2(2000)
      COMMON MS,JM,U
      COMMON JMS
      CALL PLOTS  ( DATA(1), 1024,  6  )
    4 JPM = 25
      READ(3,1)HED
    1 FORMAT (20A4)
      READ (3,112)        NUMV, VEL1  , IVOP  ,IRP  , IVPL  , IEX
  112 FORMAT ( I10,F10.0,4I10)
      NUM  =  0
      READ(3,2) ZM,CB,RO,RB ,FSC
    2 FORMAT (5F10.3)
      ZMB = (200.0*FSC - ZM)/(20.0*FSC)
      ZBT(1) = ZM
      ZBT(2) = ZM
      ZBT(3) = 200.0 *FSC
      ZBT(4) = -20.0*FSC
      ZBF(1) =  0.0
      ZBF(2) = 10.0
      ZBF(3) =  0.0
      ZBF(4) =  1.0
      DO 3 I=1,100
      Z(I) = 0.
    3 C(I) = 0.
      I=1
    5 READ (3,30) Z(I),C(I)
   30 FORMAT(2F10.3)
      IF(DABS(Z(I)-ZM)-.01)6,6,7
    7 I = I+1
      GO TO 5
    6 I = 1
      IF (IVPL.EQ.1)  GO TO 8
      DO 130  K  =  1, NUMV
      CR(NUMV -K +1)  =  C(K)
  130 ZR(NUMV -K +1)  =  Z(K)
      ZR(NUMV +1) = ZM -0.01
      ZR(NUMV +2) = ZM +50.0
      CR(NUMV  +1)  =  CB
      CR(NUMV  +2)  =  CB
      DO 185   NINY  = 1, NUMV
  185 ZR(NINY)  =  ZM - ZR(NINY)
      ZR(NUMV +3) = 200.0*FSC
      ZR(NUMV +4) = -20.0*FSC
      CR(NUMV  +3)  =  VEL1
```

```
      CR(NUMV  +4)  =  50.0
      CALL PLOT (0.0,0.0,-3)
      CALL LINE (CR,ZR,NUMV +2, 1,0,0  )
      CALL LINE (ZBF,ZBT,2,1,0,0)
      CALL SYMBOL (10.25,ZMB,0.14,6HBOTTOM,0.0,6 )
      CALL AXIS (0.0,0.0,14HSOUND VELOCITY,14,10.,0.0,CR(NUMV  +3) ,
     1CR(NUMV+4),10.0  )
      CALL AXIS (0.0,0.0,11HWATER DEPTH,11,10.0,90.0,ZR(NUMV +3)  ,
     1ZR(NUMV+4),10.0  )
      CALL PLOT (15.0,0.0,-3)
      ZR(NUMV +1) = 200.0*FSC
      ZR(NUMV +2) = -20.0*FSC
      CR(NUMV +1) =VEL1
      CR(NUMV +2) =10.0
      CALL LINE (CR,ZR,NUMV,1,0,0)
      CALL LINE (ZBF,ZBT,2,1,0,0)
      CALL SYMBOL (10.25,ZMB,0.14,6HBOTTOM,0.0,6 )
      CALL AXIS (0.0,0.0,14HSOUND VELOCITY,14,10.,0.0,CR(NUMV  +1) ,
     1CR(NUMV+2),10.0  )
      CALL AXIS (0.0,0.0,11HWATER DEPTH,11,10.0,90.0,ZR(NUMV +1)  ,
     1ZR(NUMV+2),10.0  )
      CALL PLOT  ( 15.0,0.0, -3)
    8 JP = 3
  188 WRITE(4,9)HED
    9 FORMAT (1H1,9X,20A4)
      WRITE(4,10)
   10 FORMAT(1H0,15X,4HZ,FT,5X,8HC,FT/SEC)
   11 WRITE(4,12)ZR(I),CR(I)
   12 FORMAT(1H0,9X,F10.1,F12.1)
      IF(DABS(Z(1)-ZM)-.01)14,14,13
   13 I = I+1
      JP = JP+1
      IF(JP-JPM)11,8,8
   14 READ(3,15)N,  UM ,FQ
   15 FORMAT(I10,2F10.3)
      NNN  =  N
  151 READ (3,150) ISFQ, IEFQ, NMOD, INCF
  150 FORMAT (4I10)
      IF (IRP.NE.1)  GO TO 120
      READ (3,121) IRST, IREN, IRIC, NPS, ZS, ZRC  ,FMI
  121 FORMAT (4I10, 3F10.3)
      ZS = ZM - ZS
      ZRC = ZM - ZRC
      READ (3,122)  (DD(J), J= 1,NMOD)
  122 FORMAT (4F10.5)
  120 DO 154  M=  1,NMOD
      DO 155  L= ISFQ, IEFQ,-INCF
      IF (IVOP.NE.1)   GO TO 162
      FQ  =  L
  162 P2 = 6.283185306
      W2 = (P2*FQ)*(P2*FQ)
      N  =  NNN
      FMOD = M
      IREL = 0
      IF(N)29,4,29
   29 K20 = ((W2*(CB-C(1))*(CB+C(1)))/(C(1)*C(1)*CB*CB))
      DK2= .099*K20
      K2 = -K20
```

```
 31 K2 = K2 + DK2
    IF(K2-K20)16,32,32
 32 WRITE(4,33)
 33 FORMAT(1H0,13HNO MODE FOUND)
    IEFQ  =  L  + INCF
    IF (IVOP.EQ.1)  GO TO 160
    GO TO 111
 16 FLB  =  FLOAT(N)
    H = ZM/ DBLE(FLB)
    ZP = 0.
    J = 1
    I = 1
 17 IF (ZP- Z(I+1)) 18,18,19
 19 I = I+1
    GO TO 17
 18 CZ = (C(I)*(Z(I+1)-ZP)+C(I+1)*(ZP-Z(I)))/(Z(I+1)-Z(I))
    CCC(J)  =  CZ
    G =-(W2*(C(1)-CZ)*(C(1)+CZ))/(CZ*CZ*C(1)*C(1))
    F(J) = K2 - G
    IF(ZP-ZM) 20,21,21
 20 J=J+1
    FLA  =  FLOAT(J -1)
    ZP  =  ZM*DBLE(FLA)/DBLE(FLB)
    GO TO 17
 21 U(1) = 1.0
    UP(1) =(RO/RB)*DSQRT ((W2*(CB-C(1))*(CB+C(1)))/(C(1)*(C(1)*CB*CB))
   1-K2)
    J = 1
 22 JP = 3
 25 FLA  =  FLOAT(J -1)
    FLB  =  FLOAT(N)
    ZP  =  ZM*DBLE(FLA)/DBLE(FLB)
    IF(J-N-1)27,34,27
 27 IF(DABS(U(J))-UM)28,34,34
 28 J = J+1
    JP= JP+1
    H2= H*H
    DEN = 1.0 + (H2*F(J))/6.0
    U(J)= ((1.0-(H2/3.0)*F(J-1))*U(J-1)+H*UP(J-1))/DEN
    UP(J)=((1.0-(H2*F(J))/3.0)*UP(J-1)-(F(J-1)+F(J)-(H2*F(J)*F(J-1))/
   16.0)*H*U(J-1)* 0.5)/DEN
    IF (JP-JPM)25,22,25
 34 JM = J
    CALL COUNT
195 IF (MS-M)31,35,35
 35 K2 = K2 - DK2
    DK2= DK2 / 10.0
    IF(DK2- .000001*K20 *10**(-IEX))36,36,31
 36 J = 2
    S = H*U(1)*U(1)/2.0
    S2= H*U(1)*U(1)/(2.0*CCC(1)*CCC(1))
 37 IF(J-JMS)38,39,38
 38 S = H*U(J)*U(J)+S
    S2= H*U(J)*U(J)/(CCC(J)*CCC(J))  +S2
    J = J+1
    GO TO 37
 39 S =(H*U(J)*U(J)/2.0) + S
    S2= H*U(J)*U(J)/(2.0*CCC(J)*CCC(J))  +S2
```

```
      IF (IVOP.EQ.1)  GO TO 164
      J = 1
   42 JP = 3
      WRITE(4,23)HED,N,K2,UM,FQ,M
   23 FORMAT(1H1,5X,20A4,//,2X,3HN =,I5,2X,4HK2 =,F15.8,2X,4HUM =,F6.1,
     12X,6HFREQ = ,F8.1,2X,3HM =,I5)
      WRITE(4,47) ZM,CB,RO,RB
   47 FORMAT(3X,6HZMAX = ,F10.3,4HCB = ,F10.3,4HRO = ,F15.8,4HRB = ,
     1F15.8)
      WRITE(4,24)
   24 FORMAT(1H0,17X,4HZ,FT,10X,1HU,10X,5HDU/DZ,11X,4HF(Z))
   43 ZP = ZM*( FLOAT(J-1)/ FLOAT(N))
      ZQ = ZM - ZP
      WRITE(4,26)ZQ,U(J),UP(J),F(J)
      IF(J-N-1)45,44,45
   45 IF(DABS(U(J))-UM)46,44,44
   46 J = J+1
      JP = JP+1
      IF(JP-JPM)43,42,43
   44 WRITE(4,40) S
   40 FORMAT (1H0,10X, 3HS = ,F15.5)
  164 UMAX = 0.0
      NM  =  N  +1
      DO  104  K=  1, NM
      IF  ( DABS (U(K)) - UMAX)  104,104,103
  103 UMAX  =  DABS(U(K) )
  104 CONTINUE
      DO  105  K=  1, NM
  105 UU(K) =  U(K)/UMAX
      DO 106  K= 1, NM
  106 ZZP(K)  =  ZM*(FLOAT(K -1)/FLOAT(N)  )
      GAM = DSQRT(K20 - K2)
      BA = (RO*C(1))/(2.0*RB*CB*GAM*S )
      WRITE(4,41) BA,GAM
   41 FORMAT(1H0,10X,5HB/A = ,F15.5,5X,7HGAMMA = ,F15.5 )
      SS=  RO*S/(UMAX*UMAX)+RO* RO*U(1)*U(1)/(UMAX*UMAX*2.0*GAM*RB)
      SSS= RO*S2/(UMAX*UMAX)              +       RO*RO*U(1)*U(1)/(UMAX*UMAX
     1*2.0*GAM*RB*CB*CB)
      IF(IVOP.EQ.1)  GO TO 153
      E = DEXP(-GAM*H)
      ZP = 0.0
      V = 1.0
      NN  =  1
      ZPP(1)  =  0.0
      VV(1)  = UU(1)
      WRITE(4,23)HED,N,K2,UM,FQ,M
      WRITE(4,47) ZM,CB,RO,RB
      WRITE(4,48)
   48 FORMAT(1H0,17X,4HZ,FT,10X,1HU )
   49 WRITE(4,26)ZP,V
   26 FORMAT(1H0,F22.2,F13.3,F13.3,F16.5)
   50 V = V*E
      NN  = NN  +1
      VV(NN)  =  VV(NN -1)*E
      ZPP(NN)  =  ZP -      H
      ZP = ZP-H
      IF  (ZPP(NN)  + 50.0)          110, 110,  49
  110 CALL PLOT  (  5.0,0.0, -3)
```

```
      DO 184    NINX  = 1, NN
  184 ZPP(NINX) =  ZM - ZPP(NINX)
      NINV  =  N + 1
      DO 183    NINW  = 1, NINV
  183 ZZP(NINW) =  ZM - ZZP(NINW)
      VV(NN +1)  =  -1.0
      VV(NN +2)  =  0.5
      ZPP(NN +1) = 200.0*FSC
      ZPP(NN +2) = -20.0*FSC
      ZZP(N +2)  = 200.0*FSC
      ZZP(N +3)  = -20.0*FSC
      UU(N+2)  =  -1.0
      UU(N+3)  =  0.5
      CALL  AXIS (0.0,0.0, 9HAMPLITUDE,  9,4.0,0.0,UU(N+2),UU(N+3),10.0)
      CALL AXIS (0.0,0.0,16HWATER DEPTH (FT),16,10.0,90.0,ZZP(N+2),
     1  ZZP(N +3),10.0)
      CALL LINE  (UU, ZZP,  N+1, 1,0,0)
      CALL LINE (VV, ZPP,  NN,  1,0,0  )
      CALL LINE (ZBF,ZBT,2,1,0,0)
      CALL SYMBOL (10.25,ZMB,0.14,6HBOTTOM,0.0,6 )
      CALL SYMBOL(1.3,9.50,0.14,9HAMPLITUDE,0.0,9)
      CALL SYMBOL(1.7,9.25,0.10,6HVERSUS,0.0,6)
      CALL SYMBOL(1.6,9.00,0.14,5HDEPTH,0.0,5)
      CALL SYMBOL(0.8,8.75,0.14,19HFREQUENCY         HZ,0.0,19)
      CALL NUMBER(2.2,8.75,0.14,FQ,0.0,-1)
      CALL SYMBOL(1.4,8.50,0.14,4HMODE,0.0,4)
      CALL NUMBER(2.1,8.50,0.14,FMOD,0.0,-1)
      NUM  =  NUM  +1
  153 XMP(1)  =  0.0
      ZMP(1)  =  0.0
      NM  =  N  +1
      CALL PLOT (15.0,0.0,-3)
      NSTR = 1
      NEND = N +1
      IDZ = 0
      IF(F(1).GT.0.0)   GO TO 179
  181 DO 170 K=  NSTR,NEND
      IF(F(K).GT.0.0)    GO TO 171
  170 IRTB = K
      GO TO 189
  171 COS2(IRTB +1) = F(IRTB +1)*CCC(IRTB +1)*CCC(IRTB +1)/W2
      CV  =  CCC(IRTB +1)/DSQRT(1.0 - COS2(IRTB +1))
      ZMP(2) = H*(CV - CCC(IRTB +1))/(CCC(IRTB)-CCC(IRTB +1))
      XMP(2) =  (ZMP(2) - ZMP(1))*(CCC(IRTB +1) + CV)/(CV*(DSQRT(COS2
     1 (IRTB +1))))
      ZMP(1) = FLOAT(IRTB)*H - ZMP(2)
      ZMP(2) = ZMP(1) + ZMP(2)
      NM = NM -IRTB +1
      DO 172  K = 3,NM
      TH1 = 90.0
      KO = IRTB -1 +K
      COS2(KO-1) = F(KO -1)*CCC(KO -1)*CCC(KO -1)/W2
      COS2(KO)=F(KO)*CCC(KO)*CCC(KO)/W2
      IF(CCC(KO).GE.CV) ZMP(K) = ZMP(K  -1) +H*(CV- CCC(KO -1))/(CCC(KO)
     1 -CCC(KO -1))
      IF(CCC(KO).GE.CV)   GO TO 152
      XMP(K) = XMP(K  -1) +H*(CCC(KO -1) + CCC(KO))/(CV*(DSQRT(COS2(KO-1
     1)) + DSQRT(COS2(KO))))
```

```
172 ZMP(K)  =  (KO -1)*H
    TH2 = (ACOS(SQRT(COS2(NM +IRTB -1))))*57.2958
    N =  NM -1
    GO TO 173
179 COS2(1)  =  ABS(F(1))*CCC(1)*CCC(1)/W2
    CV  =  CCC(1)/DSQRT(1.0 - COS2(1) )
    DO 140  K=  2,NM
    COS2(K -1) = ABS(F(K -1))*CCC(K -1)*CCC(K -1)/W2
    COS2(K)  =  ABS(F(K))*CCC(K)*CCC(K)/W2
    TH1 =(ACOS(SQRT(COS2(1))))*57.2958
    TH2 =(ACOS(SQRT(COS2(NM))))*57.2958
    IF( CCC(K).GE.CV)  GO TO 142
    XMP(K) = XMP(K -1) + H*(CCC(K-1) + CCC(K))/(CV*(DSQRT(COS2(K-1))+
   1 DSQRT(COS2(K))))
140 ZMP(K)  =  (K-1)*H
173 DO 141  K=  1,N
    XMP(NM +K) = 2.0*XMP(NM)  -  XMP(NM - K)
141 ZMP(NM +K) = ZMP(NM -K)
    GO TO 143
142 ZMP(K) = ZMP(K -1)  +  H*(CV - CCC(K-1))/(CCC(K) - CCC(K -1))
152 TH2  =  90.0
    XMP(K) = XMP(K -1) + (ZMP(K) - ZMP(K-1))*(CCC(K-1) + CV)/(CV*(
   1  DSQRT(COS2(K -1))))
    N = K -1
    NM  =  K
    DO 144  K=  1,N
    XMP(N+1+K) = 2.0*XMP(N+1) - XMP(N+1-K)
144 ZMP(NM +K) = ZMP(NM -K)
143 XMP(2*NM)  =  0.0
182 XMP(2*NM +1)  =  1000.0
    NIZZ = 2*NM -1
    DO 186 NINZ = 1, NIZZ
186 ZMP(NINZ) = ZM - ZMP(NINZ)
    ZMP(2*NM)  =  200.0*FSC
    ZMP(2*NM +1)  = -20.0*FSC
    WRITE (4,145) TH1,TH2  ,XMP(NM +N)
    IF (IVOP.EQ.1)  GO TO 157
145 FORMAT (3F10.3)
    CALL LINE (XMP,ZMP,NM +N,1,0,0)
    IF (IDZ.EQ.1) GO TO 650
    IDZ = 1
    CALL LINE (ZBF,ZBT,2,1,0,0)
    CALL SYMBOL (10.25,ZMB,0.14,6HBOTTOM,0.0,6 )
    CALL AXIS (0.0,0.0,10HRANGE (FT),10,12.0,0.0,XMP(2*NM)
   1XMP(2*NM +1),10.0)
    CALL AXIS (0.0,0.0,16H       DEPTH (FT),16,10.0,90.0,ZMP(2*NM),
   1 ZMP(2*NM +1),10.0 )
    CALL SYMBOL(5.0,9.50,0.14,14HRAY EQUIVALENT,0.0,14)
    CALL SYMBOL(5.0,9.25,0.14,19HFREQUENCY         HZ,0.0,19)
    CALL NUMBER(6.4,9.25,0.14,FQ,0.0,-1)
    CALL SYMBOL(5.5,9.00,0.14,4HMODE,0.0,4)
    CALL NUMBER(6.2,9.00,0.14,FMOD,0.0,-1)
    NM = NEND
650 NSTR =        IRTB + NM -1
    ZMP(1) = 0.0
    IF(NSTR.GE.NEND) GO TO 189
    GO TO 181
189 CALL PLOT (15.0,0.0,-3)
```

```
      IF (IVOP.NE.1)   GO TO 154
  157 T1(L) = TH1
      T2(L) = TH2
      FMH = SQRT(P2*FQ /(30.48*CV) )
      PM(L) = SQRT(P2)*       RO/(FMH*2.0*(SS) )
      GVEL(L) = SS/(CV*SSS)
      FQP(L) = L
      WRITE ( 4,166)  PM(L) , FMH, SS  , GVEL(L)
  166 FORMAT(4F10.3)
      IF (IRP.EQ.1) PM(M) = PM(L)
      FMH(M) = P2*FQ/CV
      IZS = ZS*FLB/ZM   +1.0
      IZR =ZRC*FLB/ZM   +1.0
      USR(M) = U(IZS)/UMAX
      URR(M) = U(IZR)/UMAX
      PMM(M) = PM(M)*USR(M)*URR(M)/RO
  155 PVEL(L) = CV
      IF (IRP.EQ.1) GO TO 154
  160 IDF   = (ISFQ - IEFQ)/INCF  +1
      LIFQ = IDF -1
      DO 161 LLL= 1, IDF
      ILL  =  (LLL  -1)*INCF
      FQP(LLL)  =  FQP(IEFQ+ILL)
      GVEL(LLL)  =  GVEL(IEFQ+ILL)
      T1(LLL)  =  T1(IEFQ+ILL)
      T2(LLL)  =  T2(IEFQ+ILL)
      PM(LLL) = PM(IEFQ + ILL)
  161 PVEL(LLL)  =  PVEL(IEFQ+ILL)
      WRITE(4,163)  (PVEL(J), GVEL(J), FQP(J), PM(J), J= 1,IDF)
  163 FORMAT (4F10.3)
      FQP(LIFQ +2)  =  0.0
      FQP(LIFQ +3) =  ISFQ/10
      PVEL(LIFQ +2)  =  3500.0
      PVEL(LIFQ +3)  =  250.0
      GVEL(LIFQ +2)  =  3500.0
      GVEL(LIFQ +3)  =  250.0
      PM(LIFQ  +2)  =  0.0
      PM(LIFQ  +3)  =  0.1
      CALL PLOT (15.0,0.0,-3)
      CALL LINE (FQP,PVEL,LIFQ +1,1,10,14)
      CALL LINE (FQP,GVEL,LIFQ +1,1,10,28)
      CALL LINE (FQP,PM,LIFQ +1,1,10,4)
      CALL AXIS (0.0,0.0,14HFREQUENCY (HZ),14,10.0,0.0,FQP(LIFQ +2),
     1 FQP(LIFQ +3),10.0)
      CALL AXIS (0.0,0.0,27HSOUND VELOCITY (FT PER SEC),27,10.0,90.0,
     1  PVEL (LIFQ +2),PVEL(LIFQ +3),10.0)
      CALL AXIS(10.0,0.0,18HEXITATION PRESSURE,-18,10.,90.0,PM(LIFQ +2),
     1 PM(LIFQ +3),10.0)
      CALL SYMBOL(2.4,9.50,0.14,38HSOUND VELOCITY AND EXCITATION PRESSUR
     1E,0.0,38)
      CALL SYMBOL(4.7,9.25,0.10,6HVERSUS,0.0,6)
      CALL SYMBOL(4.4,9.00,0.14,9HFREQUENCY,0.0,9)
      CALL SYMBOL(4.5,8.75,0.14,4HMODE,0.0,4)
      CALL NUMBER(5.2,8.75,0.14,FMOD,0.0,-1)
      CALL SYMBOL(4.7,8.50,0.10,14HPHASE VELOCITY,0.0,14)
      CALL SYMBOL(4.2,8.50,0.10,14,0.0,-1)
      CALL SYMBOL(4.7,8.25,0.10,14HGROUP VELOCITY,0.0,14)
      CALL SYMBOL(4.2,8.25,0.10,28,0.0,-1)
```

```
      CALL SYMBOL(4.7,8.00,0.10,19HEXCITATION PRESSURE,0.0,19)
      CALL SYMBOL(4.2,8.00,0.10,4,0.0,-1)
       T1(LIFQ  +2)  = 90.0
       T1(LIFQ +3)  = -10.0
       T2(LIFQ +2)  = 90.0
       T2(LIFQ  +3)  = -10.0
      CALL PLOT (15.0,0.0,-3)
      CALL LINE (FQP, T1,LIFQ +1,1,10,4)
      CALL LINE (FQP, T2,LIFQ +1,1,10,5)
      CALL AXIS (0.0,0.0,14HFREQUENCY (HZ),-14,10.,0.0,FQP(LIFQ +2),
     1 FQP(LIFQ +3),10.0)
      CALL AXIS (0.0,0.0,28HANGLE OF INCIDENCE (DEGREES),28, 9.0,90.0,
     1  T1(LIFQ +2), T1(LIFQ +3),10.0)
      CALL SYMBOL(3.7,9.50,0.14,18HANGLE OF INCIDENCE,0.0,18)
      CALL SYMBOL(4.7,9.25,0.10,6HVERSUS,0.0,6)
      CALL SYMBOL(4.4,9.00,0.14,9HFREQUENCY,0.0,9)
      CALL SYMBOL(4.5,8.75,0.14,4HMODE,0.0,4)
      CALL NUMBER(5.2,8.75,0.14,FMOD,0.0,-1)
      CALL SYMBOL(4.5,8.50,0.10,25HBOTTOM ANGLE OF INCIDENCE,0.0,25)
      CALL SYMBOL(4.0,8.50,0.10,4,0.0,-1)
      CALL SYMBOL(4.5,8.25,0.10,26HSURFACE ANGLE OF INCIDENCE,0.0,26)
      CALL SYMBOL(4.0,8.25,0.10,5,0.0,-1)
  154 CALL PLOT (15.0,0.0,-3)
      IF (IRP.NE.1)  GO TO 111
  123 DO 124 IP=  1,NPS
      READ (3,125)  NMS
  125 FORMAT (I10)
      READ (3,126)  (MDS(J),  J=1,NMS)
  126 FORMAT (6I10)
      DO 131 IR = IRST, IREN, IRIC
      IREO = (IR -IRST)/IRIC  +1
      PCT(IREO)  =  0.0
  131 PST(IREO)  =  0.0
      DO 127  IQ= 1,NMS
      M=  MDS(IQ)
      DO 129 IR = IRST, IREN, IRIC
      RR  =  IR
      IREO = (IR -IRST)/IRIC  +1
      DDT(M) = 10.0**(-DD(M)*RR/20.0)
      PST(IREO)  =  PST(IREO)+PMM(M)*DDT(M)        *SIN(FMR(M)*RR-P2/8.0)
      PCT(IREO)=    PCT(IREO)+PMM(M)*DDT(M)        *COS(FMR(M)*RR-P2/8.0)
  129 CONTINUE
  127 CONTINUE
      DO 132 IR = IRST, IREN, IRIC
      RR  =  IR
      IREO = (IR -IRST)/IRIC  +1
      PPT(IREO) = SQRT(PCT(IREO)*PCT(IREO) + PST(IREO)*PST(IREO))*RO/
     1SQRT(RR/3.0)
      FR = FQ/1000.0
      A = ( 0.1*FR**2/(1.0 +FR**2)) + (40.0*FR**2/(4100.0 +FR**2))
     1 + (.000275*FR**2)
      PPT(IREO        ) =-20.0*ALOG10(PPT(IREO))    +A*IR/3000.0
  132 RP(IREO         )  = FLOAT(IR)/6000.0
      WRITE (4,128) (PPT(J),  J= 1,IREO    )
  128 FORMAT (10F10.5)
      RP(IREO +1)  =  0.1533
      RP(IREO +2)  =  FMI
      PPT(IREO +1)  =  130.0
```

```
      PPT(IREO +2)  =  -20.0
      ZS = ZM - ZS
      ZRC = ZM - ZRC
      CALL LINE (RP,PPT,IREO,1,10,4)
      CALL AXIS(0.0,0.0,13HRANGE (MILES),13,20.0,0.0,RP(IREO +1),
     1 RP(IREO +2),10.0)
      CALL AXIS(0.0,0.0,21HPROPAGATION LOSS (DB),21,10.0,90.0,
     1 PPT(IREO +1),PPT(IREO +2),10.0)
      CALL SYMBOL(8.9,9.50,0.14,16HPROPAGATION LOSS,0.0,16)
      CALL SYMBOL(9.7,9.25,0.10,6HVERSUS,0.0,6)
      CALL SYMBOL(9.7,9.00,0.14,5HRANGE,0.0,5)
      CALL SYMBOL(8.9,8.75,0.14,18HFREQUENCY        HZ,0.0,18)
      CALL NUMBER(10.3,8.75,.14,FQ,0.0,-1)
      CALL SYMBOL(8.6,8.50,0.14,20HSOURCE DEPTH       FT,0.0,20)
      CALL NUMBER(10.5,8.50,0.14,ZS,0.0,-1)
      CALL SYMBOL(8.6,8.25,0.14,22HRECEIVER DEPTH       FT,0.0,22)
      CALL NUMBER(10.6,8.25,0.14,ZRC,0.0,-1)
      CALL SYMBOL (8.6,8.0,0.14,5HMODES,0.0,5)
      DO 187  J=  1,NMS
      FDS(J)  =  MDS(J)
  187 CALL NUMBER (9.1  +0.5*J,8.0,0.14,FDS(J),0.0,-1)
      CALL PLOT (15.0,0.0,-3)
  124 CONTINUE
      CALL PLOT (15.0,0.0,-3)
  111 CALL PLOT (15.0,0.0,-3)
      END
      SUBROUTINE COUNT
      DIMENSION U(500)
      DOUBLE PRECISION U
      COMMON MS,JM,U
      COMMON JMS
      MS=0
      J=1
      IS=1
      JMS=1
    5 IF (U(J)) 1,2,3
    3 IS1=IS
      IS=1
    7 IF (IS-IS1) 4,2,4
    4 MS=MS+1
      JMS=J
    2 J=J+1
      IF (J-JM-1) 5,6,5
    1 IS1=IS
      IS=0
      GO TO 7
    6 RETURN
      END
```

Appendix B

LIST OF PROGRAM S1548

```
      DOUBLE PRECISION     F,U,UP
      DOUBLE PRECISION               K2,    W2,P2,H,ZP,    CZ,G,H2,DEN
      DOUBLE PRECISION S,K20,DK2,GAM,BA
      DOUBLE PRECISION E,V
      DOUBLE PRECISION  UMAX
      DOUBLE PRECISION  COS2 , CCC  , CV
      DIMENSION HED(20),Z(100),C(100),F(500),UP(500) ,U(500) ,
     1  ZMP(1000), XMP(1000), COS2(500), CCC(500)
     1  , ZZP(500) , ZPP(500),  VV(500),  DATA(1024) , UU(500)
     1  ,PM(4000)  ,  ICVP(200)  , IADS(200)  ,CC(500), ZZ(500)
     1  , ZR(500) , CR(500) ,RP(1000),ZBT(5) , ZBF(5)
     1,DD(100),PPT(1000),PCT(1000),PST(1000),MDS(100),USR(100),URR(100),
     1  PMM(100),FMR(100)  ,FDS(100),DDS(100), DDT(100)
     1 ,GVEL(4000), PVEL(4000), FQP(4000), T1(4000), T2(4000)
     1,FKB(100),ERS(100),GKB(100),ER(100),PMI(100) ,GMR(100)
      COMMON MS,JM,U
      COMMON JMS
      CALL PLOTS  ( DATA(1), 1024,  6  )
      READ(3,1)HED
    1 FORMAT (20A4)
      READ (3,126)  NPCS, NVPC , NADS ,NCOR, NMOD
      READ (3,126)  (ICVP(J),  J= 1, NVPC)
      READ (3,126)  (IADS(J),  J= 1, NADS)
      READ (3,196)  IRIC, NPS, ZS, ZRC, FMI ,FSC ,FMJ, FMK
  196 FORMAT (2I10, 6F10.3)
      FINC = 30*(NADS*NMOD +NVPC)
      CALL PLOT (FINC ,0.0,-3)
      DO 111  L= 1,NPCS
      NMF = 0
      DO 189 J= 1,NVPC
      IF (ICVP(J).EQ.L)   GO TO 4
  189 CONTINUE
      GO TO 14
    4 JPM = 25
      FINC =30*NADS*NMOD+(NVPC -J +1)*30
      CALL PLOT (-FINC,0.0,-3)
      READ (3,112)         NUMV, VEL1  ,  IVPL  ,IEX
  112 FORMAT ( I10,F10.0,3I10)
      NUM  =  0
      READ(3,2) ZMM,CB
    2 FORMAT (4F10.3)
      ZMB = (200.0*FSC -ZMM)/(20.0*FSC)
      ZBT(1) = ZMM
      ZBT(2) = ZMM
      ZBT(3) = 200.0*FSC
      ZBT(4) = -20.0*FSC
      ZBF(1) =  0.0
      ZBF(2) = 10.0
      ZBF(3) =  0.0
      ZBF(4) =  1.0
      DO 3 I=1,100
      ZZ(I)  =  0.0
    3 CC(I)  =  0.0
      I=1
    5 READ (3,30) ZZ(I),  CC(I)
   30 FORMAT(2F10.3)
      IF(DABS(ZZ(I) - ZMM) - .01) 6,6,7
```

```
  7 I = I+1
    GO TO 5
  6 I = 1
    IF (IVPL.EQ.1)  GO TO 8
    DO 130  K  =  1, NUMV
    CR(NUMV -K +1)  =  CC(K)
130 ZR(NUMV -K +1)  =  ZZ(K)
    ZR(NUMV +1) = ZMM - 0.01
    ZR(NUMV +2) = ZMM + 50.0
    CR(NUMV  +1)  =  CB
    CR(NUMV  +2)  =  CB
    DO 185   NINY  = 1, NUMV
185 ZR(NINY) = ZMM - ZR(NINY)
    ZR(NUMV +3) = 200.0*FSC
    ZR(NUMV +4) = -20.0*FSC
    CR(NUMV  +3)  =  VEL1
    CR(NUMV  +4)  =  50.0
    CALL LINE (CR,ZR,NUMV +2, 1.0,0  )
    CALL LINE (ZBF,ZBT,2,1,0,0)
    CALL SYMBOL (10.25,ZMB,0.14,6HBOTTOM,0.0,6 )
    CALL AXIS (0.0,0.0,14HSOUND VELOCITY,14,10.,0.0,CR(NUMV  +3) ,
   1CR(NUMV+4),10.0  )
    CALL AXIS (0.0,0.0,11HWATER DEPTH,11,10.0,90.0,ZR(NUMV +3)  ,
   1ZR(NUMV+4),10.0  )
    CALL PLOT (15.0,0.0,-3)
    ZR(NUMV +1) = 200.0*FSC
    ZR(NUMV +2) = -20.0*FSC
    CR(NUMV +1) =VEL1
    CR(NUMV +2) =10.0
    CALL LINE (CR,ZR,NUMV,1,0,0)
    CALL LINE (ZBF,ZBT,2,1,0,0)
    CALL SYMBOL (10.25,ZMB,0.14,6HBOTTOM,0.0,6 )
    CALL AXIS (0.0,0.0,14HSOUND VELOCITY,14,10.,0.0,CR(NUMV  +1) ,
   1CR(NUMV+2),10.0  )
    CALL AXIS (0.0,0.0,11HWATER DEPTH,11,10.0,90.0,ZR(NUMV +1)  ,
   1ZR(NUMV+2),10.0  )
    CALL PLOT (-15.,0.0,-3)
    CALL PLOT (FINC ,0.0,-3)
  8 JP = 3
188 WRITE(4,9)HED
  9 FORMAT (1H1,9X,20A4)
    WRITE(4,10)
 10 FORMAT(1H0,15X,4HZ,FT,5X,8HC,FT/SEC)
 11 WRITE(4,12)ZR(I),CR(I)
 12 FORMAT(1H0,9X,F10.1,F12.1)
    IF(DABS(ZZ(I) -ZMM) - 0.01)  14,14,13
 13 I = I+1
    JP = JP+1
    IF(JP-JPM)11,8,8
 14 IF (L.NE.1)  GO TO 197
    READ (3,15)  N, UM, FQ
 15 FORMAT(I10,2F10.3,I10)
    NNN  =  N
    IF (L.NE.1)  GO TO 197
    DO 204  J= 1, NM
    FKB(M) = 0.0
    DDS(M) = 0.0
204 ERS(M) = 0.0
```

```
197 READ (3,195)  ZM, IRST , IREN
195 FORMAT (F10.0, 2I10)
    READ (3,2)  CB , RO , RB  ,XI
    READ (3,122)  (DD(J), J= 1,NMOD)
122 FORMAT (4F10.5)
    IPOS = 0
    IF (ZRC.GT.ZM)  IPOS = 1
    ZS = ZM - ZS
    ZRC = ZM - ZRC
    ZMB = (200.0*FSC -ZM )/(20.0*FSC)
    DO 200 J= 1,NUMV
    C(J) = CC(J)
200 Z(J) = ZZ(J)  -  (ZMM -ZM)
    DO 201 J= 1,NUMV
    IF(Z(J).LT.0.1)  GO TO 201
    GO TO 202
201 CONTINUE
202 IF (J.EQ.1)  GO TO 120
    C(J -1) = C(J   ) +(C(J) -C(J -1))*-Z(J)/(Z(J) - Z(J -1))
    Z(J -1) = 0.0
    JJJ = NUMV -J +2
    DO 203  JJ= 1,JJJ
    C(JJ) = C(JJ +J  -2)
203 Z(JJ) = Z(JJ +J  -2)
    JJJ= JJJ  +1
    DO 205  JK = JJJ,NUMV
    C(JK) = 0.0
205 Z(JK) = 0.0
120 DO 154  M=  1,NMOD
162 P2 = 6.283185306
    W2 = (P2*FQ)*(P2*FQ)
    N  =  NNN
    FMOD = M
    IF(N)29,4,29
 29 K20 = ((W2*(CB-C(1))*(CB+C(1)))/(C(1)*C(1)*CB*CB))
    DK2= .099*K20
    K2 = -K20
 31 K2 = K2 + DK2
    IF(K2-K20)16,32,32
 32 WRITE(4,33)
 33 FORMAT(1H0,13HNO MODE FOUND)
    NMF = 1
    DO 295  J= 1, NMOD
295 DDS(J) = DDS(J) +DD(J)*FLOAT(IREN)
    GO TO 123
 16 FLB  =  FLOAT(N)
    H = ZM/ DBLE(FLB)
    ZP = 0.
    J = 1
    I = 1
 17 IF (ZP- Z(I+1)) 18,18,19
 19 I  =  I  +1
    GO TO 17
 18 CZ = (C(I)*(Z(I+1)-ZP)+C(I+1)*(ZP-Z(I)))/(Z(I+1)-Z(I))
    CCC(J)  =  CZ
    G =-(W2*(C(1)-CZ)*(C(1)+CZ))/(CZ*CZ*C(1)*C(1))
    F(J) = K2 - G
    IF(ZP-ZM) 20,21,21
```

```
 20 J=J+1
    FLA   =  FLOAT(J -1)
    ZP    =  ZM*DBLE(FLA)/DBLE(FLB)
    GO TO 17
 21 U(1) = 1.0
    UP(1) =(RO/RB)*DSQRT ((W2*(CB-C(1))*(CB+C(1)))/(C(1)*(C(1)*CB*CB))
   1-K2)
    J = 1
 22 JP = 3
 25 FLA   =  FLOAT(J -1)
    FLB   =  FLOAT(N)
    ZP    =  ZM*DBLE(FLA)/DBLE(FLB)
    IF(J-N-1)27,34,27
 27 IF(DABS(U(J))-UM)28,34,34
 28 J = J+1
    JP= JP+1
    H2= H*H
    DEN = 1.0 + (H2*F(J))/6.0
    U(J)= ((1.0-(H2/3.0)*F(J-1))*U(J-1)+H*UP(J-1))/DEN
    UP(J)=((1.0-(H2*F(J))/3.0)*UP(J-1)-(F(J-1)+F(J)-(H2*F(J)*F(J-1))/
   16.0)*H*U(J-1)* 0.5)/DEN
    IF (JP-JPM)25,22,25
 34 JM = J
    CALL COUNT
    IF (MS-M)31,35,35
 35 DO 289 J= 1,N
    IF (F(J).GT.0.0) GO TO 290
289 CONTINUE
290 IJ1 = J +1
    DO 291  J= IJ1,  N
    IF(F(J).LT.0.0)  GO TO 292
291 CONTINUE
    GO TO 294
292 IJ2 = J +1
    DO 293  J= IJ2, N
    IF(F(J).GT.0.0)  GO TO 31
293 CONTINUE
294 K2 = K2 - DK2
    DK2= DK2 / 10.0
    IF(DK2- .000001*K20*10**(-IEX)) 36,36,31
 36 J = 2
    IF (XI.GT.0.0)   GO TO 502
    GO TO 501
502 READ (3,500)  (U(II)  ,  II= 1,N)
500 FORMAT (8D10.5)
501 S = H*U(1)*U(1)/2.0
    S2= H*U(1)*U(1)/(2.0*CCC(1)*CCC(1))
 37 IF(J-JMS)38,39,38
 38 S = H*U(J)*U(J)+S
    S2= H*U(J)*U(J)/(CCC(J)*CCC(J))  +S2
    J = J+1
    GO TO 37
 39 S =(H*U(J)*U(J)/2.0) + S
    S2= H*U(J)*U(J)/(2.0*CCC(J)*CCC(J))  +S2
    J = 1
 42 JP = 3
    DO 206 KK= 1, NADS
    IF(IADS(KK).EQ.L)  GO TO 208
```

```
206 CONTINUE
    GO TO 43
208 WRITE(4,23)HED,N,K2,UM,FQ,M
 23 FORMAT(1H1,5X,20A4,/,2X,3HN =,I5,2X,4HK2 =,F15.8,2X,4HUM =,F6.1,
   12X,6HFREQ = ,F8.1,2X,3HM =,I5)
    WRITE(4,47) ZM,CB,RO,RB
 47 FORMAT(3X,6HZMAX = ,F10.3,4HCB = ,F10.3,4HRO = ,F15.8,4HRB = ,
   1F15.8)
    WRITE(4,24)
 24 FORMAT(1H0,17X,4HZ,FT,10X,1HU,10X,5HDU/DZ,11X,4HF(Z))
 43 ZP = ZM*( FLOAT(J-1)/ FLOAT(N))
    ZQ = ZM - ZP
    DO 207 KK= 1, NADS
    IF(IADS(KK).EQ.L)  GO TO 209
207 CONTINUE
    GO TO 44
209 WRITE(4,26)ZQ,U(J),UP(J),F(J)
    IF(J-N-1)45,44,45
 45 IF(DABS(U(J))-UM)46,44,44
 46 J = J+1
    JP = JP+1
    IF(JP-JPM)43,42,43
 44 WRITE(4,40) S
 40 FORMAT (1H0,10X, 3HS = ,F15.5)
164 UMAX = 0.0
    NM  =  N  +1
    DO  104  K=  1, NM
    IF  ( DABS (U(K)) - UMAX)  104,104,103
103 UMAX  =  DABS(U(K) )
104 CONTINUE
    DO  105  K=  1, NM
105 UU(K) =  U(K)/UMAX
    DO 106  K= 1, NM
106 ZZP(K)  =  ZM*(FLOAT(K -1)/FLOAT(N)  )
    GAM = DSQRT(K20 - K2)
    BA = (RO*C(1))/(2.0*RB*CB*GAM*S )
    WRITE(4,41) BA,GAM
 41 FORMAT(1H0,10X,5HB/A = ,F15.5,5X,7HGAMMA = ,F15.5 )
    SS=  RO*S/(UMAX*UMAX)+RO* RO*U(1)*U(1)/(UMAX*UMAX*2.0*GAM*RB)
    SSS= RO*S2/(UMAX*UMAX)            +       RO*RO*U(1)*U(1)/(UMAX*UMAX
   1*2.0*GAM*RB*CB*CB)
    E = DEXP(-GAM*H)
    ZP = 0.0
    V = 1.0
    NN  =  1
    ZPP(1)  =  0.0
    VV(1)  = UU(1)
    WRITE(4,23)HED,N,K2,UM,FQ,M
    WRITE(4,47) ZM,CB,RO,RB
212 DO 210  KK= 1,NADS
    IF(IADS(KK).EQ.L)  GO TO 211
210 CONTINUE
    GO TO 50
211 WRITE(4,48)
 48 FORMAT(1H0,17X,4HZ,FT,10X,1HU )
 49 WRITE(4,26)ZP,V
 26 FORMAT(1H0,F22.2,F13.3,F13.3,F16.5)
 50 V = V*E
```

```
      NN  = NN  +1
      VV(NN)  =  VV(NN -1)*E
      ZPP(NN)  =  ZP -       H
      ZP = ZP-H
      IF  (ZPP(NN)  + 50.0)          110, 110,  212
  110 DO 190 J= 1, NADS
      IF ( IADS(J).EQ.L)  GO TO 193
  190 CONTINUE
      GO TO 192
  193 FINC = 30*(NADS*NMOD -J +1)  -(NMOD -M)*30
      CALL PLOT (-FINC,0.0,-3)
      DO 184   NINX  = 1, NN
  184 ZPP(NINX) =  ZM - ZPP(NINX)
      NINV  =  N + 1
      DO 183   NINW  = 1, NINV
  183 ZZP(NINW) =  ZM - ZZP(NINW)
      VV(NN +1)  =  -1.0
      VV(NN +2)  =  0.5
      ZPP(NN +1) = 200.0*FSC
      ZPP(NN +2) = -20.0*FSC
      ZZP(N +2)  = 200.0*FSC
      ZZP(N +3)  = -20.0*FSC
      ZBT(1) = ZM
      ZBT(2) = ZM
      UU(N+2)  =  -1.0
      UU(N+3)  =  0.5
      CALL  AXIS (0.0,0.0, 9HAMPLITUDE,  9,4.0,0.0,UU(N+2),UU(N+3),10.0)
      CALL AXIS (0.0,0.0,16HWATER DEPTH (FT),16,10.0,90.0,ZZP(N+2),
     1  ZZP(N +3),10.0)
      CALL LINE  (UU, ZZP,  N+1, 1,0,0)
      CALL LINE (VV, ZPP,  NN,  1,0,0  )
      CALL LINE (ZBF,ZBT,2,1,0,0)
      CALL SYMBOL (10.25,ZMB,0.14,6HBOTTOM,0.0,6 )
      CALL SYMBOL(1.3,9.50,0.14,9HAMPLITUDE,0.0,9)
      CALL SYMBOL(1.7,9.25,0.10,6HVERSUS,0.0,6)
      CALL SYMBOL(1.6,9.00,0.14,5HDEPTH,0.0,5)
      CALL SYMBOL(0.8,8.75,0.14,19HFREQUENCY         HZ,0.0,19)
      CALL NUMBER(2.2,8.75,0.14,FQ,0.0,-1)
      CALL SYMBOL(1.4,8.50,0.14,4HMODE,0.0,4)
      CALL NUMBER(2.1,8.50,0.14,FMOD,0.0,-1)
  192 NUM  =  NUM  +1
  153 XMP(1)  =  0.0
      ZMP(1)  =  0.0
      NM  =  N  +1
      CALL PLOT (15.0,0.0,-3)
      NSTR = 1
      NEND = N +1
      IDZ = 0
      IF(F(1).GT.0.0)   GO TO 179
  681 DO 170 K=  NSTR,NEND
      IF(F(K).GT.0.0)    GO TO 171
  170 IRTB = K
      GO TO 689
  171 COS2(IRTB +1) = F(IRTB +1)*CCC(IRTB +1)*CCC(IRTB +1)/W2
      CV  =  CCC(IRTB +1)/DSQRT(1.0 - COS2(IRTB +1))
      ZMP(2) = H*(CV - CCC(IRTB +1))/(CCC(IRTB)-CCC(IRTB +1))
      XMP(2) =  (ZMP(2) - ZMP(1))*(CCC(IRTB +1) + CV)/(CV*(DSQRT(COS2
     1 (IRTB +1))))
```

```
      ZMP(1) = FLOAT(IRTB)*H - ZMP(2)
      ZMP(2) = ZMP(1) + ZMP(2)
      NM = NM -IRTB +1
      DO 172  K = 3,NM
      TH1 = 90.0
      KO = IRTB -1 +K
      COS2(KO-1) = F(KO -1)*CCC(KO -1)*CCC(KO -1)/W2
      COS2(KO)=F(KO)*CCC(KO)*CCC(KO)/W2
      IF(CCC(KO).GE.CV) ZMP(K) = ZMP(K  -1) +H*(CV- CCC(KO -1))/(CCC(KO)
     1 -CCC(KO -1))
      IF(CCC(KO).GE.CV)    GO TO 152
      XMP(K) = XMP(K  -1) +H*(CCC(KO -1) + CCC(KO))/(CV*(DSQRT(COS2(KO-1
     1)) + DSQRT(COS2(KO))))
  172 ZMP(K)  =  (KO -1)*H
      TH2 = (ACOS(SQRT(COS2(NM +IRTB -1))))*57.2958
      N =  NM -1
      GO TO 173
  179 COS2(1)  =  ABS(F(1))*CCC(1)*CCC(1)/W2
      CV  =  CCC(1)/DSQRT(1.0 - COS2(1) )
      DO 140  K=  2,NM
      COS2(K -1) = ABS(F(K -1))*CCC(K -1)*CCC(K -1)/W2
      COS2(K)  =  ABS(F(K))*CCC(K)*CCC(K)/W2
      TH1 =(ACOS(SQRT(COS2(1))))*57.2958
      TH2 =(ACOS(SQRT(COS2(NM))))*57.2958
      IF( CCC(K).GE.CV)  GO TO 142
      XMP(K) = XMP(K -1) + H*(CCC(K-1) + CCC(K))/(CV*(DSQRT(COS2(K-1))+
     1 DSQRT(COS2(K))))
  140 ZMP(K)  =  (K-1)*H
  173 DO 141  K=  1,N
      XMP(NM +K) = 2.0*XMP(NM)  -  XMP(NM - K)
  141 ZMP(NM +K) = ZMP(NM -K)
      GO TO 143
  142 ZMP(K) = ZMP(K -1)  +  H*(CV - CCC(K-1))/(CCC(K) - CCC(K -1))
  152 TH2  =  90.0
      XMP(K) = XMP(K -1) + (ZMP(K) - ZMP(K-1))*(CCC(K-1) + CV)/(CV*(
     1  DSQRT(COS2(K -1))))
      N = K -1
      NM  =  K
      DO 144  K=  1,N
      XMP(N+1+K) = 2.0*XMP(N+1) - XMP(N+1-K)
  144 ZMP(N +1 +K) = ZMP(N +1 -K)
  143 XMP(2*NM)  =  0.0
  182 XMP(2*NM +1)  =  1000.0
      NIZZ = 2*NM -1
      DO 186 NINZ = 1, NIZZ
  186 ZMP(NINZ) = ZM - ZMP(NINZ)
      ZMP(2*NM)  =  200.0*FSC
      ZMP(2*NM +1)  = -20.0*FSC
      WRITE (4,145) TH1,TH2,XMP(NM +N)
  145 FORMAT (3F10.3)
      DO 691 J= 1, NADS
      IF ( IADS(J).EQ.L)  GO TO 194
  691 CONTINUE
      GO TO 157
  194 CALL LINE (XMP,ZMP,NM +N,1,0,0)
      IF (IDZ.EQ.1) GO TO 650
      IDZ = 1
      CALL LINE (ZBF,ZBT,2,1,0,0)
```

```
      CALL SYMBOL (10.25,ZMB,0.14,6HBOTTOM,0.0,6 )
      CALL AXIS (0.0,0.0,10HRANGE (FT),10,12.0,0.0,XMP(2*NM)    ,
     1XMP(2*NM +1),10.0)
      CALL AXIS (0.0,0.0,16H       DEPTH (FT),16,10.0,90.0,ZMP(2*NM),
     1 ZMP(2*NM +1),10.0 )
      CALL SYMBOL(5.0,9.50,0.14,14HRAY EQUIVALENT,0.0,14)
      CALL SYMBOL(5.0,9.25,0.14,19HFREQUENCY         HZ,0.0,19)
      CALL NUMBER(6.4,9.25,0.14,FQ,0.0,-1)
      CALL SYMBOL(5.5,9.00,0.14,4HMODE,0.0,4)
      CALL NUMBER(6.2,9.00,0.14,FMOD,0.0,-1)
      NM = NEND
  650 NSTR =       IRTB + NM -1
      ZMP(1) = 0.0
      IF(NSTR.GE.NEND) GO TO 689
      GO TO 681
  689 CALL PLOT (-15.0,0.0,-3)
      CALL PLOT (FINC ,0.0,-3)
  157 T1(L) = TH1
      T2(L) = TH2
      FMH = SQRT(P2*FQ /(30.48*CV) )
      PM(L) = SQRT(P2)*      RO/(FMH*2.0*(SS) )
      GVEL(L) = SS/(CV*SSS)
      FQP(L) = L
      WRITE ( 4,166)  PM(L) , FMH, SS   , GVEL(L)
  166 FORMAT(4F10.3)
      PM(M)  =  PM(L)
      FMR(M) = P2*FQ/CV
      FKB(M) = FKB(M) + FMR(M)*FLOAT(IREN)
      DDS(M) = DDS(M) +DD(M)*FLOAT(IREN)
      IF (L.EQ.NCOR)PMI(M)= PM(L)
      IZR =ZRC*FLB/ZM +1.0
      IZS = ZS*FLB/ZM   +1.0
      IF(L.EQ.NCOR)USR(M)= U(IZS)/UMAX
      IF(IPOS.EQ.1) GO TO 155
      URR(M) = U(IZR)/UMAX
      PMM(M) = SQRT(PM(M)*PMI(M))*USR(M)*URR(M)/RO
      WRITE (4,166)  PMM(M),PMI(M), USR(M), URR(M)
      WRITE(4,126)  L, NCOR
  155 PVEL(L) = CV
  154 CONTINUE
  123 ZS = ZM - ZS
      ZRC = ZM - ZRC
      IREN = IRST + IREN
      DO 124 IP=  1,NPS
      IF (L.NE.1)  GO TO 198
      READ (3,125)  NMS
  125 FORMAT (I10)
      READ (3,126)  (MDS(J),  J=1,NMS)
  126 FORMAT (6I10)
  198 DO 131 IR = IRST, IREN, IRIC
      IREO = (IR -IRST)/IRIC  +1
      PCT(IREO)  =  0.0
  131 PST(IREO)  =  0.0
      IF (NMF.EQ.1)  GO TO 111
      DO 127  IQ= 1,NMS
      M=  MDS(IQ)
      DO 129 IR = IRST, IREN, IRIC
      IF (L.EQ.NMOD)RI= FLOAT(IRST)
```

```
      GKB(M) = FKB(M) - FLOAT(IREN - IR)*FMR(M)
      DDT(M) = DDS(M) -FLOAT(IREN -IR)*DD(M)
      IF (GKB(M).LE.0.0)  GO TO 214
      GKB(M) = GKB(M)/(FLOAT(IR) -RI)
  214 RR  =  IR
      IF(L.EQ.NMOD)GKB(M)= FMR(M)
      GMR(M) = GKB(M) + ERS(M)/RR
      ER(M) = FMR(M) - GKB(M)
      IF(IREN -IR.GE.IRIC)  WGT = IRIC
      IF(IREN -IR.LT.IRIC)  WGT = IREN -IR
      ERS(M) = ERS(M) + ER(M)*WGT
      IREO = (IR -IRST)/IRIC  +1
      IF(IPOS.EQ.1)  GO TO 129
      DDT(M) = 10.0**(-DDT(M)/20.0)
      PST(IREO)  =  PST(IREO)+PMM(M)*      DDT(M)  *SIN(GMR(M)*RR-P2/8.0)
      PCT(IREO)=    PCT(IREO)+PMM(M)*      DDT(M)  *COS(GMR(M)*RR-P2/8.0)
  129 CONTINUE
  127 CONTINUE
      IF(IPOS.EQ.1)  GO TO 113
      DO 132 IR = IRST, IREN, IRIC
      RR  =  IR
      IREO = (IR -IRST)/IRIC  +1
      PPT(IREO) = SQRT(PCT(IREO)*PCT(IREO) + PST(IREO)*PST(IREO))*RO/
     1SQRT(RR/3.0)
      FR = FQ/1000.0
      A = ( 0.1*FR**2/(1.0 +FR**2)) + (40.0*FR**2/(4100.0 +FR**2))
     1 + (.000275*FR**2)
      PPT(IREO        ) =-20.0*ALOG10(PPT(IREO))    +A*IR/3000.0
  132 RP(IREO        )  = FLOAT(IR)/6000.0
      WRITE (4,128) (PPT(J), J= 1,IREO   )
  128 FORMAT (10F10.5)
  113 RP(IREO +1)  =  0.0
      RP(IREO +2)  =  FMI
      PPT(IREO +1)  =  FMJ
      PPT(IREO +2)  =  FMK
      IF(IPOS.EQ.1)  GO TO 114
      CALL LINE (RP,PPT,IREO,1,10,4)
  114 IF (L.NE.NCOR) GO TO 111
      CALL AXIS(0.0,0.0,13HRANGE (MILES),13,20.0,0.0,RP(IREO +1),
     1 RP(IREO +2),10.0)
      CALL AXIS(0.0,0.0,21HPROPAGATION LOSS (DB),21,10.0,90.0,
     1 PPT(IREO +1),PPT(IREO +2),10.0)
      CALL SYMBOL(8.9,9.50,0.14,16HPROPAGATION LOSS,0.0,16)
      CALL SYMBOL(9.7,9.25,0.10,6HVERSUS,0.0,6)
      CALL SYMBOL(9.7,9.00,0.14,5HRANGE,0.0,5)
      CALL SYMBOL(8.9,8.75,0.14,18HFREQUENCY        HZ,0.0,18)
      CALL NUMBER(10.3,8.75,.14,FQ,0.0,-1)
      CALL SYMBOL(8.6,8.50,0.14,20HSOURCE DEPTH       FT,0.0,20)
      CALL NUMBER(10.5,8.50,0.14,ZS,0.0,-1)
      CALL SYMBOL(8.6,8.25,0.14,22HRECEIVER DEPTH       FT,0.0,22)
      CALL NUMBER(10.6,8.25,0.14,ZRC,0.0,-1)
      CALL SYMBOL (8.6,8.0,0.14,5HMODES,0.0,5)
      DO 187  J=  1,NMS
      FDS(J)  =  MDS(J)
  187 CALL NUMBER (9.1  +0.5*J,8.0,0.14,FDS(J),0.0,-1)
  199 FINC  =  IP*25
      CALL PLOT (20.0,0.0,-3)
  124 CONTINUE
```

```
      DO 220  J= 1,NPS
  220 CALL PLOT (-20.0,0.0,-3)
  111 CONTINUE
      CALL PLOT (15.0 ,0.0,-3)
      END
      SUBROUTINE COUNT
      DIMENSION U(500)
      DOUBLE PRECISION U
      COMMON MS,JM,U
      COMMON JMS
      MS=0
      J=1
      IS=1
      JMS=1
    5 IF (U(J)) 1,2,3
    3 IS1=IS
      IS=1
    7 IF (IS-IS1) 4,2,4
    4 MS=MS+1
      JMS=J
    2 J=J+1
      IF (J-JM-1) 5,6,5
    1 IS1=IS
      IS=0
      GO TO 7
    6 RETURN
      END
```

UNCLASSIFIED

Security Classification

DOCUMENT CONTROL DATA - R & D

Security classification of title, body of abstract and indexing annotation must be entered when the overall report is classified)

1. ORIGINATING ACTIVITY (Corporate author)
Naval Underwater Systems Center
Newport, Rhode Island 02840

2a. REPORT SECURITY CLASSIFICATION
UNCLASSIFIED

2b. GROUP

3. REPORT TITLE
COMPUTER PROGRAMS TO CALCULATE NORMAL MODE PROPAGATION AND APPLICATIONS TO ANALYSIS OF EXPLOSIVE SOUND DATA IN THE BIFI RANGE

4. DESCRIPTIVE NOTES (Type of report and inclusive dates)
Research Report

5. AUTHOR(S) (First name, middle initial, last name)
William G. Kanabis

6. REPORT DATE	7a. TOTAL NO. OF PAGES	7b. NO. OF REFS
6 November 1972	108	23

8a. CONTRACT OR GRANT NO.

b. PROJECT NO. A-650-09
SF 11 552-008-14054

c.

d.

9a. ORIGINATOR'S REPORT NUMBER(S)
TR 4319

9b. OTHER REPORT NO(S) (Any other numbers that may be assigned this report)

10. DISTRIBUTION STATEMENT
Distribution limited to U. S. Government agencies only; Test and Evaluation; 6 November 1972. Other requests for this document must be referred to the Naval Underwater Systems Center.

11. SUPPLEMENTARY NOTES

12. SPONSORING MILITARY ACTIVITY
Department of the Navy

13. ABSTRACT

This report describes two computer programs that use normal mode theory to predict acoustic propagation and discusses the use of these programs in analyzing explosive data taken in a series of shallow water tests. Program S1441 calculates normal mode propagation in a medium in which the stratification is constant with range; program S1548 computes normal mode propagation when the horizontal stratification is assumed to vary slowly with range. The results of the tests indicate that the introduction of horizontal stratification in program S1548 provides an improved comparison with measured data. Physical explanations are provided for the previously observed minimum in propagation loss at about 125 Hz and for the nonlinear relationship, at certain frequencies, between propagation loss and size of the negative sound gradient observed. In addition, bottom loss was determined in the BIFI (Block Island Fishers Island) range for a wide range of frequencies and thermal conditions.

DD FORM 1 NOV 65 1473 (PAGE 1)

S/N 0102-014-6600

UNCLASSIFIED

Security Classification

14 KEY WORDS	LINK A		LINK B		LINK C	
	ROLE	WT	ROLE	WT	ROLE	WT
BIFI range						
Normal mode theory						
Acoustic propagation						
Horizontal stratification						
Explosive data						
Bottom loss						
Shallow water						
Computer programs						

INITIAL DISTRIBUTION LIST

Chief of Naval Operations, Op-311
- Op-32
- Op-95
- Op-96
- Op-9420
- Op-950
- Op-954
- Op-9814
- Op-23T

Oceanographer of the Navy
Office of Naval Research, Code 400-A2
- Code 466
- Code 468
- Code 480
- Code 481
- Code 485
- Code 102-OS

Naval Oceanagraphic Office, Code 7200
- Code 9320

Naval Ship Systems Cammand, PMS-302
- PMS-302-4
- PMS-302-4B
- PMS-302-44
- PMS-302-441

ASW Systems Project Office (CNM-PM-4), ASW-211
- ASW-22
- ASW-23
- ASW-24

Cammander, Fleet Numerical Weather Central
Naval Air Development Center, Johnsville, Pa.
Naval Ordnance Laboratory, White Oak, Md.
Navy Undersea Center, San Diego, Calif.
Naval Research Laboratary, Washingtan, D. C.
Applied Physics Labaratory, University of Washingtan
Marine Physical Laboratory, Scripps Institution of Oceanagraphy
Ordnance Research Labaratary, Pennsylvania State University
Woods Hole Oceanographic Institutian
Naval Pastgraduate School, Monterey, Calif.
Center of Naval Analyses
Committee on Undersea Warfare, National Research Council
Naval Air Development Center, Johnsville, Pa.
Deputy Director of Defense Research and Engineering
Naval Electronic Systems Command (PME-124)
Defense Documentation Center (DDC)